

Silesian University of Technology
Faculty of Mechanical Engineering
Institute of Engineering Processes Automation
and Integrated Manufacturing Systems

SELECTED ENGINEERING PROBLEMS

NUMBER 5

Gliwice 2014

SCIENTIFIC COMMITTEE

Professor Andrzej Buchacz, Silesian University of Technology – Chairman
Professor Aleksander S. Bokhonsky, Sewastopol National Technical University, Ukraine
Professor Piotr Gendarz, Silesian University of Technology, Poland
Professor Ivan M. Gostev, National Research University Higher School of Economics, Moscow, Russia
Professor Aleksander N. Mikhaylov, Donetsk National Technical University, Ukraine
Professor Dumitru Nedelcu, Technical University "Gheorghe Asachi" of Iasi, Romania
Professor Tetiana Roik, National Technical University of Ukraine "Kyiv Polytechnic Institute", Kiev, Ukraine
Professor Bożena Skołod, Silesian University of Technology, Poland
Professor Jerzy Świder, Silesian University of Technology, Poland
Professor Edward Tomasiak, Silesian University of Technology, Poland
Professor Pavel Topala, State University of Russo -Alecuc Republic of Moldova
Associate Professor Andrzej Baier, Silesian University of Technology, Poland
Associate Professor Gabriel Kost, Silesian University of Technology, Poland
Associate Professor Tomasz Trawiński, Silesian University of Technology, Poland
Associate Professor Waldemar Świdorski, Military Institute of Armament Technology, Zielonka, Poland

EDITORIAL BOARD

Andrzej Wróbel - Editor in Chief
e-mail: andrzej.wrobel@polsl.pl, phone.: (+48) 32-237 1603
Marek Płaczek – Deputy Editor in Chief
e-mail: marek.placzek@polsl.pl, phone: (+48) 32-237 2437
Magdalena Bączkiewicz
e-mail: magdalena.baczkowicz@polsl.pl, phone: (+48) 32-237 1657
Małgorzata Olender
e-mail: malgorzata.olender@polsl.pl, phone: (+48) 32-237 1219

Articles published on the basis of materials supplied by the authors.

ISSN 2299-954X

© Copyright by
Institute of Engineering Processes Automation and Integrated Manufacturing Systems, Faculty of
Mechanical Engineering, Silesian University of Technology.

The publication, in whole or in a part, may not be reproduced or distributed by copying, recording or other ways, also may not be used distributed in digital form, both on the Internet and local networks without the prior written consent of the copyright owners.

CONTENTS

BAIER M., DUSIK D. BELT VIBRATIONS MEASUREMENTS AND RELATIVE EFFICIENCY OF THE POWERTRAIN STUDY ON THE ENGINE TEST STAND FOR <i>SILESIA GREENPOWER VEHICLE</i>	5
BĄCZKOWICZ M., GWIAZDA A. IMPROVEMENT OF THE PIECE PRODUCTION SYSTEM USING LEAN MANAGEMENT APPROACHES	11
BOGNÁR E., Ozsváth P., Kertész A., Pelyhe L., Dévényi L. ANALYSIS AND DEVELOPMENT OF THE ADHESION OF STENT COATINGS	15
ĆWIKŁA G., GRABOWIK C., KALINOWSKI K. APPLICATION OF LEAN AND SIX SIGMA METHODOLOGY IN IMPROVING OF PRODUCTION PROCESSES	21
FOIT K. SVG GRAPHICS LANGUAGE AS A DESCRIPTION OF A 2D PATH IN ROBOT PROGRAMMING TASKS	27
GAWLAS-MUCHA A., NOWOSIELSKI R., BABILAS R., GUWER A. SELECTED ASPECTS OF MAGNESIUM ALLOYS MELTING TECHNOLOGY	33
GOLDA G., KAMPA A. A MICROLOGISTIC SYSTEM ANALYSIS ON EXAMPLE OF ROBOTIZED RAPID PROTOTYPING CELL	37
GRABOWIK C., KALINOWSKI K., ĆWIKŁA G., JANIK W. ALTERNATIVE METHODS OF THE ARTIFICIAL FISH LURES MANUFACTURING – CASE STUDY	41
GUWER A., NOWOSIELSKI R., GAWLAS-MUCHA A., KILJAN A., BABILAS R. THE INFLUENCE OF MILLING AND INTERVAL TIME ON THE AMORPHIZATION PROCESS OF Cu-Ti ALLOYS	47
JANIK W., GRABOWIK C., ĆWIKŁA G., KALINOWSKI K. MANUFACTURING PROCESSES OPTIMIZATION WITH APPLICATION OF GRIP NC PROGRAMMING LANGUAGE	53
KAMPA A., GOLDA G. RAPID MACHINING WITH INDUSTRIAL ROBOT	57
Klarecki K., Rabsztyn D., Hetmańczyk M. THE EFFECT OF BACKGROUND CURRENT INTENSITY ON THE HYSTERESIS OF PROPORTIONAL VALVES	63

Krenczyk D. THE AUTOMATED PROCESS OF CREATING SIMULATION MODELS	67
Mandla Ł., Krzystała E. THE USE OF BIOMECHANICAL INDEX TO ESTIMATE SOLDIER'S LEVEL OF THREAT	71
MICHALSKI P., TKOCZ K. THE ALGORITHMS SUPPORT FOR VISUALISATION OF INDUSTRIAL ROBOT MOVEMENTS	81
MIKOŁAJCZAK M., KALINOWSKI K., GRABOWIK C., ĆWIKŁA G., JANIK W. THE REORGANIZATION OF THE INPUT STORE OF STEEL RAW MATERIALS IN THE MANUFACTURING SYSTEM - CASE STUDY	87
Moczała M., Hetmańczyk P. THE MINIATURE PHOTOVOLTAIC SYSTEM WITH SUN-TRACKING ALGORITHM	93
Monica Z., Gwiazda A. OPTIMIZATION OF A PRODUCTION SYSTEMS USING VIRTUAL MODELS OF WORKPLACES	99
NOWOSIELSKI R., KILJAN A., GUWER A., BABILAS R. CHARACTERIZATION OF SELECTED MG-BASED AMORPHOUS ALLOY	103
Pilarczyk W., Majchrzak M. THE IDENTIFICATION OF HAZARDS IN THE PROCESS OF PRODUCTION AND EXAMINATION OF BULK METALLIC GLASSES WITH FERROUS MATRIX	109
Placzek M. A CONCEPT OF THE MECHATRONIC SYSTEM DESIGNED FOR FREIGHT CARS MANAGEMENT	113
Sakiewicz P., Nowosielski R., Babilas R., Pilarczyk W., Cesarz-Andraczke K. WEEE CONTAINING NANOWASTE - RISK FOR ENVIRONMENT AND HEALTH & SAFETY	119
Zbiciak R. THE ORIGINAL SOFTWARE SUPPORTING DESIGN OF GEARS IN SIEMENS NX ENVIRONMENT	123
INDEX OF AUTHORS	129

SELECTED ENGINEERING PROBLEMS

NUMBER 5

INSTITUTE OF ENGINEERING PROCESSES AUTOMATION
AND INTEGRATED MANUFACTURING SYSTEMS

Maja BAIER¹, Dawid DUSIK²

Institute of Engineering Processes Automation and Integrated Manufacturing Systems,
Faculty of Mechanical Engineering, Silesian University of Technology, Gliwice,
Poland¹maja.baier@gmail.com, ²dawid.dusik@gmail.com

BELT VIBRATIONS MEASUREMENT AND RELATIVE EFFICIENCY OF THE POWERTRAIN STUDY ON THE ENGINE TEST STAND FOR *SILESIA GREENPOWER* VEHICLE

Abstract: The process of designing and building a professional test stand for measuring efficiency of the drive system in Silesian Greenpower vehicle was described in this paper. The fundamental aim of the study was to obtain an optimum belt tension at which the vehicle will be able to achieve the highest speed. The work depicts a description of the stand construction, research methodology, presentation of results, summary and conclusions. In particular, the article focuses on the measurement of belt vibrations and the study of the drive system efficiency on the constructed stand. One of the tasks was also to determine influence of proper belt tension on vehicle efficiency. The final effect of the research is a compilation of results for each belt tension and conclusions concerning practical correlations of studies with the trend in development of Silesian Greenpower vehicle design.

1. Introduction

The ground on which this research was conducted stems from the need of reducing resistance and maximising efficiency in Silesian Greenpower vehicles – the electric racing cars participating in annual events held on prestigious motor circuits in Great Britain. The rules of the races determine the same motor and batteries for each competitor, so engineers have to seek for other factors which will lead them to the victory.

One of the most crucial elements of the vehicle is the powertrain. In order to increase its efficiency toothed belt transmission was chosen. However, the system will not work properly unless the optimum belt tension is maintained. The article describes the professional engine test stand designed especially for the research and tests which were conducted on the stand, including belt vibrations measurement and tests of relative efficiency of the powertrain.

2. Engine test stand construction

The base of the stand (Fig. 1.) is a modular construction, which provides two types of measurement. The first is the test directly on the vehicle, which is not the subject of the paper, and the second is the use of a separate drive system mounted on the stand. The greatest advantage of this way of research is the possibility of redesigning the powertrain without the necessity of altering the vehicle construction.

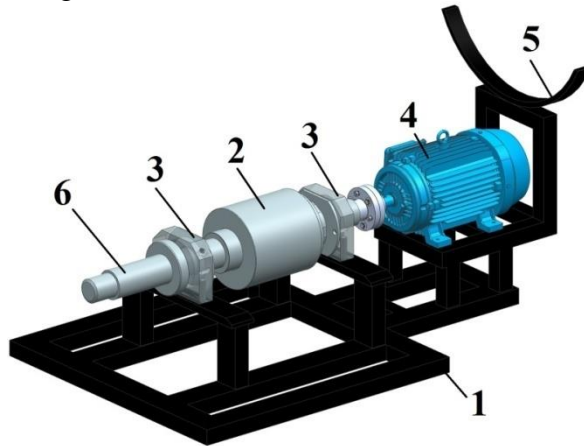


Fig. 1. CAD model of the base of the test stand

The base of the test stand consists of six main parts: 1- steel frame, 2- shaft with a track on which driven wheel drives, 3-self-aligning bearings fixing the shaft, 4- electric motor which can model braking forces of aerodynamics, 5- the support of the rear non-driven wheel, 6- place provided for the attachment of additional loads which simulate inertial deceleration by braking torque generated by the mass. During tests using the stand only, the force pushing the wheel to the shaft is maintained by 25 kilograms weight hung on a steel cable in rollers system. The whole stand construction was designed in CAD system – Siemens NX 8.5 and built by authors afterwards (Fig. 2.).

1– base of the test stand, 2– frame of the test stand,
3– equipment board, 4– linear bearings,
5– trapezoidal screw, 6– driven wheel

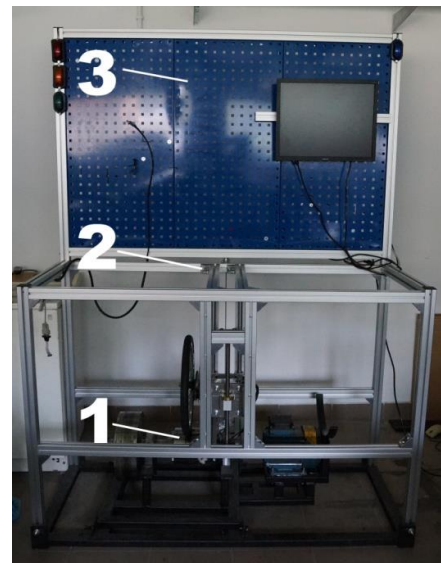


Fig. 2. The engine test stand

3. Belt vibrations measurement

The research conducted on the test stand was performed for six different tensions of the belt: named from A to F (tension A was too weak to transfer the rotation movement). The aim was to calculate frequency and assign maximum speed for each tension which then would lead to optimum solution. To measure acceleration of vibrations and then calculate frequency, the hammer was tapped on the belt near the place of attachment of the sensor with the same conditions for all tensions.

In order to determine the frequency of belt vibrations, acceleration-time graph (Fig. 4.) was plotted availing the measuring apparatus (Fig. 3.).

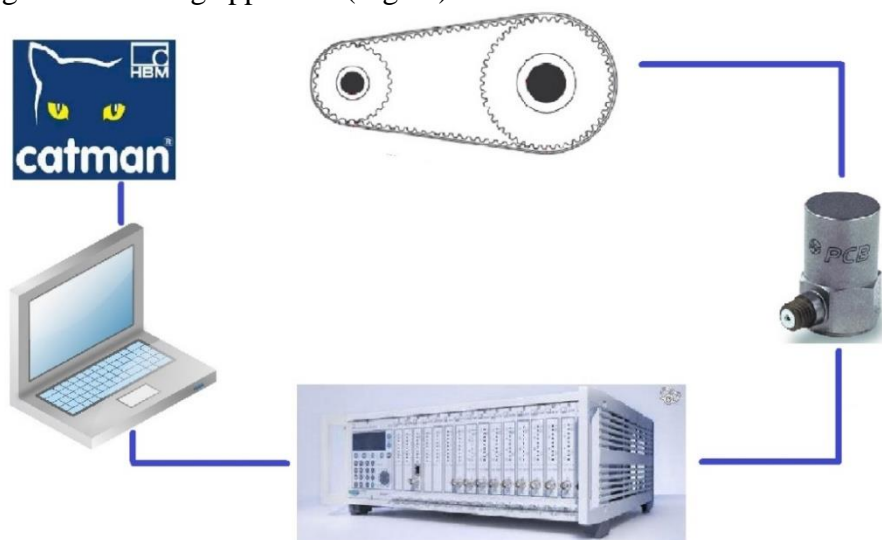


Fig. 3. Diagram of the measuring apparatus

The PCB Piezoelectronics sensor, called also piezoelectronic transducer, is attached to the belt with technical wax. The sensor avails piezoelectronic effect to convert the alterations in electrical voltage. The next element is the amplifier - MGCplus AB22AA HBM whose task is to enhance the signal from the sensor, its processing and enabling data archiving. The device has a modular design that allows measurement of many physical values by using proper expansion cards. For this study the AP 180 HBM card was used. The amplifier is connected via USB port to the computer with Catman Easy. The program has proper configuration parameters set and characteristics of a piezoelectronic sensor defined.

The results of the tests were presented as acceleration-time graphs. The first part of curve was neglected because of nearly the same amplitudes. The subject of analysis was the second part where intensive damping of vibrations occurred. To make all six graphs easily comparable, the scale of X axis was limited from 0 to 0,5 and Y axis form -100 to 100. The graphs differ significantly as for tension A period equals 0,03 s and for tension F – 0,007 s, which proofs that spectrum of tensions being tested was chosen properly.

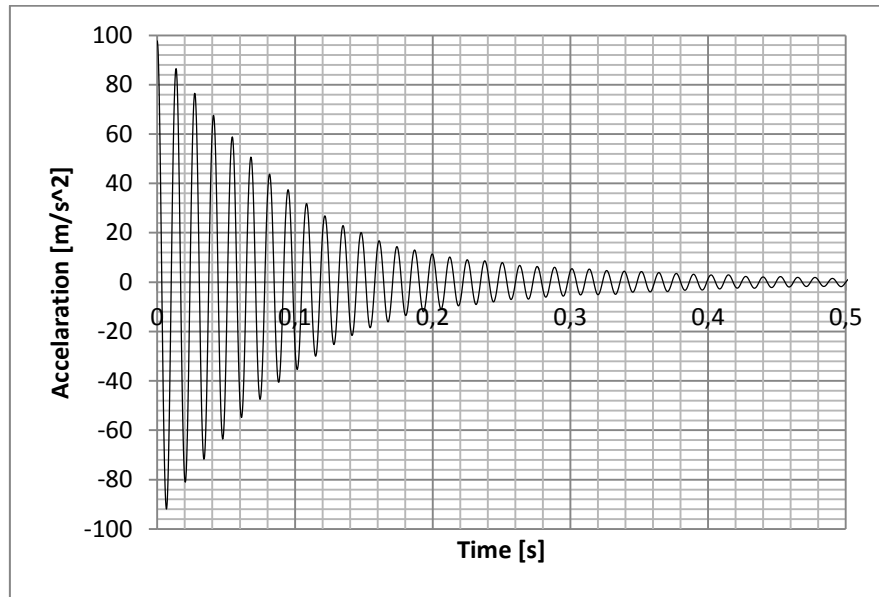


Fig. 4. Acceleration-time graph for tension C

The calculation of frequency values allowed the calculation of the force with which the belt is pulled. In this regard, equations on the belt span (1) and the force of tension (2), which are available in the controller of the mobile SKF belt tension meter [6], were used. Data used in this calculations are shown in (Tab.1).

$$S = \sqrt{CD^2 - \frac{(D-d)^2}{4}} \quad (1)$$

$$N = 4 \cdot m_p \cdot S^2 \cdot f^2 \quad (2)$$

S – belt span, CD – distance between toothed wheels' axles, D – bigger toothed wheel diameter, d - smaller toothed wheel diameter, N – force of tension, m_p – weight of belt per linear meter, f – frequency.

Tab. 1. Data used in calculation of the force of tension

Parameter	Symbol	Unit	Value
Smaller toothed wheel diameter	d	m	0,055
Bigger toothed wheel diameter	D	m	0,110
Distance between toothed wheels' axles	CD	m	0,190
Weight of belt per linear meter	m_p	kg/m	0,036

4. Relative efficiency of the powertrain

In order to create certain scheme of tests, the tension of the belt was set as usually and duty cycle of cars power was set to 100 per cent. This was followed by the tests of the more and

less tensioned belt. Thanks to the tests, the maximum speed with which the drive system mounted on a test bench can drive with a ratio of 2.25 was received. This also allowed the determination of time the car reaches the average speed, namely about 45 seconds.

After initial attempts to set a constant course, which will be accelerated with the car at each tension. Sample time was 60 seconds, the first 10 s was with 60% duty cycle, the next 30 seconds with 100%, another 10s - 60% and the last 10s without a drive. This course was designed to simulate the car turning, faster driving on the short straight and entering the next turn.

Research carried out on the test stand consisted of three tests for each tension, except for A which occurred to be too weak to transfer the rotation movement. The tension fixing was maintained by screwing the trapezoidal screw to which the motor was attached on two linear bearings (Fig. 2.) – the difference between two tensions (e. g. A and B) corresponds to one pitch of the screw.

The tests resulted in generating text files and graphs which can be easily pre-analysed thanks to an application created specially for Silesian Greenpower project by one of the members. Screenshot of application (Fig. 5.) shows graphs of speed, duty cycle, voltage, current (filtered and unfiltered). After comparing the graphs in the application, the data were exported to a spreadsheet in Microsoft Excel. Out of all the parameters, speed, duty cycle and current were selected and one graph was created. However, in order to improve the legibility of the function of the speed, it was approximated by a polynomial of the third degree. The speed values were averaged in order to find the representative value of all three tests for each tension. The maximum value of speed was read from the original tabular data. The numerical results are shown in Tab. 2.

Tab. 2. Comparison of results for different belt tensions

Parameter	Unit	Tension A	Tension B	Tension C	Tension D	Tension E	Tension F
Vibrations frequency	Hz	33,2	66,06	75	93	104,34	144
Belt tension force	N	5,5	22	33	41	52	105
Maximum speed	km/h	0	41,27	45,5	45	42,3	42

The results indicate the value of the transmission belt tension to be between 33 and 41 N to ensure optimal functioning of the drive system. In addition, these tensions were characterised by specific string sound which was absent in other tests. Overall analysis shows that managing the optimal belt tension is crucial to maintain the highest maximum speed of the car, otherwise, the value of maximum speed may decrease even by 10% (Tension B compared to Tension C). Neither too weak, nor too strong belt tension is acceptable.

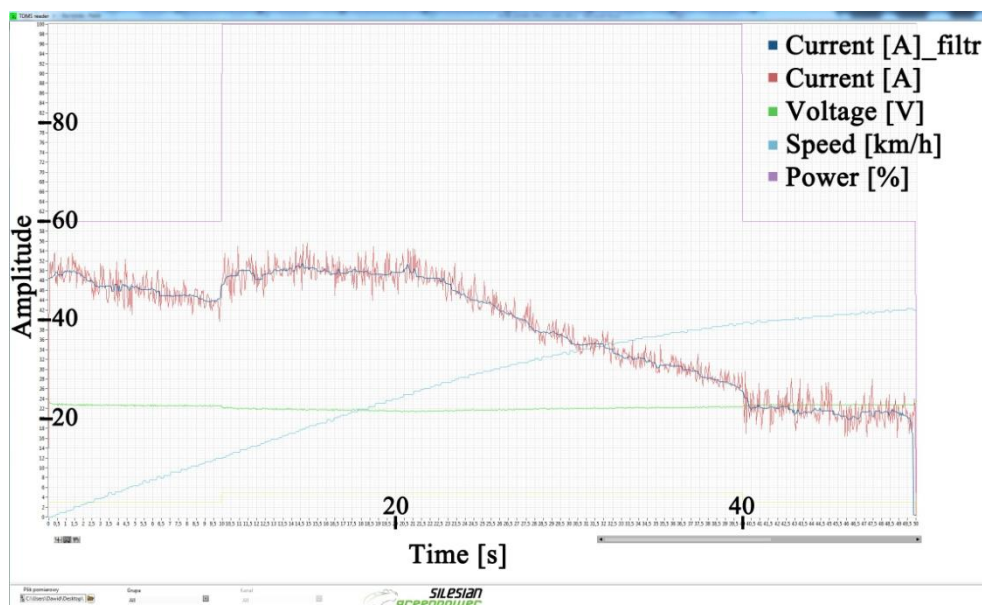


Fig. 5. The application used to read data from the stand

5. Conclusion

In this paper influence of belt tension on the relative efficiency of the powertrain was analysed. The study depicted a linear relation of belt tension on the efficiency of the powertrain. It was stated how to define the optimal belt tension and how to measure it in laboratory conditions. The final results have significant impact on further development of the Silesian Greenpower vehicle and its optimal performance on the motor circuits. The further research will cover measuring and maintaining optimal belt tension in real conditions during tests on the motor circuit and monitoring the variation of powertrain efficiency due to different belt tensions.

References

1. Jelaska D.: Gears and gear drives. Chichester: Wiley, 2012.
2. Kurmaz L.: Podstawy Konstrukcji Maszyn. Warszawa: Wydawnictwo Naukowe PWN, 1999.
3. Siłka W.: Teoria ruchu samochodu. Warszawa: Wydawnictwo Naukowo Techniczne, 2002.
4. Smith E.: Mechanizing laboratories: research and development with speed and efficiency. London : Iliffe Books, 1965.
5. Ubysz A.: Energochłonność samochodu a zużycie paliwa w złożonych warunkach ruchu. Gliwice: Wydawnictwo Politechniki Śląskiej, 2003.
6. The controller of the mobile SKF belt tension meter documentation http://uni-lager.pl/image/katalogi/Miernik_sily_napiecia_pasow.pdf (6.07.2014)

SELECTED ENGINEERING PROBLEMS

NUMBER 5

INSTITUTE OF ENGINEERING PROCESSES AUTOMATION
AND INTEGRATED MANUFACTURING SYSTEMS

Magdalena BĄCZKOWICZ^{1*}, Aleksander GWIAZDA¹

¹ Institute of Engineering Processes Automation and Integrated Manufacturing Systems,
Faculty of Mechanical Engineering, Silesian University of Technology,
Konarskiego 18a Street, 44-100 Gliwice, Poland
* magdalena.baczkowicz@polsl.pl

IMPROVEMENT OF THE PIECE PRODUCTION SYSTEM USING LEAN MANAGEMENT APPROACHES

Abstract: The paper presents a lean management approach to the production system organisation. The scope of the presented work includes problems considered with both production engineering and workflow management in the context of non-time added task. The main applied tools is the 5S method of work scene ordering and visual control of manufactured parts. The utilisation of proposed approach is described basing on the example of the production of industrial boilers in conditions of a piece production. The application of 5S method allows shortening by 3 day the production cycle. It was considered with the workplace ordering and decreasing the auxiliary times. While the introduction of a visual control let to improve the operation of failure detection and instructing employees. Typically this operation occupied 2 days and has been shorten of 25% and 1,5 day for directing employees work instructions . It is also recommended to introduce to the production practice the utilisation of formalized approach basing on written documents.

1. Introduction

The piece production is very specific, taking into account its management and logistic system. Each production system is elaborated one time for the ordered type of an industrial boiler which is individually design each time. In this paper is presented such type of production system. The chosen enterprise is a limited liability company, and its activity can lead to the Polish territory and abroad. The share capital of the company amounts to 100 000 PLN. Main business for the company is production for order oversized water and steam boilers and serial production of other parts used in energy industry which is done by production department. Mostly in serial production they manufacture different types of pressure parts, steam superheaters, water heaters, membrane walls, screens, reducing stations, collectors, slag traps, flanges, cyclones, separators and other custom products. The company also provides services related to the installation and modernization of boilers executed by assembly – repair department. The enterprise currently employs 128 people of which 67 production employees, 4 employees in “tool room”, 11 employees in construction and design department, 8 employees in quality control department, 3 employees in department of

supplies, 9 employees in service department and other administrative and management staff. The company has 2 production halls but nowadays is using just a new build hall where 121 production machine are located in. Old production hall is an unused space where the company is storing temporarily sheets of metal and pipes.

2. The 5S method in Lean Management

The article focuses on the Japanese point of view of 5S because the method was invented by them and is implemented and used with excellent effects. Japanese 5S method is an elementary factor that allowed developing the world production systems. This method is described in five Japanese words: *seiri*, *seiton*, *seiso*, *seiketsu* and *sitsuke*. The introduction of 5S method is concerned with the JiT systems. The objective of a JiT system is to reduce costs by reducing inventory taking into account the whole process of enterprises logistics. It also helps to minimize the production area, which increases the unit efficiency. For such a system it should be made the most possible simplification of individual processes. *The 5 S are the basis - or pillars - of a workplace, where we set the flow of production, visual inspection, standard operations and other JiT components* [1]. The 5S method in Hirano work is based on the five steps [2]: sorting, setting in order, shining, standardizing and sustaining. In the first step, the elements of the production system are sorted. For this purpose, special markers are used to indicate items for which it should be decide about their suitability. Currently, there are three markers: red (useless items), yellow (items possible needed), and green (needed items). In the first step red marked items are eliminated. The second step is to organize other elements of the system (yellow and green) what leads to its simplification. This step is also known as stabilization of the work system after a change. In the third step is realized the implementation of procedures for the permanent “cleaning” of the production system in order to keep it at a high level through sweeping its “contaminations”. Then is carried out the standardization of the most desirable changes induced by previous steps by developing appropriate standards of an organization. This allows to make the workplace more “transparent”. Finally, according to the last recommendation everyone should always keep the new state of a system.

3. Improvements of the analysed production system

After many visits and conducted interviews with employees in the company, the biggest weakness that have been observed was disorder in production hall and especially in “tool room” (place of storage of tools used mainly for the repair of production machines). Non value added time was established based on the analysis of the production process of the recovery boiler OS-5. The production hall does not have a sufficient quantity of suitable signs to help employees with their work. The company does not use any containers for the storage of scrap metal and other production waste, also tools and other items needed in manufacturing process are deposited at random racks or random places ate production hall. That is the main reason why it is difficult to find a desired element in a short period of time during manufacturing process. The “tool room” lacks of specialized tooling cabinets, lockers, shelving and tables designed to maintain order. Most of the tools are stored in unmarked boxes. Each workstation has a redundant tools that should be stored in the “tool room”. Employees need to be very careful because of moving gantry transporting boiler elements,

since production hall does not have a clear path for walking (fig.1). In the production hall there is only one theoretically safe zone marked with yellow paint, and often in the separated area there are various cables, cans, gas cylinders and other items.



Fig.1. View of the production hall - current status

Work instructions and all other information concerning manufacturing process, for example: amount of raw materials needed for production or how to make an item are transmitted orally. There is no documentation relating to the procedures of manufacturing of the parts. The place where the complete 5 S method will be introduced is a “tool room”, the production hall will be sorted and unnecessary tools and other parts will be transferred to the “tool room”. The introduction of 5S will be held in the following steps:

- *Sorting* – initially the tools and other necessary items must be extract. Damaged tools and components must be separated and removed, best way for the company is to sold them as metal scraps. The selection was done using red, yellow and green labels and after that selection protocol was created.
- *Setting in order* - list of all objects in the “tool room” was created to determine their permanent storage places. The inventory was hanged on the information board in the workspace. To help with the cleaning the company purchased needed cabinets and blackboard tool (fig. 2). Each tool was allocated to the appropriate place.



Fig. 2.Types of used cabinets and blackboard tool

- *Shining* – at the end of each working day employees are required to clean their workplace and leave all the objects arranged by inventory list according to the schedule.
- *Standardizing* – there are always two people working in “tool room” during each shift. Each employee needs to know what are his responsibilities and when to do them. To help employees, liability schedule was created, describing all the duties, person responsible for them and dates. The schedule was put on the information board in “tool room”.

- *Sustaining* - employees were trained on the importance of maintaining order in the workplace and monthly control of employees and their workspaces were introduced using appropriate filling control protocols of the current state.

The visual control method was implemented in the entire production hall. First marked floor of the production hall using top floor marking adhesive tapes type AT8, designed to function in the industry (yellow - transition - do not block, green – work stations, blue - storage areas for raw materials, red – test workstation “hydrostatic test”, black - space for production waste). Because the company does not use forklift trucks, established minimum paths between machines and other devices with a width of 1 meter for two-way traffic (accordance with the applicable standards). Finished goods are stored outside, therefore, there was no space in the hall marked for storage. Table of signs must be hung on information board in production hall, and the staff must be familiarize with the new order. Also introduced illuminated signs indicating the course of production process and each work stations provided with a special tablet that contains 4 buttons with colors corresponding to the certain states during production (green, blue, red, yellow). Information from the tablets are send to construction and design department, which provided with a light board with every workstation can solve the occurring problem. If the work proceeds without interference automatically green light (production is working fluently) is on, and if e.g. machine failure occurs than the red button is pushed informing about the problem allowing to quickly eliminate it. The blue light informs about lack of raw materials and yellow light tells that production of the item has been completed. Information signboards were placed on each machine. The signs help to informed about the risks relating to the use of the device, and contain basic technical specification. Also work instructions are delivered to each employee in the form of paper from the start of production of the new order. The sheet will contain basic guidelines for manufacturing the item for each workstations.

4. Conclusion

Analyzed manufacturing process of the recovery boiler OS–5 and based on conducted measurements and observation established duration of the production cycle which was min. 73,55 and max. 79,8 days depending on used mode of transport. Non value added time was 30,5 days including 3 days needed for searching tools, 2 days wasted on failure detection and 1,5 day for familiarizing employees with work instructions. Those are 3 wastes that can be easily eliminated using 5S and visual control methods. Introduction of selected methods does not exposes the company to significant cost and can be achieve relatively quickly. The company should establish a timetable for the implementation of changes to correctly and quickly implement new solutions.

References

1. Hirano H., 5 Pillars of the Visual Workplace: The Sourcebook for 5s Implementation, New York: Productivity Press, 1995.
2. Moulding E., 5S: A Visual Control System for the Workplace, Author House, Milton Keynes 2010
3. Nyaude A., The 5S Code For Workplace Organization: Implementing a Sustainable 5S Program, Create Space, New York 2014

SELECTED ENGINEERING PROBLEMS
NUMBER 5
INSTITUTE OF ENGINEERING PROCESSES AUTOMATION
AND INTEGRATED MANUFACTURING SYSTEMS

Eszter BOGNÁR^{1,2*}, Péter OZSVÁTH³, Anna KERTÉSZ¹, Liza PELYHE^{1*}, László DÉVÉNYI¹

¹ Department of Materials Science and Engineering, Faculty of Mechanical Engineering, Budapest University of Technology and Economics, Budapest, Hungary

² MTA–BME Research Group for Composite Science and Technology, Muegyetem rkp. 3., H-1111 Budapest, Hungary

³ Department of Vehicle Manufacturing and Repairing, Faculty of Transportation Engineering and Vehicle Engineering, Budapest University of Technology and Economics, Budapest, Hungary

* eszter@eik.bme.hu, liza@eik.bme.hu

ANALYSIS AND DEVELOPMENT OF THE ADHESION OF STENT COATINGS

Abstract: The influence of the surface roughness on adhesion strength of polyurethane coating on stainless steel alloy (316LVM) is introduced. These coatings are one of the development directions in coronary stent production. One of the widely spread stent base material is the 316LVM, so in the presented study these materials were involved. The samples were prepared by etching and electro-polishing. The current density and polishing time were changed to create samples with different surface roughness. After electro-polishing polyurethane (Chronoflex[®]) coating was applied. The adhesion of the coating on different surfaces was tested by scratch test (nano indenter technique). The increasing surface roughness gives stronger adhesion. According to our experiments it was concluded that the coronary stents, treated by etching without polishing could cut out the balloons during expansion, therefore the surface roughness should be under this value. It is recommended to use an electro-chemical treatment that is resulting Ra=1.5-2.0 μm roughness.

1. Introduction

The significance of biomedical engineering is continuously increasing all over the world [1]. There has been a great leap forward in the field of surface treatments for metallic coronary stents to improve their biocompatibility. Stent coating is an important factor for stent design, influencing both angiographic and clinical outcomes [2,3]. The coating can protect the metallic surface of the stent from corrosion attack caused by the biological environment [4] though coatings in general have potential disadvantages relating to cracks and discontinuities, fluid seepage, and delamination [5].

However, usage of bare metal stents is widespread, in order to reduce non-desirable complications, new coatings have been developed. The hope of overcoming the natural

roughness of bare metal was one of the first reasons to coat bare metal stents with polymers [6,7].

Non-biodegradable polymer coatings can serve as a shield against corrosion and also as a platform for improving the biocompatibility of the device [6,8,9] adhesion of such films to their substrates has been the subject of several studies [10]. E. Gallino et al. developed a process to coat the stainless steel surface from the biological environment by depositing an ultra-thin uniform, cohesive and adhesive plasma polymerized allylamine coating [4]. F. Lewis et al investigated the adhesion properties of fluorocarbon films of three different thicknesses deposited by plasma polymerization. Among the coatings with different thicknesses studied, only those with a thickness of 36 nm exhibited the required cohesion and interfacial adhesion to resist the stent expansion without cracking or delaminating. Otherwise, cracks were detected in the coatings having thicknesses equal or superior to 100 nm, indicating a lack of cohesion [11]. Polymeric coatings should be resistant during implantation and expansion of the stent [12]. The CSM Scratch Testers are ideal instruments for characterizing the surface mechanical properties of thin films and coatings [13]. S. J. Bull et al investigated scratch adhesion behaviour of relatively thick hard coatings on soft substrates thin hard coatings on hard substrates. The residual stress in the coating has been carefully determined and the quantification is expected to be more accurate [14]. D. Vodnick et al. used a new energy-based method has been proposed to quantitatively assess the interfacial adhesion of soft films on compliant substrates with complex geometries. The method utilizes a scratching technique to determine energy required to delaminate a unit of area of coating while taking into account energy lost to substrate deformation [15].

Widely spread technique is the scratch test to characterize the adhesive strength of the coating-substrate system. During the scratch test, the sample is displaced at constant speed and at a certain load, damage occurs along the scratch path. This load value is the critical load [16]. The critical load depends on coating adhesion, but also on several other parameters; some are directly related to the test itself whereas others are related to the coating-substrate combination [17,18].

In our study we submit the impact of the surface roughness on adhesion strength of polyurethane coating on 316LVM substrate exemplified with results of a complex materials analysis process.

2. Materials and methods

Samples: Stainless steel alloy (316LVM) tube slices were used as samples, which were produced by laser cutting in longitudinal direction at every 120 degree of a tube, which original measures were 1800 μm diameter and 120 μm wall thickness. Two small holes were placed at the ends of the tube slices to fix the samples without damage. The lengths of the specimens were 11 mm. This type of tube is already used in stent production.

Sample preparation: The laser cut process of the samples is followed by the surface preparation, which is extremely important for the coating's adhesion and the removing of the laser-cutting burr. The first step of the surface preparation is the etching. Etching was done by using etchant and ultrasonic agitation. The etchant was mixed from equal portion of HCl 35% w/w (hydrogen chloride) and HNO_3 65% w/w (nitric acid) which was diluted in 1:3 proportions (50 ml etchant mixed with 150 ml distilled water). Each etching process lasted for

5 minutes because this way the elimination of the oxide layer and burr, created by the laser cutting, was ensured.

Electro-polishing (EP) was applied on the etched and dried samples. The composition of the electrolyte was $\text{H}_2\text{O} + \text{H}_3\text{PO}_4$ 88% w/w (phosphorus acid) + H_2SO_4 96% w/w (sulphuric acid) with the same rate. To reach different surface roughness the polishing parameters were changed.

The surface area of the tube slices was 73.68 mm^2 . The base material particles issued by laser cutting process, have exfoliated by the etching. Then the following electro-polishing have resulted a smooth surface.

The coating: By using the dipping technology a passive, i.e. even surface polyurethane coating was created. The etched and electro-polished tube slices were coated in three layers by a 2% solution of Chronoflex[®] polyurethane. The coatings were prepared from a not mixed and evenly dried solution on room temperature.

Measuring of the surface roughness: Evenness and smoothness of surface of the tube slices was influenced by the electro-polishing parameters in order to examine the relation between the surface roughness and the adhesion (0.01 A/mm^2 and 30 s, 60 s, 90 s, 120 s, 150 s). The current density of the electro-polishing was chosen to be 0.01 A/mm^2 because the further augmentation of the electricity in the case of such sample had caused a rough surface and the foaming of the electrolyte. The decrease of the current significantly increased the necessary time for polishing because the elimination of the greater roughness summits has higher time consumption. In the course of electro-polishing one of the tube slice holes was used to grip and we hang the samples into the electrolyte to polish. Then the surface roughness of the samples was examined with Zeiss LSM 510 META confocal microscope, so thus an objective and numerical result was received regarding to the average roughness. Before applying the coating, the effect of the different electro-polishing parameters on the surface roughness was examined on the surface treated samples. The samples were examined with equal settings at the same location, i.e. in the middle of the sample. Both the external and the internal surfaces of the samples were examined which is important because the stent is fabricated from the same type of tube, so it must be determined the two surfaces.

The measuring of the adhesion of the coatings: The adhesion of the coating on different surfaces was tested by scratch test (nano indenter technique), because this method is appropriate for such a small devices, as stents. A CSM Micro Combi Tester (MCT) was used to examine the coating's adhesion. In the process the MCT pulls a diamond Rockwell indenter along a straight line with a controlled normal force (FN) on the sample's surface. During this, the frictional force, the acoustic emission and the needle's penetration depth are registered. The evaluation is based once on the optical microscopy analysis of the scratches and secondly on the order of the coating's typical scaling methods to the normal force value on a given section.

The indenter's loading was increased from 0.04 N to 1.5 N according to the linear program of 2.09 N/min loading rate, the indenter's moving speed was 10 mm/min as well as it was set at the pre-experiments. The length of the scratches varied between 2.5 mm and 7 mm.

Examination of coating topography: The topography of the coated samples was examined by atomic force microscopy (AFM). AFM was used in contact mode to analyse the samples.

3. Results

The examination results show that the increasing electro-polishing time decreases the surface roughness until a certain limit in both inner and external surfaces. Figure 1a shows the results of the electro-polishing. One can see in Figure 1a reaching 150 s the sample's surface becomes smooth and the surface roughness does not decrease further; thus the external surface was considered significant because this territory attaches with the vascular wall and gets the highest level of stress as well. The parameters that are belonging to lowest surface roughness are 0.01 A/mm² and 90-150 s. These parameters give 1.2 μm average surface roughness. However to achieve a better adhesion of the coating a rougher surface was needed than the lowest roughness.

The surface topology was evaluated according to pictures created by a confocal microscope once in normal mode and then in inverse mode. The comparison of them shows clearly that quite a lot of pits exist on the surfaces that cannot be removed even with electro-polishing. This means that the coating is going to be thicker at these which phenomenon is not disadvantageous; moreover, it can correct the surface's adhesion with filling the hole by shape closing (anchoring effect).

Earlier experiences show that the etching in itself is not suitable as a stent surface treatment process, because the high surface roughness can cause damage of the balloon. The coating has a smoothing effect because the coating layer which is adhered to the sharp edges makes them rounded. Chronoflex[®] polyurethane coating was applied in 3 layers made from a 2% solution on the surface of the etched and electro-polished tube slices. Untreated samples were also involved, but the coating did not fully cover its surface due to the sample's high surface roughness, so it was excluded from further examinations. The 90-150 s electro-polishing times result closely the same surface roughness therefore 30 s, 60 s and the 90 s electro-polished samples were examined by scratch test.

The scratching techniques were defined (the loading program and the indenter radius) which can examine the sensitive layers in the MCT machine's mN measuring domain. At pre-experiments indenters with a 10 μm or 50 μm radius were used, but in these cases the coatings immediately peeled off and the needle started to scratch the 316 LVM raw material too. Finally, a diamond indenter with 200 μm tip radius was used for the measurements.

During the scratch tests, the average normal force was measured what can cause the laceration of the coating. The indenter forced to penetrate into the coating by this force (FN) which is normal to the plane of the coating.

The coating of 30 s electro-polished tube slice (by 0.01 A/mm²) started to lacerate at FN=0.36 N average normal force, but according to Figure 1b the increasing electro-polishing time (which means smaller surface roughness) cause decreasing normal force. We can conclude that decrease of the surface roughness come with the decreasing of the coating adhesion. One can see in Figure 1b the normal force which is belongs to the 90 s electro-polished samples is FN=0.2 N.

One can see in Figure 2a the 60 s electro-polished (the average surface roughness is 1.48 μm) and coated surface of a tube slice. This picture has been captured when the normal force has reached the critical value what is necessary to lacerate the coating. Figure 2a shows the indenter remove the coating but do not harm the surface of the substrate. So the measured value is not affected by the substrate, it is represent only the adhesion of the coating.

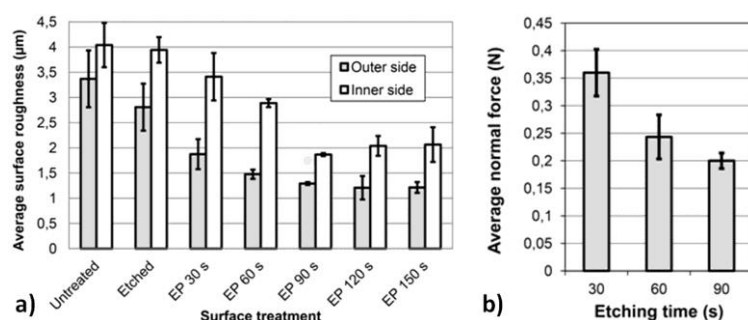


Fig. 1 a) The average outer and inner roughness of the differently electro-polished samples
 b) Normal force where the coating is peeled off during the scratch test (200 µm radius; 2,09 N/min loading rate)

The etchant attacks primarily the significantly prominent roughness peaks and grain boundaries, so we do not recommend using the simply etched surfaces because it can damage the balloon. The atomic force microscopic image (Figure 2b) shows clearly, that the surface roughness of the etched samples cannot significantly decreased by the coating especially in the case of high surface level differences. Figure 2b shows a simply etched sample which is coated in 1% polyurethane solution with 3 layers. The grain boundaries are still recognizable over the coating in the form of through of wave.

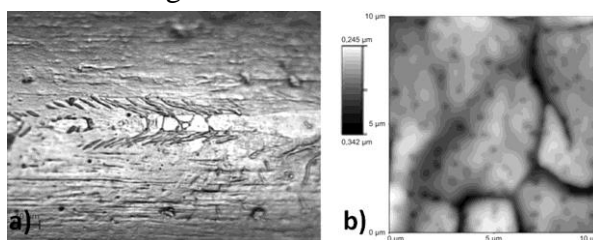


Fig. 2 a) The damaged coating after scratch test (FN=0.25 N)
 (Scratch direction: left to right; indenter radius: 200 µm; EP parameters: 0.01 A/mm² and 60 s)
 b) AFM contact mode image of coated (1% PUR solution 3 times) sample

The surface roughness resulted by etching is too high, that is why it is not admissible. Further electro-polishing is necessary to remove the highest surface peaks.

4. Conclusion

At diagnosing the maximum roughness, it is necessary to take into consideration the requirements of the stent-production technology as well. According to our experiments, those stents that have been treated simply by etched might cut out the balloons during expansion. The coating itself cannot palliate significantly the sharp edges. Besides this, the electro-polishing through the evolved oxide layer makes the surface more resistance against corrosion, thus the surface becomes passive.

In virtue of this, considering both the Chronoflex[®] coating's adhesion characteristics and the potential maximum useable with material detaching requirements of the stent production technology, in order to reach the strongest adhesion of the stent coatings, it is expedient to use an electrochemical treatment of an Ra=1,5-2,0 µm rated roughness on the external surface. To reach the suggested surface roughness in case of 316LVM substrate is necessary 5 minutes chemical etching and electro-polishing (0.01 A/mm²; 30 s).

References

1. Tayapiwatna C.: Multidisciplinary research and development: The biomedical engineering approach. "Maejo International Journal of Science and Technology" 2007, Vol. 01, pp. 98 – 99.
2. Hara H., et al.: Role of stent design and coatings on restenosis and thrombosis. "Advanced Drug Delivery Reviews" 2006, Vol. 58, pp. 377 – 386.
3. Martin D.M., Boyle F.J.: Drug-eluting stents for coronary artery disease: A review. "Medical Engineering & Physics" 2011, Vol. 33, pp. 148 – 163.
4. Gallino E., et al.: Plasma polymerized allylamine films deposited on 316L stainless steel for cardiovascular stent coatings. "Surface and Coatings Technology" 2010, Vol. 205, pp. 2461 – 2468.
5. Palmaz J.C., et al.: Influence of stent design and material composition on procedure outcome. "Journal of Vascular Surgery" 2002, Vol. 36, pp. 1031 – 1039.
6. Bakhshi R., et al.: Polymeric coating of surface modified nitinol stent with POSS-nanocomposite polymer. "Colloid Surfaces B" 2011, Vol. 86, pp. 93 – 105.
7. Unger F., et al.: Poly(ethylene carbonate): A thermoelastic and biodegradable biomaterial for drug eluting stent coatings?. "Journal of Controlled Release" 2007, Vol. 117, pp. 312 – 321.
8. Crowder S.W., et al.: Modular polymer design to regulate phenotype and oxidative response of human coronary artery cells for potential stent coating applications. "Acta Biomaterialia" 2012, Vol. 8, pp. 559 – 569.
9. Mani G., et al.: Coronary stents: A materials perspective. "Biomaterials" 2007, Vol. 28, pp. 1689 – 1710.
10. Shan W.L., et al.: Adhesion and cohesion in structures containing suspended microscopic polymeric films. "Acta Biomaterialia" 2012, Vol. 8, pp. 1469 – 1480.
11. Lewis F., et al.: Study of the adhesion of thin plasma fluorocarbon coatings resisting plastic deformation for stent applications. "Journal of Applied Physics" 2008, Vol. 41, pp. 045310 – 045400.
12. Bian H., et al.: In vitro study of poly(ethylene carbonate) as a drug-eluting stent coating. "Progress in Natural Science: Materials International" 2012, Vol. 22, pp. 295 – 302.
13. CSM Instruments: Advanced Mechanical Surface Testing. In: CSM Instruments application note, Peseux, Switzerland, 2006.
14. Bull S.J., Berasetegui E.G.: An overview of the potential of quantitative coating adhesion measurement by scratch testing. "Tribology International" 2006, Vol. 39, pp. 99 – 114.
15. Vodnick D., Nay R.: Interfacial Adhesion of Viscoelastic Coatings on Medical Stents. Hysitron application note, Hysitron, Eden Prairie, MN, USA, 2011.
16. Barnes D., Johnson S., Snell R., Best S.: Using scratch testing to measure the adhesion strength of calcium phosphate coatings applied to poly(carbonate-urethane) substrates. "Biomedical Materials" 2012, Vol. 6, pp. 128 – 138.
17. Ichimura H., Ishii Y.: Effects of indenter radius on the critical load in scratch testing. "Surface and Coatings Technology" 2003, Vol. 165, pp. 1 – 7.
18. Randall N.X. et al.: The effect of intrinsic parameters on the critical load as measured with the scratch test method. "Surface and Coatings Technology" 2001, Vol. 137, pp. 146 – 151

SELECTED ENGINEERING PROBLEMS

NUMBER 5

INSTITUTE OF ENGINEERING PROCESSES AUTOMATION
AND INTEGRATED MANUFACTURING SYSTEMS

Grzegorz ĆWIKŁA^{1*}, Cezary GRABOWIK^{1*}, Krzysztof KALINOWSKI^{1*}, Witold JANIK^{1*}

¹Institute of Engineering Processes Automation and Integrated Manufacturing Systems,
Faculty of Mechanical Engineering, Silesian University of Technology, Gliwice

* {grzegorz.cwikla, cezary.grabowik, krzysztof.kalinowski, witold.janik}@polsl.pl,

APPLICATION OF LEAN AND SIX SIGMA METHODOLOGY IN IMPROVING OF PRODUCTION PROCESSES

Abstract: This paper describes example of LEAN and SIX SIGMA methodology application in order to improve production processes. The aim of the study was to improve the production processes of wire sheaves for electrical installations of cars and agricultural machinery. The main problem was the high production costs and long lead times of technological process in case of the prototypes and sheaves produced in small series. Significant number of manufacturing defects has also been a problem. The analysis carried out in accordance with the methodology DMAIC and SIX SIGMA allowed identification of the main problems and development of solutions. As a result of the work proper solutions has been developed and implemented to streamline the production processes, as well as improve the quality and efficiency of the production system in the studied area.

1. Introduction

Companies operating in today's globalized market are forced to constantly seek for methods of optimization of their activity, leading to a reduction of production costs and increase of the efficiency of equipment. The continuous improvement of production quality in order to meet the demands of customers and to ensure the smooth operation of production lines leading to the timely execution of customer's orders is also important [1].

There are many methods allowing companies to get closer to that goal. Most often mentioned are such methodologies as lean manufacturing, Kaizen, Value Stream Mapping, TQM and SIX SIGMA, mostly focusing on continuous improvement of company's processes and improving the quality of production [2]. Especially SIX SIGMA methodology is often used in the automotive industry. Car manufacturers using this methodology expect the highest quality of components and, consequently, so in consequence SIX SIGMA should be used also by suppliers of components for assembly [4].

This paper presents an attempt to apply the SIX SIGMA methodology to streamline production processes in a plant producing the wire sheaves for the electrical system of cars, construction and agricultural machinery.

2. Description of the problem

The production facility which is the subject of analysis produces a variety of the wire sheaves to the electrical system in vehicles [3]. Most of these are sheaves produced in long series in large quantities. Production processes of that type of sheaves are optimized and profitable. In this part of the production high quality and low number of defects are obtained, which means that the manufacturing processes are properly organized.

The second part of this manufacturer offer are sheaves produced in small series (usually sold in the aftermarket, for car mechanics workshops) or single prototype sheaves. In this part of offer plant does not reach the expected financial results, production lead times are long, there is also a significant number of defects (waste). The aim of the analysis was therefore to identify the sources of problems and to implement the solutions allowing to eliminate or reduce it [3].

Production processes

The main production processes are cutting wires and insulating sleeves into pieces of required length, connecting it accordingly to the assembly scheme, and then installation of sockets and plugs. Final production operations are assembly of additional layers of insulation and waterproofing [3].

The production process of the prototype wire sheaves consists of the following steps:

- Preparation of project documentation (including list of components and wiring diagram)
- Cutting of wires into pieces of required length
- Cutting of insulating sleeves into pieces of required length
- Arrangement of wires in insulating sleeves according to the scheme
- Assembly of connectors
- Assembly of sockets and plugs
- Assembly of additional insulation layers
- Quality control

A typical order for the prototype sheaves normally includes two pieces of sheaves, a typical small series consists of 5 - 30 pieces, and sheaves for aftermarket are produced in a series of 2 to 10 sheaves. Performance of the analysed prototypes department is about 10% comparing to the series production department.

3. Application of SIX SIGMA in analysis of problems of low quality and performance in the electrical wire sheaves manufacturing processes

In order to solve the problems it was decided to apply the DMAIC model (Define - Measure - Analyse - Improve - Control) used in the SIX SIGMA method [4].

Define

In the problem definition phase SIPOC diagram (Supplier, Input, Process, Output, Customer) has been developed for the analyzed process. The next step in defining the problem is to create a process map based on SIPOC diagram. Process map should show where the potential bottlenecks, faults in the process, and the actions that do not create added value are

located. Then Ishikawa cause and effect diagram (Fig. 1) has been developed, which allows to locate the most important reason of the problems.

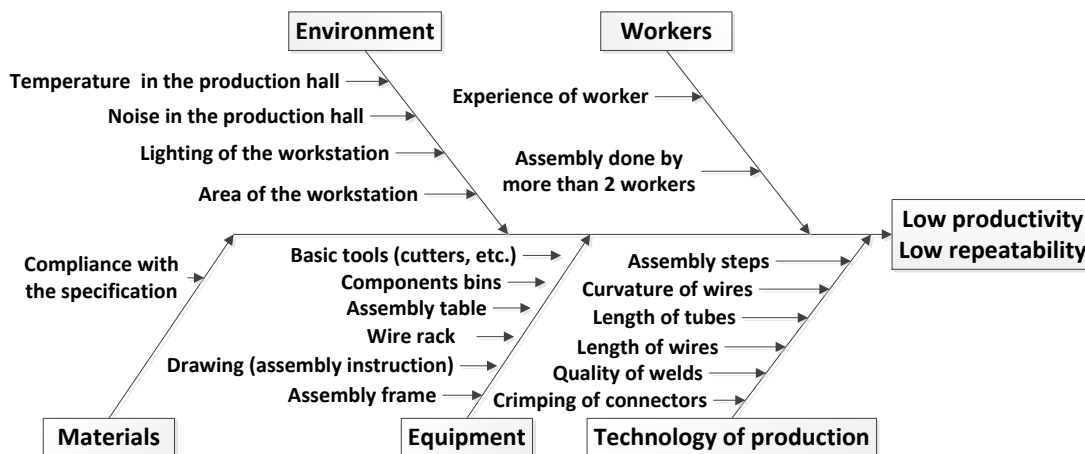


Fig. 1. Ishikawa diagram - simplified

Measure

Measurement of the characteristics of the analysed production processes were carried out on the basis of technological documentation and measurement of the real order execution time. Statistical analysis on the quality of the produced wire sheaves has been also carried-out. For example, the length of the wire ends and compliance with the scheme has been subject of the control. The results of measurements has been processed in the STATISTICA.

Results of statistical analysis of length of exemplar wire are presented on Fig. 2.

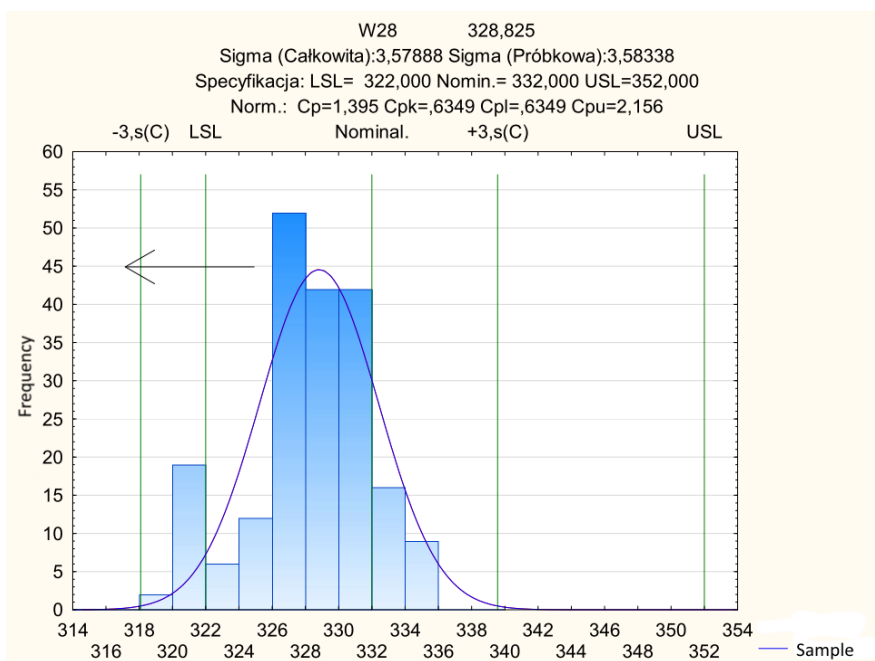


Fig. 2. Results of SIX SIGMA statistical analysis of W28 wire lengthmeasures

Analyse

Analysis of the problem of low (10%) performance was difficult, because not all data were available in the form compatible with the STATISTICA. During the analysis the documentation in the form of photos of the current equipment has been collected.

Current production station for prototype sheaves (Fig. 3) is a universal assembly table, which base is composed of Bosh profile plates. The assembly table currently is not equipped with any brackets (cable holders) for the wire sheaf, which could ensure repeatability of the final product and made assembly easier. Admittedly, table design allows for mounting brackets, but their installation requires the use of additional tools and is long lasting.

Contrary, assembly tables used in mass production (Fig. 4) are equipped with brackets for the wires and hangers for components, located directly within reach of the employee.

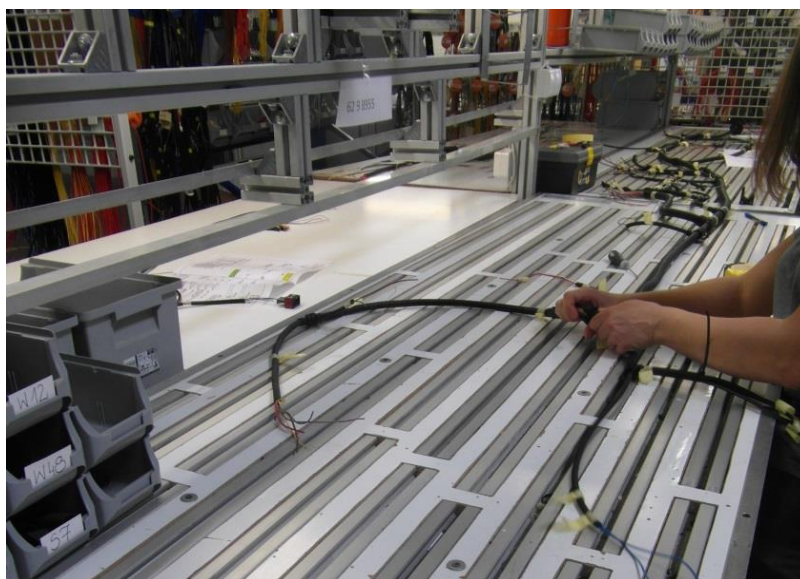


Fig. 3. Assembly table for prototype wire sheaves



Fig. 4. Assembly table for middle-series and mass production of wire sheaves

Comparison of the time of assembly of sheaves obtained using a universal table for prototyping and special table used in the series production indicates that the special equipment significantly reduces assembly time. The use of special equipment, however, is not possible in the production of prototypes and small series due to the high cost of such a solution – mass production assembly table is customized for production of given type of sheaves.

Improve

On the basis of results of the analysis it was decided to implement the following improvements in the production processes:

- The new organizational unit in the Production Preparation Department has been created, which is responsible for the preparation of 1:1 scale CAD assembly drawings before starting production.
- The new universal assembly table has been designed. The table has a layered construction (plywood, polystyrene, perforated steel sheet). The 1:1 CAD drawing can be placed on the surface of the table. It is possible to set easy to use magnetic wire holders for cables or nails, placed in locations marked on the drawing (Fig. 5).

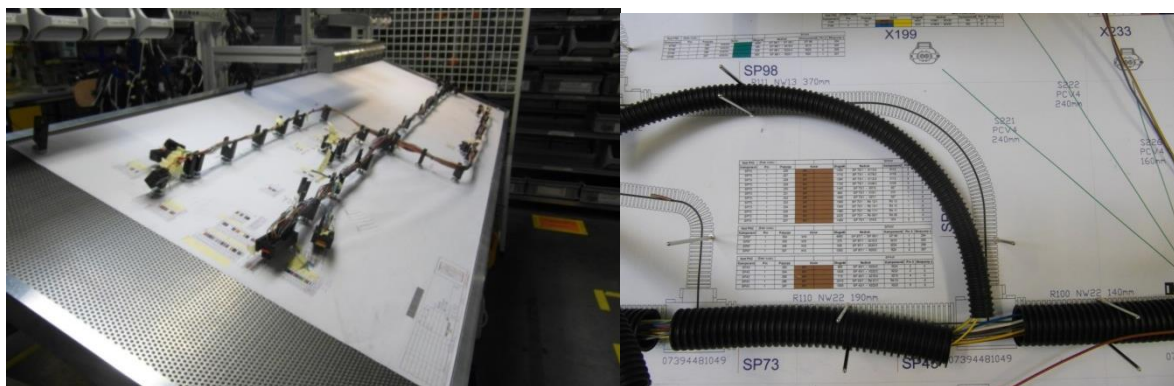


Fig. 5. New universal assembly table with CAD drawing and magnetic cable holders

Control

Control stage consisted of analysing the quality and productivity of the modified production station, measurement of the length of the wires and the control of the performance after the improvements. Statistical analysis (Fig. 6) showed improvement of the quality, the productivity rose from an initial 10% to 30%, which is a good result obtained at a low cost.

4. Conclusion

The case study shows the validity of the application of the SIX SIGMA methodology in order to improve quality and organisation of the production processes. Application of the methodology has allowed to identify the factors responsible for the low productivity and quality of produced prototype wire sheaves, analyse the problem and develop solutions to improve the production processes. Developed solutions have been implemented and tested in practice. As the result satisfactory improvement in the efficiency and quality of the manufactured prototype wire sheaves have been achieved.

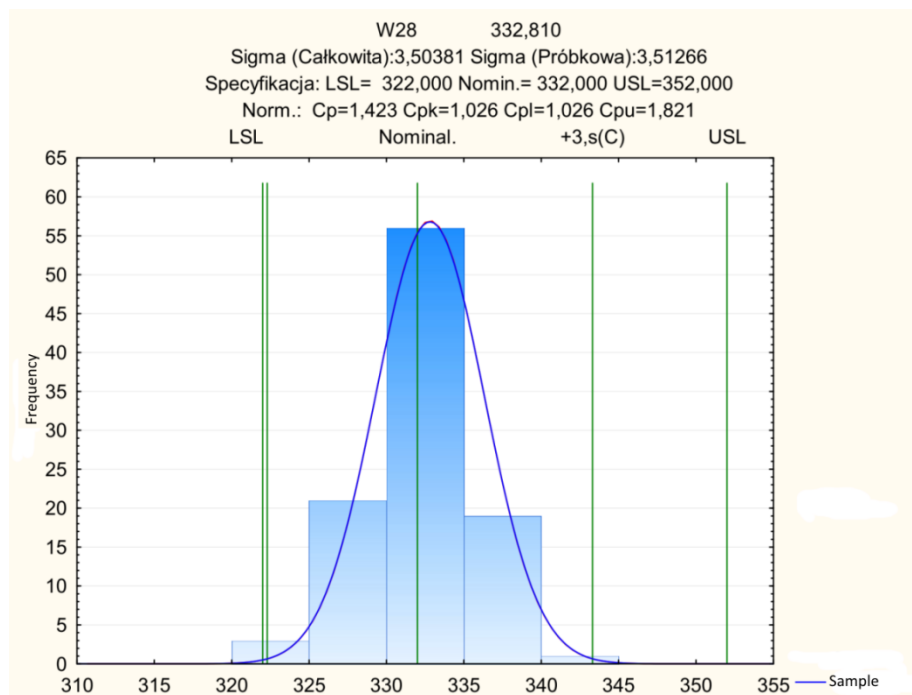


Fig. 6. Results of statistical analysis of W28 wire length measured after changes

References

1. Chunho Kim, Baldwin, D.F.: Design guidelines to implement Six Sigma in assembly process yield of area array solder interconnect packages. Electronic Components and Technology Conference, 2002, Proceedings. 52nd, pp. 1560-1568.
2. Law, R.C., Li Zhang, Beh, H.Y., Kmetec, J., Wall, F., Chan, C.E., Koay, H.K.: Six sigma methodology in improving assembly yield of high-power and high-brightness light-emitting diodes packages for automotive Applications. Electronic Manufacturing Technology Symposium, 2008, 33rd IEEE/CPMT International, pp. 1-7.
3. Pater K.: Doskonalenie procesów produkcyjnych na przykładzie zakładu produkującego wiązki do samochodowej instalacji elektrycznej [in Polish:] Improvement of production processes on the example of a plant producing a sheaves for the car electrical system. Praca dyplomowa magisterska (Master Thesis). Politechnika Śląska, Wydział Mechaniczny Technologiczny, Gliwice 2014.
4. Zymonik Z., Hamrol A., Grudowski P.: Zarządzanie jakością i bezpieczeństwem [in Polish:] Quality and work safety management. PWE, Warszawa, 2013.

SELECTED ENGINEERING PROBLEMS

NUMBER 5

INSTITUTE OF ENGINEERING PROCESSES AUTOMATION
AND INTEGRATED MANUFACTURING SYSTEMS

Krzysztof FOIT

Institute of Engineering Processes Automation and Integrated Manufacturing Systems
krzysztof.foit@polsl.pl

SVG GRAPHICS LANGUAGE AS A DESCRIPTION OF A 2D PATH IN ROBOT PROGRAMMING TASKS

Abstract: In this paper, the issue of programming of the complex path of robot effector will be discussed. It should be noted that the most of accurate tracks with complex shape are implemented for operations like milling, deburring, applying seals, adhesives, etc. These tasks are usually performed on the plane. Programming of these operations usually requires a lot of effort – operator should indicate successive points that are necessary to define the path of movement. Using dedicated software, greatly simplifies this task, but its purchase is often associated with considerable costs and attachment to a particular platform. The solution, proposed in this paper, uses the SVG graphics to define the effector's path. It is based on open standards that simplify implementation of the method on a variety of hardware platforms. SVG files are also easy to process, because of its textual form that refers to the XML.

1. Introduction

In addition to the transport and manipulative tasks, industrial robots are often used in the technological process to carry out such tasks as welding, deburring, applying adhesives and sealants, etc. [1,2]. A common feature that connects these operations is a large degree of complexity of the tool path and the fact that the individual operations are often carried out in the same plane.

Due to the considerable complexity of the path, the robot is often programmed using CP (Continuous Path) trajectory planning, or – in the case of less complex path – PTP (Point-To-Point) trajectory planning. Both methods require a fairly significant effort, amount of time and – in the case of planning CP – direct interaction with the robot.

Some attempts are being made to simplify the procedure of programming of complex paths. This is particularly noticeable in the case of welding robots, due to the frequency of use. The literature [3-7] contains descriptions of special graphic interfaces or programming languages intended for rapid prototyping of a robot program. The manipulators are also equipped with special vision systems, which allow the real-time adjustment of program parameters, according to the environmental conditions. These solutions are often dedicated to a particular type of robot and the use of vision systems significantly increases the overall cost of implementation.

One of the ways to reduce the cost of deploying new software is to use the applications under a free license, or open standards. Large companies – where robotized production lines are a kind of standard – decide not to use such software or open standards, in fear of improper level of assistance. It seems to be the most important reason for using closed solutions, supplied by machine manufacturers. However there is a middle ground: the use of open standards that are supported by major software vendors. Such standards include, inter alia, the XML markup language and SVG graphics standard that is the derivative of the XML.

The SVG was earlier used in the field of robotics as a part of the control interfaces [4-6], but is rarely used as a key part of the programming system [7-8].

This paper presents the concept of using SVG graphic to describe the path of tool mounted on the robot wrist.

2. The SVG standard

The SVG acronym stands for “Scalable Vector Graphics”. Although the name suggests a graphic standard, SVG is a programming language that operates on the graphics elements of the drawing. In addition to the typical description of attributes, it also allows to make the transformations (including translation, rotation and scale) or even animations, which in turn allows creating complex patterns that are based on the definitions of simple figures. Another quite important feature of the SVG standard is that the file, which stores image information, has the text form and drawing can be edited using an ordinary, plain text editor.

The SVG standard uses vector representation of a drawing. It means that every geometric entity is treated as the object, not as a set of pixels. This makes the objects easy to manage, however can cause some problems during the transformation of drawing into a bitmap.

The development of the SVG standard started in 1998, in order to unify web vector graphics standard. In that time, several competing formats have been developed and all of them were revised by W3C group (World Wide Web Consortium), which is an international community that develops standards used in the World Wide Web. The SVG is based on the XML language (Extensible Markup Language), so it inherits its text format and all other dependencies [9]. This property is a very important advantage, because the file can be embedded into other XML documents, databases, HTML etc. The SVG can handle three types of objects: vector graphics, raster graphics and text.

The declaration of the SVG in the documents is similar to the declaration of the XML object (Fig. 1)

```
<svg xmlns="http://www.w3.org/2000/svg" version="1.1">
    .....
    Graphics_objects
    .....
</svg>
```

Fig.1. The declaration of the SVG root object

In case of SVG, the root object has the form of <svg> tag. The “xmlns” variable is required by some browsers in order to correctly handle SVG graphics.

The SVG standard defines seven types of shapes: a rectangle, a circle, an ellipse, a line, a polygon, a polyline and a path. Additionally there is a special shape named “text”, which allows placing a text in the drawings. It differs from the other objects, because a text is defined as letters, words, and sentences – not as geometrical shapes.

Every SVG object and its attributes use descriptive names, so in many simple cases there is no need to use graphics editor in order to create or edit a simple drawing. As a result the user could use any simple text editor to create or edit a document. In many cases this is enough to make minor corrections in a code. It is a major advantage, when we taking into consideration the cooperation with the robot’s controller, using simple computer or other IT equipment.

It is worth to mention about the SVG “path” object and describe it in a few words. Its definition covers a wide variety of graphics shapes, and selection of the proper shape is done by setting values of the object’s attributes. These attributes control the movement of the virtual pen within the borders of the canvas as well as define complicated shapes, like cubic or quadratic Bezier curves. It is done by placing a special, one letter commands in the attribute’s value string. The command could be written in upper- or lowercase. The uppercase refers to the global coordinate system, while lowercase initiates operation in relation to the current position of the pen. The most important commands, selected from the set of all “path” object attributes, are:

- M – moves the pen to the specific point,
- L – draws a line,
- A – draws an arc,
- Q – creates the quadratic Bezier curve,
- C – creates the cubic Bezier curve,
- Z – closes the path.

Other commands extend the previously listed ones. They relate to the special definitions of the objects, like cubic and quadratic Bezier curves or horizontal/vertical lines. They are as follows:

- H – draws horizontal line,
- V – draws vertical line,
- S – draws smooth cubic Bezier curve,
- T – draws smooth quadratic Bezier curve.

All of the mentioned commands are the subsystem of the “path” object that have considerable drawing capabilities and could replace almost all of remaining SVG graphics objects, like circle, polyline or rectangle. There is no objections to create the SVG file in a text editor, where the simple objects (like circle, rectangle etc.) could be described by editing the SVG code. On the other hand, in case of complex paths, it is recommended to use an SVG editor. The example of the code that uses the “path” object and the result of its interpretation are shown in Figure 2.

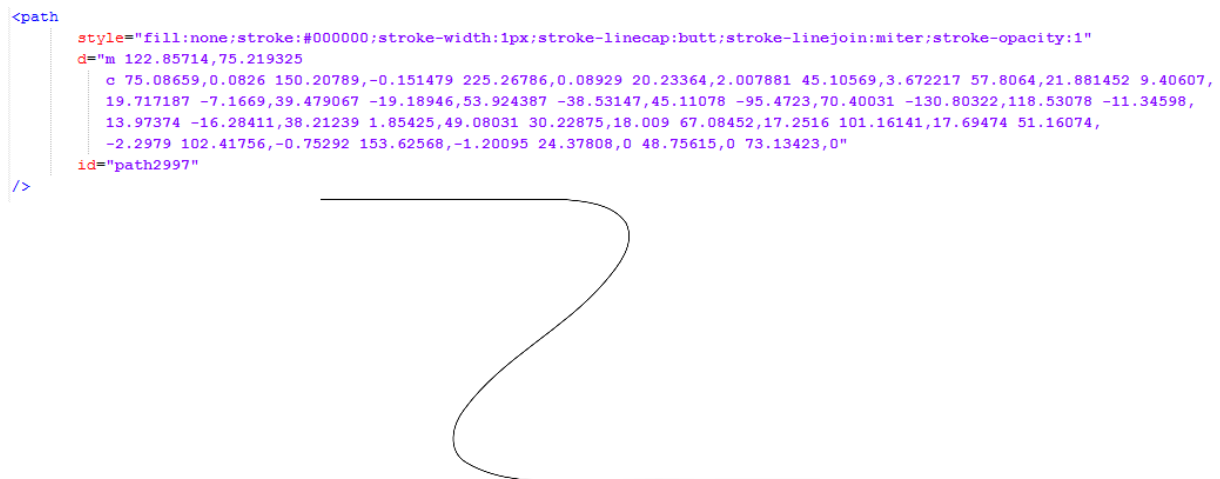


Fig.2. The example of “path” object declaration (cubic Bezier curve) and its graphical interpretation

The SVG file is saved as a XML text file with the “.svg” extension. It is also possible to save the file in a compressed form (using gzip deflate algorithm) with the “.svgz” extension. The compressed file is still readable by most programs, but the direct editing (using text editor) is no longer possible without the prior decompression.

The SVG files could also contain animated objects or hyperlinks, what makes them a very powerful tool among the World Wide Web standards.

All of the mentioned properties of SVG make this standard very attractive in a manner of creating user interfaces or graphics presentation. In the next part of the paper, it will be shown that this form of notation could be also used for development of robot’s tool path.

3. Conversion of the SVG objects to the robot’s tool path

The SVG standard, thanks to its versatility and wide processing capabilities, can be used to store information about the path of the tool mounted on the robot’s wrist. Due to the SVG limitations, it can store information only about points on the plane. This is not a major disadvantage, because – as it was mentioned earlier – most of the tasks, which require high accuracy with a significant degree of path complexity, take place on a plane. The orientation of this plane (on which the task is realized), may require defining a new coordinate system, which is done by using the appropriate robot’s control functions.

The transformation of the SVG path into the form that will be “understood” by the robot’s controller may cause some difficulties. The paths or object, like circle or rectangle, should be transformed to a set of discrete points, which will describe the following segments of the tool path [8]. The transformation could be done in two manners:

- the vector graphics could be transformed to the bitmap, then the list of points, which contain every pixel that belongs to the SVG object, should be created,
- every objects should be sampled into the set of the discrete points, and every curve should be converted into segments.

The second case could be done more efficiently by using optimization. Some points on the straight segment of the path could be omitted, but on the curved sections the points must be

arranged more densely in order to achieve adequate accuracy. The optimization can cause some problems during the movement of the effector, because speed changes may occur. In order to avoid this problem, sometimes it is better to find the optimal step that will be compromise between changes of velocity and accuracy. One of the possible solutions of the sampling problems is to export the drawing to a HPGL file. This format was created especially for plotters, enabling the possibility to control a pen or cutting tool on the XY plane. Export to the HPGL format can be performed from any application that supports SVG, by using the print command, selecting the correct driver and the option to write to a file. Some applications, like Dia, Inkscape and some graphics converters, allow direct export to the HPGL. The both ways of getting the coordinates from the SVG path are illustrated in Fig. 3.

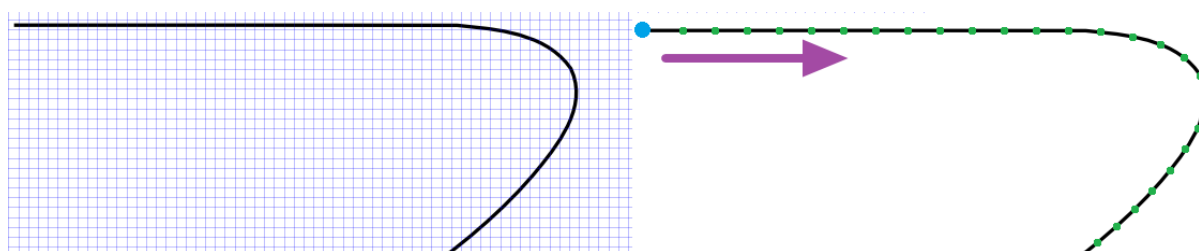


Fig.3. The rasterization (on the left) and sampling (on the right) of the SVG path

Regardless of the method used for acquisition of coordinates, the preparation of data for the robot program proceeds in a similar manner (Fig. 4). The preceding stage of the creation of the core of program is to arrange the appropriate coordinates into groups, corresponding to the individual objects (paths) of the SVG graphics. If the SVG drawing was exported to the HPGL file, this operation is quite simple, because the exporting algorithm arranges the coordinates automatically. In the case of rasterization, the whole bitmap must be scanned in order to acquire the coordinates of the points. The arrangement of the coordinates according to the objects requires more effort and special algorithms (e.g. nearest-neighbor search). Also excessive accuracy, resulting from the neighboring arrangement of bitmap's pixels, could cause some problems. It could results in robot's memory overload (due to the large number of coordinates) and excessively slow movement of the manipulator. It is therefore advisable to exclude some points from the set of pixels and optimize the resultant path..

4. Conclusion

The SVG is open standard and it is consistently evolving. This means that new features can be expected in the future releases of the SVG, together with growing support, documentation and software implementation. The use of SVG standard in robotics is very limited so far. Its main purpose is to create graphical user interfaces. The method presented in this paper changes the approach by introducing the ability to define manipulator path in graphical manner, using a flexible standard and widely available software tools. The advantages of using open standards are not only financial savings, but also the possibility of managing the code on different platforms, including the mobile devices, which are gaining more and more popularity today.

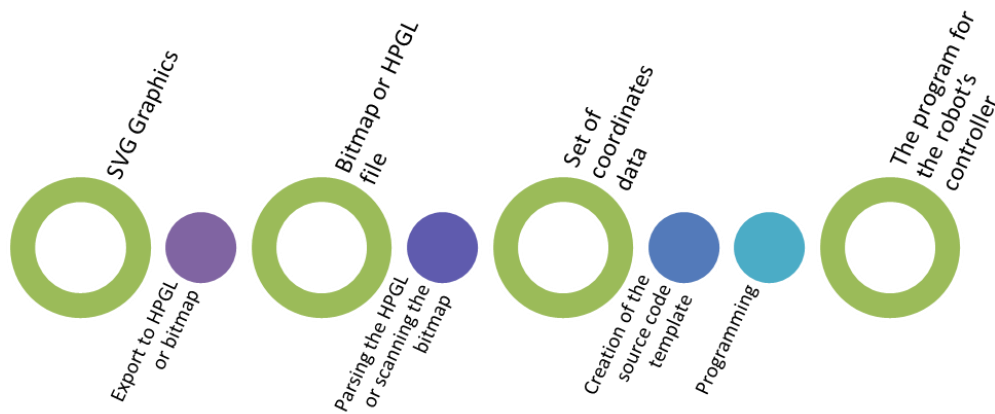


Fig.4. The process of preparation of the robot's program from the path designed in SVG

The main disadvantage of the presented method is its 2D nature, which means the inability to extend it to the general cases of robot's programming. On the other hand this drawback is not particularly problematic, since the most of precise actions performed by the robot, takes place on the plane.

Future work will focus on creation of a system, which will support the use of SVG graphics for planning of a manipulator path.

References

1. Ardayfio D.: Fundamentals of robotics, Taylor & Francis, 1987
2. Pires J.N., Loureiro A., Bölmsjö G.: Welding robots: Technology, system issues and applications, Springer 2006.
3. Dai W., Kampker M.: User oriented integration of sensor operations in a offline programming system for welding robots. In Robotics and Automation, 2000. Proceedings. ICRA'00. IEEE International Conference on (Vol. 2, pp. 1563-1567). IEEE
4. Jo S., Shahab Q. M., Kwon Y. M., Ahn, S. C.: Indoor modeling for interactive robot service. In SICE-ICASE, 2006. International Joint Conference (pp. 3531-3536). IEEE
5. Jo S., Ki J., Jeon K. W., Kwon Y. M., Ahn S. C.: Human-Robot Interaction with Indoor Virtual Model. In Robot and Human interactive Communication, 2007. RO-MAN 2007. The 16th IEEE International Symposium on (pp. 493-498). IEEE
6. Reinicke C., Buss M.: Towards multi-modal mobile telepresence and telemanipulation, The Internet Challenge: Technology and Applications (Ed. Hommel G., Huanye S.), Springer, Netherlands, 2002, 55-62
7. Cassinis R., Tampalini F.: AMIRoLoS an active marker internet-based robot localization system. Robotics and Autonomous Systems, 55(4), 306-315.
8. Foit K.: Controlling the movement of the robot's effector on the plane using the SVG markup language, Advanced Materials Research, vol. 837 1662-8985, Trans Tech Publications 2014, pp. 577-581
9. Scalable Vector Graphics (SVG) 1.1 (Second Edition), W3C Recommendation 2011, 2011, [online] Retrieved June 25, 2013 from <http://www.w3.org/TR/SVG/Overview.html>

SELECTED ENGINEERING PROBLEMS

NUMBER 5

INSTITUTE OF ENGINEERING PROCESSES AUTOMATION
AND INTEGRATED MANUFACTURING SYSTEMS

Agnieszka GAWLAS-MUCHA*, Ryszard NOWOSIELSKI, Rafał BABILAS,
Aleksandra GUWER

Institute of Engineering Materials and Biomaterials, Faculty of Mechanical Engineering
Silesian University of Technology, ul. Konarskiego 18a, 44-100 Gliwice, Poland
*agnieszka.gawlas-mucha@polsl.pl

SELECTED ASPECTS OF MAGNESIUM ALLOYS MELTING TECHNOLOGY

Abstract: Magnesium alloys are new class of biodegradable materials usually called as bioresorbable biomaterials for orthopedic applications. The potential benefits of Mg alloys are the nearer modulus of elasticity to the bone than stainless steel or titanium, biocompatibility and bone-active properties and the elimination of necessity of a second operation to remove the implant body. Two-component Mg-Ca alloy is characterized by a solid solution limit, and creates a stable intermetallic phase Mg_2Ca . Studied samples were prepared by melting starting material in an induction furnace in a quartz crucible. The micro chemical analysis of samples using a scanning electron microscope with EDS was performed. Values of the microhardness of materials were compared before and after remelting.

1. Introduction

Metallic materials used for implants, such as plates, screws or pins used to secure the fracture, must be removed during the second surgical operation, after a time sufficient for the healing of tissues. Magnesium alloys are promising new class of degradable structural biomaterials which provide advantageous properties, eg. high strength with respect to weight of the alloy, Young's modulus nearer to elasticity modulus of bone compared with titanium implants, biocompatibility, osseointegration, improving the growth of apatite in a living body. The advantage of using biodegradable material is that there is only one operation, thereby eliminating the time and expense of a second operation and / or the cost of the new implant. Magnesium metabolism and excretion in the kidney process is a natural physiological process in the human body [1-3].

The development of appropriate biodegradable implants is a multidisciplinary challenge. Suitable time resides in the body and uniform distribution of implant constitute the biggest problem in designing of degradable materials.. The prospective patient may avoid additional operations, which lead to the reduction of risk with an unnecessary stress and complications after surgery. Light and degradable orthopedic implants with a specific rate of corrosion may be assumed as a new generation of implant materials [1-3].

2. Magnesium–calcium alloys

Magnesium–calcium alloys are applicable as biodegradable materials. Calcium reduces the tendency to oxidize in the liquid state and in the state after heat treatment. As well as increases susceptibility to mechanical working. Calcium concentrations higher than 0.3% by weight promotes cracking during welding.

In the Mg–Ca alloys calcium forms intermetallic phases such as Mg_2Ca occurring at the grain boundaries of the solid solution α -Mg. It also increases the strength properties and creep resistance. The best properties are obtained when the calcium concentration is about 3% by weight. Calcium allows the original grain refinement of magnesium alloys Mg–Al and Mg–Zn [6-9].

Preparation of the alloy consists of melting the components in an induction or resistance furnace and casting them into the mold. Further processing can be hot-rolling and pressing. Casting of magnesium alloys forces need to use a protective atmosphere, due to high oxidation of the magnesium during the melting. The protective layer is obtained by various methods, the inert gases or fluxes could be used. The primary task of the protective atmosphere is to protect the molten metal against to the formation of unwanted compounds [6-9].

The using of flux is designed to obtain the surface of the protective layer on liquid metal from contact with air. The next task is to remove undesirable molten oxides, nitrides and other harmful substances formed during the melting process. Fluxes are usually mixtures of various salts mainly on the basis of fluorides and chlorides of alkali metals, eg. $BaCl_2$, $CaCl_2$, CaF_2 , KCl , $NaCl$, $MgCl_2$, and carnallite ($CaCO_3 \cdot KCl \cdot 2H_2O$) [1,6, 7].

Due to a huge number of disadvantages and difficulties associated with the use of fluxes, another alternative protection against oxidation of magnesium alloys is using a protective gas atmosphere. The most commonly used protective gases are dry air, argon, helium, nitrogen, carbon dioxide, sulfur hexafluoride (SF_6), sulfur dioxide (SO_2), boron hexafluoride (BF_3). Sulfur hexafluoride allows melting of the magnesium at temperatures above $700^\circ C$, while giving good results in view of the protective sealing cover the surface of the molten alloy [6-9].

3. Research techniques and results

Melting and casting of magnesium alloys is quite a complicated process during which an oxide layer is formed on the surface. It is a tight barrier against further oxidation. This phenomenon necessitates the use of a protective layer [4]. The protective layer is obtained by various methods. Among other things, we can distinguish the use of protective gases or special protective fluxes. [4-5].

Melting the magnesium alloys with calcium was done in an induction furnace. Magnesium and calcium are placed in a quartz crucible and then introduced into the furnace. Melting temperature was $700^\circ C$. Protective atmosphere is assured at all times during the process. The weight composition of prepared samples is presented in Table 1.

Tab. 1. The composition of the mass of elements used for boiling the samples

Element	Wt. [%]	T _t [°C]
Magnesium	95	650
Calcium	5	842

The analysis of the chemical composition of the ingot was conducted by using a scanning electron microscope (SEM) Zeiss Supra 35 equipped in energy-dispersive spectrometer (EDS).

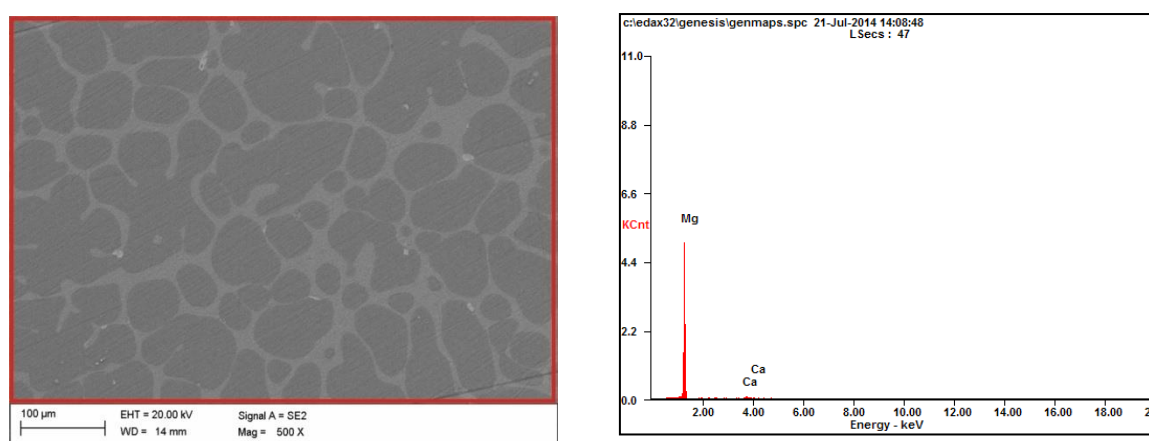


Fig.1. Alloy structure Mg 99% by weight. - Ca 5 wt%. obtained as a result of research carried out in a scanning electron microscope SEM (a) together with the results of the chemical composition microanalysis (b)

Table 2 presents the average microhardness of fabricated Mg-5Ca alloy with microhardness of pure Mg and Ca in as-delivery state. Alloy Mg-5%(wt) Ca showed significantly lower microhardness (HV 43) than its individual components Mg (57 HV) and Ca (81 HV).

Tab. 2. Average microhardness values of pure element Mg and Ca in the form of slug in as-delivery state

Material	Average microhardness [HV]
Mg	57
Ca	81

Results of microhardness measurements of received ingot are presented in Table 3. The fabricated ingot was seven times examined. The largest value of microhardness which occurred was 94 HV, whereas the lowest value was 52 HV. The average value of microhardness was 70 HV. These results indicate a slight heterogeneity of different areas of the ingot.

Tab. 3. Results of microhardness measurements of Mg-5(wt%)Ca sample after resistance melting

Number of measurement	Microhardness [HV]	Averagemicrohardness [HV]
1	94	70
2	52	
3	94	
4	82	
5	69	
6	76	
7	80	

4. Conclusion

The results obtained after preparation and examination of Mg5Ca ingot allowed to state the following conclusions:

- EDS demonstrated occurrence of magnesium and calcium elements in studied alloys. Moreover the concentration of alloying elements is almost the same as the starting composition alloy.
- Mg5Ca alloy has the average value of microhardness 43 HV. The difference between the measurements of the microhardness was 13 VH. The measurements of hardness is only a preliminary study. It is necessary to conduct further examination of mechanical properties.

References

1. Dudek J., Fajkiel A., Reguła T., Saja K.: Wybrane zagadnienia technologii przygotowania ciekłego stopu magnezu AZ91, Prace Instytutu Odlewnictwa, 2009, Vol. XLIX.
2. Fajkiel A., Obrzeski A., Dudek P., Reguła T.: Nowoczesne stopy oraz metody odlewania magnezu w zastosowaniach motoryzacyjnych, Przegląd Odlewnictwa Vol. 59, nr 1-2, 2009, pp. 48-55.
3. Staiger M., Piertak A., Huadmai J., Dias G.: Magnesium and its alloys orthopedic biomaterials: A review, Biomaterials vol 27, pp. 1728–1734, 2006.
4. Nowosielski R., Gawlas-Mucha A., Borowski A., Guwer A.: Fabrication and properties of magnesium based alloys Mg-Ca, Journal of Achievements in Materials and Manufacturing Engineering, Vol. 61, issue 2 December 2013.
5. Martynowicz-Lis K., Pachota M., Kryczek A.: Odlewnictwo w Polsce – wyniki roku 2006, Odlewnictwo współczesne – Polska i świat 1- 2, p. 12 – 15, 2008.
6. Orman M., Orman Z.: Technologia magnezu i jego stopów, wydawnictwo Śląsk, Katowice 1965.
7. Fajkiel A., Obrzeski A., Dudek P., Reguła T.: Nowoczesne stopy oraz metody odlewania magnezu w zastosowaniach motoryzacyjnych, Przegląd Odlewnictwa Vol. 59, nr 1-2, , pp. 48-55, 2009.
8. Holtzer M., Bobrowski A.: Atmosfery ochronne stosowane przy topieniu i odlewaniu stopów magnezu, Przegląd odlewnictwa, 2008 Vol. 58, nr 3 E.C. Lee, C.Y. Nian, Y.S. Tarng, Design of a materials processing technologies, Archives of Materials Science and Engineering 28, pp. 48-56, 2007.
9. Hartwig A.: Role of magnesium in genomic stability, Mutation Research 475, pp. 113–121, 2001.

SELECTED ENGINEERING PROBLEMS

NUMBER 5

INSTITUTE OF ENGINEERING PROCESSES AUTOMATION
AND INTEGRATED MANUFACTURING SYSTEMS

Grzegorz GOŁDA^{1*}, Adrian KAMPA¹

¹Institute of Engineering Processes Automation and Integrated Manufacturing Systems Department,
The Faculty Of Mechanical Engineering, Silesian University of Technology, Gliwice

*grzegorz.golda@polsl.pl

A MICROLOGISTIC SYSTEM ANALYSIS ON EXAMPLE OF ROBOTIZED RAPID PROTOTYPING CELL

Abstract: The article presents a proposal of a robotized rapid prototyping cell configuration. This cell is treated as an elementary micrologistics system. The real example of existing system was described. The main aim of the researches is establishment and development of methodology for the analysis of complete, integrated logistics systems in a new product prototyping, production and assembly. Realization of the technology is developed for the purposes of the didactic processes and the research project, proposed by one of mechanical enterprise, in area of construction the prototyping cell with machining robots.

1. Introduction

According to current trends in the development of automated systems in product design and manufacturing use of industrial robot is growing. In addition to standard applications of industrial robots in typical production cells, like: fixing parts on the machines, part manipulation and handling, welding, painting, polishing, etc., a new proposals for the use of robot as a technological machine for rapid prototyping processes will appear, e.g.: milling, turning, 3D printing [1]. In conducted studies authors attempted to use a industrial robot (Fanuc ArcMate 100iB) in the processes of rapid prototyping a new parts and these production. The industrial robot is here both as a manipulation and technological machine. This should shorten the duration of the prototype manufacturing and reduce costs [2,3,4].

Proper planning of whole robotized system is essential to cope with the modern trends of shortening the time to produce the prototypes and striving minimize the manufacturing costs [3]. Therefore, robotized system is treated as an elementary micrologistics system forming part of larger, integrated system of material and information flow which is whole enterprise. So, we can use computer simulation tools for robots programming using off-line method (e.g. Roboguide software [5]) and application to analyse queueing systems and logistics (e.g. Enterprise Dynamics 8 software [6]). Results obtained during two-step simulation will be compared with actual measurements of the robotized rapid prototyping cell productivity to validate the correctness of the model. Then, we can start to use a properly functioning model to predict parameters of micrologistics system for prototyping or manufacturing, a new, different parts and products.

2. The robotized rapid prototyping system

The use of conventional machining technologies and incremental rapid prototyping techniques by robot as a technological machine is still on the margins of research. This is due to use in that process the classical and modern CNC machines or 3D printers [1,2,3,4]. Apply industrial robot only as a manipulation device in prototyping processes (treated as a job or single-batch production) by machining is too expensive. On the other hand, the working space limitations of typical 3D printers give possibility to make only small objects, besides that, the process is very long. Thus, the use of the industrial robot with six (or more) degrees of freedom, long-range arms, possibility of automatic tools and grippers change will allow for faster and cheaper production of individual prototypes. While trying to apply the robot for rapid prototyping we should remember about limitations like: stiffness of the kinematic chain, accuracy of robot positioning, payload depended on the manipulator size [2].

In the course of research the station with FANUC ArcMate100iB robot (Fig. 1) was used (degrees of freedom - 6, maximum range of arm - 1373 mm, load capacity - 6 kg, position accuracy - 80 μm , semi-continuously regulated feed rate, the linear and circular interpolation). Due to parameters of the manipulator and pneumatic milling machine mounted in the robot wrist (nominal pressure - 6 bar, spindle speed - 2200 r/min, tool - end mill Φ 12 mm) the study was started from easy-machinable materials (styrodur - XPS, plastics, machinable wax).



Fig. 1. The rapid prototyping station with FANUC ArcMate100iB industrial robot

The material was a XPS plate fixed on machining table. First, theoretical parameters of milling (cutting speed, feed rate, depth of cut layer, number of transitions, processing time) was calculated for different surfaces like: flat surfaces, fillets, chamfers, holes, keyways etc. Then experimentally the impact of processing parameters controlled by the robot was tested by changing their types and values. The range of changes was the following: type of interpolated movement (linear, circular in options: precise and with inaccurate), cutting speed: 20-80 m/min (dependent on the pressure, difficult for precise adjustment), feed rate of milling tool: 1-100 mm/s (the setpoint speed of the tool center point - TCP), depth of the cut layer: 0,5-5 mm.

During the tests the cutting parameters was chosen experimentally, so that surface accuracy is comparable with standard 3D printing. In view of the fact that XPS is easy to machining process, with its high compression resistance and low hardness, the cutting force influence on the machining accuracy is small (deflection of the kinematic chain and tool fixed in industrial robot wrist).

Considering the low cost of the material and short time of machining the application of industrial robot in the rapid prototyping process seems justified. In connection with the need to estimate the processing time of the any other prototype and minimize the time it was decided to treat the rapid prototyping station as a micrologistics system consisting of subsystems: production (robot and machining table), manipulation and transport (robot) and warehouses. For the analysis of the micrologistics system a creation of a simulation model was proposed. The productivity tests of the model are the next step.

3. The simulation of robotized rapid prototyping cell

Modelling of robotized rapid prototyping cell begins by choice of appropriate robot, creation of elements of robotized station and data acquisition on the shape and dimensions of the prototype (workshop drawing made in a CAD application, e.g. Siemens NX 8.5 [7] saved in the iges format). The next step is to prepare the off-line robot subprogram of the processing by defining the trajectory and motion parameters of TCP, relative to the starting raw material (machining operations) and subprogram with the trajectory of manipulation (transport, gripping and fixing of the workpiece on the station). In this case, it is necessary, to calibrate the robot and to define coordinate systems associated with the tool, workpiece, and other elements of the robotized station. As a computer simulation software the Roboguide (demo version - Fig. 2) was used [5]. Prepared off-line program, after optimization, was loaded into control system of the real Fanuc ArcMate 100iB and successfully executed [3].

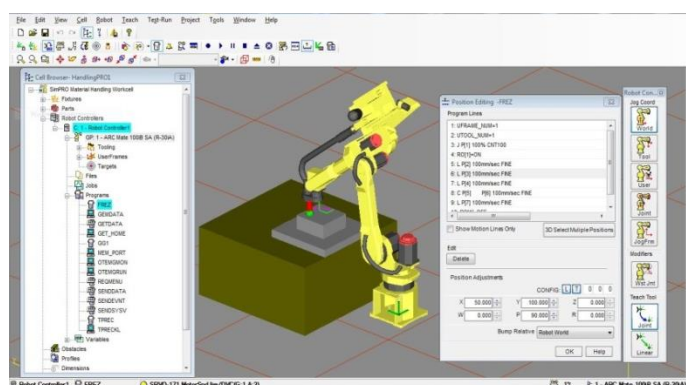


Fig. 2. Modelling of the rapid prototyping station in Roboguide software

During the simulation of rapid prototyping process, for different parts, in Roboguide software, the execution time of manipulation and machining was measured. Then the reconstruction of micrologistics system (robotized cell) was created in Enterprise Dynamics 8 - Logistics Suite (Fig. 3) [6]. A study of the system productivity was conducted. The main aim was a compare the results for two dedicated simulation systems to the next researches. A further target of these activities is the proper location of the prototyping station elements, selection the optimal material flow parameters (in storage, manipulation, transport and production operations) in order to minimize the total manufacturing time and the cost reduction of a new prototype.

The next stage will be to extend the existing micrologistics model of the rapid prototyping system to additional equipment, including more developed structures of the prototyping, manufacturing, assembly and logistics system.

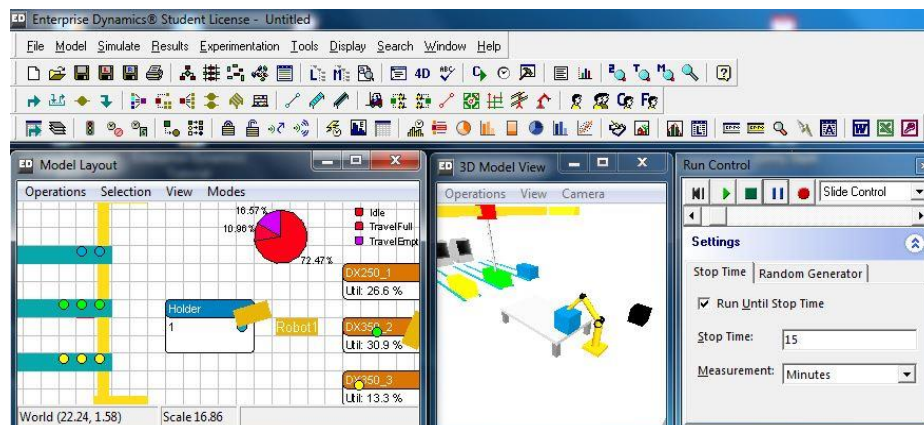


Fig. 3. The created model and productivity tests of micrologistics rapid prototyping system in Enterprise Dynamics 8-Logistics Suite software

This will estimate the time needed to produced batches of finished product using machining operations using industrial robots during rapid prototyping and production of final products.

4. Conclusion

At the article the proposal of micrologistics system analysis on the example of robotized rapid prototyping system are presented. Described methodology (simulation in virtual reality and real prototype manufacturing) is used during the laboratory didactic classes in the field of rapid prototyping techniques. Realized technology represents a preliminary study for the research project which consists in creation of rapid prototyping cell with machining robot. It's provides the basis for the further research on the use of computer simulation in an automated and robotized production using alternative methods for current manufacturing techniques. Activities in this area are intended to shorten the time from placing the order for a new product to its delivery to the final customer and reduce whole production costs.

References

1. Pandremenoset J., et al. Machining with robots: a critical review. In: 7th International Conference on Digital Enterprise Technology. Proceedings. Athens, Greece, September 28–30, 2011, pp. 152-159.
2. Gołda G., Kampa A.: Modelling of Cutting Force and Robot Load During Machining. Advanced Materials Research Vol. 1036, 2014, pp. 715-720.
3. Gołda G., Kampa A.: The application of industrial robots in the rapid prototyping process. Progress of robotics Vol. 2, Publishing House of Warsaw University of Technology, Warsaw 2014, pp. 579-586.
4. Kampa A., et al. Impact of rapid prototyping techniques for the manufacturing of new products. In: Selected Engineering Problems Vol. 3, Gliwice 2012, pp. 93-96.
5. Fanuc Robotics. Roboguide – Technical documentation.
6. Incontrol Simulation Software. Enterprise Dynamics - Technical documentation.
7. Siemens. NX 8.5 - Technical documentation.

SELECTED ENGINEERING PROBLEMS

NUMBER 5

INSTITUTE OF ENGINEERING PROCESSES AUTOMATION
AND INTEGRATED MANUFACTURING SYSTEMS

Cezary GRABOWIK^{1*}, Krzysztof KALINOWSKI^{1*}, Grzegorz ĆWIKŁA^{1*}, Witold JANIK^{1*},
Jarosław MAZUR^{1*}

¹Institute of Engineering Processes Automation and Integrated Manufacturing Systems,
Faculty of Mechanical Engineering, Silesian University of Technology, Gliwice
* {cezary.grabowik, grzegorz.cwikla, krzysztof.kalinowski, witold.janik}@polsl.pl,

ALTERNATIVE METHODS OF THE ARTIFICIAL FISH LURES MANUFACTURING – CASE STUDY

Abstract: In this paper alternative methods of the artificial lures manufacturing are presented. Proposed approach is based on application of various contemporary techniques it is reverse engineering rapid prototyping and manufacturing and middle-end CAD modeler. It is proposed to use reverse engineering not only for gathering of existing parts 3D geometry but also for acquiring it just from fish. Moreover if there is a possibility to gather information about fish skin texture, with high end 3D scanners, the real-looking fishing lures would be produced. These scanned models are usually sufficiently good for production with rapid prototyping apparatus. In order to meet a client needs application of the middle-end CAD modeler – Inventor is proposed. It allows modeling a product geometry which is well matched to a client needs and requirements. Finally vacuum casting rapid manufacturing method for a small batch production of soft fishing lures is suggested. This paper gives an application example of each above mentioned methods.

1. Introduction

Currently there are the two basic manufacturing techniques used in a mass production of artificial lures. The first is a highly developed technique of the injection moulding of the polymers materials used in case of manufacturing of soft baits lures (see the figure 1). The second most popular manufacturing technique is stamping used for manufacturing of the artificial lures such as inline spinner baits and spoon lures (see the figure 3). The last considered in the paper type of hard-bodied fishing lures is wobbler. It can have a solid or hollow body made out of a light weight material such as plastic or balsa. In some designs a wobbler body is separated into two pieces joined by a small flexible link to improve the impression of a fish whipping its tail fin. Wobbler is manufactured, depending on type of the raw material, with combination of removal and gluing techniques.

Injection moulding is generally used for manufacturing of soft bait lures such as rippers and twister tail fishing lures. The manufacturing process is being realised cyclically with injection moulding machine. During the injection process the raw material it is granulated or powder material is heated to required temperature and next extruded into an injection mould.

The most expensive part of the injection moulding machine is a mould mostly because of high mould raw materials cost and need of mould manufacturing with CNC controlled machine.



Fig. 1. Exemplary soft artificial lures

The input product of the injection moulding process is a moulded piece which is additionally treated by removing flashes and runners [4].

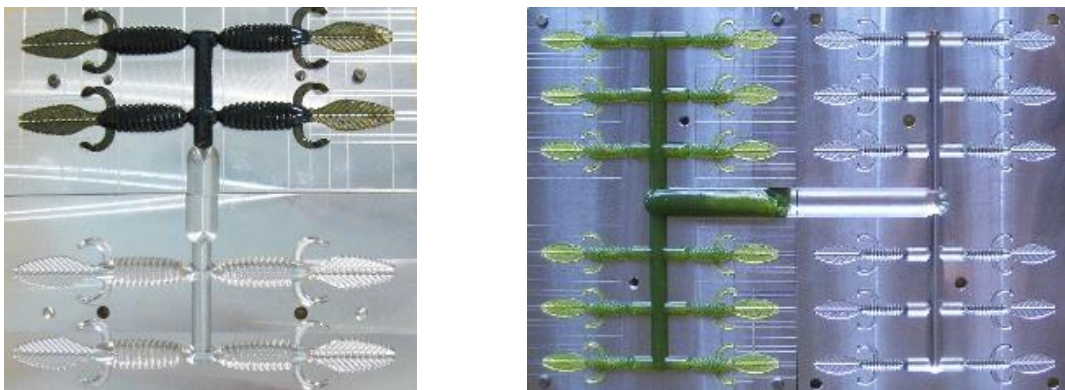


Fig. 2. Aluminium injection moulds used for a cavity moulding of the soft lures [9]

As it has been previously mentioned the second group of the fishing lures consists of inline spinner baits and spoon lures. The characteristic feature of this kind of baits is that the main part of each, it is a spoon or blade respectively, is made of steel brass or copper shaped by stamping. This process is being carried out in the three steps as follows (see the figure 3).



Fig. 3. Stages of the spoon lures manufacturing process [9]

In the first stage a press presses down a sheet brass to a die block in order to make a company trade-mark and drawing: size, a slot in the middle and a hole in the lower part of the

spoon lure. During the second stage the spoon outer contour is marked out, in the third stage of the manufacturing process the desired shape is obtained by cutting. The manufacturing cost in case of stamping is relatively low in comparison to other manufacturing methods [1, 4].

2. Alternative method of the artificial fishing lures manufacturing

In the proposed solution the alternative method of the artificial fishing lures manufacturing is based on application of the following contemporary techniques such as inverse engineering, rapid prototyping and vacuum casting [2, 3, 4, 7, 8, 11]. The reverse engineering process was used for gathering geometrical information. Reverse engineering process was carried out with application of the non-contact scanning method. As a subject of the scanning process a wobbler made of balsa was chosen (fig. 4). The process was performed with SMARTTECH 3D dual volume scanner.



Fig. 4. The wobbler model [11]

For the scanning process purpose from the wobbler model treble hooks and rings were removed. During the scanning process the wobbler model was scanned from the 8 directions, it is the front, back, left and right sides of the model and the four model diagonals.



Fig. 5. The scanning process of the wobbler model, a) the wobbler model fixed in the handle, b) the appearance of the wobbler model in 3D Mesh software

As a result the 8 points' clouds were obtained. These points' clouds were next processed with 3D Mesh and Geomagic Studio respectively. During the post processing the following imperfections such as noise, handle elements and random objects from clouds' points were removed. After completing the post processing stage the 3D CAD model of the scanned product was automatically prepared in Geomagic Studio (see the fig. 6).

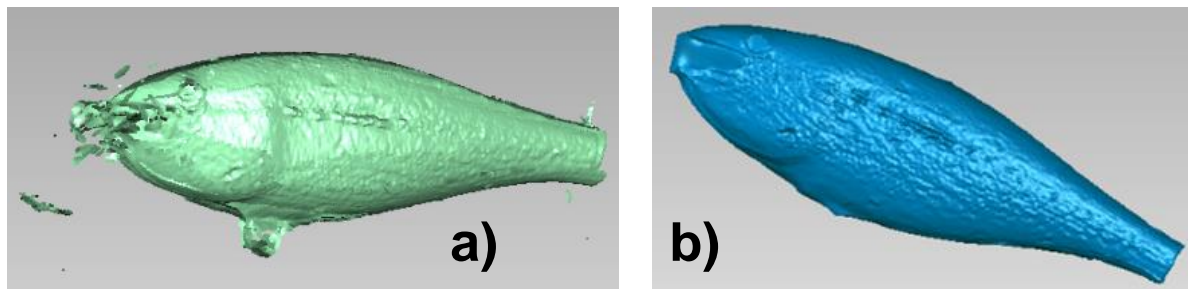


Fig. 6. The scanning process of the wobbler model, a) the appearance of the wobbler model after joining points' clouds together, b) the appearance of the wobbler 3D CAD model [10]

The wobbler CAD model was next sent to the NX 8.5 Siemens environment in order to prepare its STL model.

Having this model prepared it was possible to set about choosing the manufacturing technique. In the considered case selection of the manufacturing methods was limited, according to laboratory potential to the two; it is fused deposition modelling and 3D printing. Finally fused deposition modelling process was selected taking into account material characteristic of models manufactured with it. The wobbler model was made with Stratasys FDM 360 MC machine. The final product in the picture 7 is shown.



Fig. 7. The wobbler model made with fused deposition modelling on FDM 360 MC machine [10]

Taking into account the model surface quality it is appearance of staircase effect characteristic for RP manufactured parts it was necessary to apply additional finishing treatment [4, 5]. There are several methods of fused deposition modelling manufactured parts finishing but the most often used are abrasive machining and chemical treatment with acetone. The choice of treatment method is determined by the final product surface requirements.

In case when the part surface should be smooth it is recommended to apply acetone bath (acetone liquid bath or acetone fumes bath). If a product surface painting is needed then abrasive machining and primer painting ought to be applied. Taking into consideration above in presented case the second treatment method was chosen.

2.1. Application of a CAD modeler in custom fit fishing lures and vacuum casting

In the presented work Inventor CAD modeler was applied for modelling of custom fit fishing lures which are the best fitted to a client needs and requirements as it is only possible. During research the following models were made (see the figure 8): a twister and rippers. These models were next transformed into STL files and manufactured with FDM 360 MC apparatus.

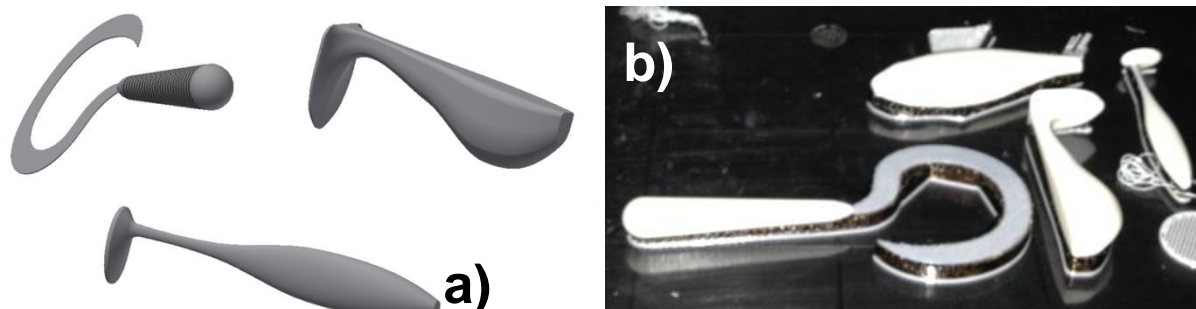


Fig. 8. The fishing lures CAD models (a), models manufactured with fused deposition modelling technique on the FDM 360 MC apparatus (b) [10]

Having fishing lures models manufactured (used next as master models) it was possible to set about choosing a small batch production method. There several rapid manufacturing methods for instance HSM machining, HSC cutting or casting. It was decided to apply vacuum casting method. Manufacturing process was carried out in the following steps: a moulding box preparation, supporting scaffold design, gating system and degassing system design, silicone mould fabrication, silicone mould cutting, mould heating, mould casting (see the figure 9).

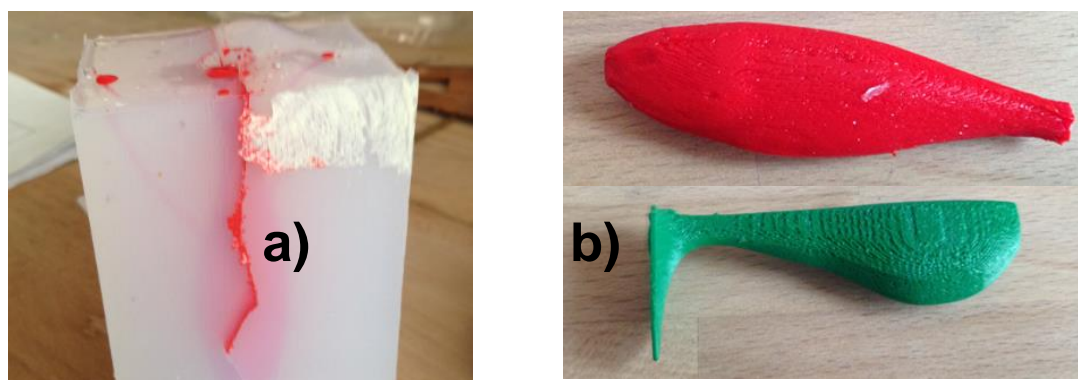


Fig. 9. The silicone mould with the casted part (a), final casted parts (b) [10]

3. Conclusion

Basis on the conducted research the following conclusions were drawn. Proposed alternative methods of artificial fishing lures manufacturing appeared to be time and labour-consuming because of the great number of manual work. It means that they are not the best choice in case of mass or series production but good in small batch production or custom fit

production. Vacuum casting methods is especially sensitive to correct selection of the following process parameters: components ratio, pigments amount, process' temperatures such as soaking heat and fluidization temperature, overall processing time. Moreover this method allows making parts with dimensions limited to the size of the working chamber. In case of casting of small and precise parts there is a danger of appearing of the final model geometry imperfections. Silicone moulds in vacuum casting technology have a limited life-span so the number of parts that can be casted with a particular mould equals to maximum dozens. In series or mass production it is suggested to use an alternative technology such as pressure die casting or injection moulding. Reverse engineering process is expensive mostly because of the high application cost of FDM. However it allows getting a product CAD model from the real object fast and makes the process of a design reconstruction relatively easy. Proposed in the paper approach can be used in prototyping, model verification and small or batch production.

References

1. Grabowik C., Kalinowski K.: Object-Oriented Models in an Integration of CAD/CAPP/CAP Systems. LNAI 6678. Springer, vol. II, 2011, pp. 405–412.
2. Grabowik C., Janik W., Kalinowski K.: The die reconstruction of the sterile inflatable nasal tubes for haemorrhage prevention. Selected Engineering Problems 2013 nr 4, pp. 91-96.
3. Grabowik C., Janik W.: The concrete casting matrixes inserts design preparation based on the master models. Advanced Material Research 2013 vol. 702, pp. 259-262.
4. Kalinowski K., Grabowik C., Janik W.: Analysis and testing of the dimensional accuracy of parts made with the FDM technology. Selected Engineering Problems 2013 nr 4, pp. 103-108.
5. Grabowik C., Kalinowski K.: A review of rapid tooling technologies in technical production preparation. Selected Engineering Problems 2012 nr 3, pp. 87-92.
6. Grabowik C., Kalinowski K.: A review of rapid tooling technologies in technical production preparation - a vacuum casting practical example. Selected Engineering Problems 2012 nr 3, pp. 81-86.
7. Janik W.: The implementation of the material loss detection method in the author computer aided overhaul software, Advanced Materials Research vol. 1036 (2014) pp. 652-655.
8. Janik W.: The practical verification of the material loss detection method for cylindrical shape parts”, Advanced Materials Research Vol. 1036 (2014) pp. 656-661.
9. http://www.lsbait.com/Craws-and-Creature-Baits_c7.htm [access: 30.06.2013].
10. Mazur J.: Alternatywne metody wytwarzania wędkarskich przynęt sztucznych. Master thesis, Silesian University of Technology, Gliwice 2014.
11. Kampa A.: Impact of rapid prototyping techniques for the manufacturing of new products. Selected Engineering Problems 2012 nr 3, Gliwice, 2012, pp. 93-96.
12. <http://www.rapala.com/rapala/lures/shallow-shad - apandreg/Shallow+Shad+Rap.html?start =47&cgid=rapala-lures>

SELECTED ENGINEERING PROBLEMS

NUMBER 5

INSTITUTE OF ENGINEERING PROCESSES AUTOMATION
AND INTEGRATED MANUFACTURING SYSTEMS

Aleksandra GUWER*, Ryszard NOWOSIELSKI, Agnieszka GAWLAS-MUCHA, Anna
KILJAN, Rafał BABILAS

Institute of Engineering Materials and Biomaterials, Faculty of Mechanical Engineering,
Silesian University of Technology, Gliwice, Poland
* aleksandra.guwer@polsl.pl

THE INFLUENCE OF MILLING AND INTERVAL TIME ON THE AMORPHIZATION PROCESS OF Cu-Ti ALLOYS

Abstract: The aim of this paper is describing a preparation, investigation and comparison of the structure size and shape of the $\text{Cu}_{50}\text{Ti}_{50}$ amorphous and nanocrystalline powders depending of the milling and interval time in cycle. The $\text{Cu}_{50}\text{Ti}_{50}$ alloy was obtained by mechanical alloying (MA) in a high energy ball mill SPEX 8000. The structure of $\text{Cu}_{50}\text{Ti}_{50}$ powders was examined by X-ray diffraction (XRD). Chemical composition, particle size and shape of the prepared powders was investigated by scanning electron microscopy (SEM). Amorphous $\text{Cu}_{50}\text{Ti}_{50}$ alloy can be prepared by a high energy ball milling. Milling and interval time determined an amorphization process of starting elements. The SEM analysis showed that the increase of milling time caused the increasing of powder particle size. The shape changing of the particles was also observed.

1. Introduction

Bulk metallic alloys exhibit many superior properties in comparison with crystalline alloys. Lately, it has been notified that rods and ribbons obtained from Cu – based alloy exhibit high tensile strength, fatigue strength, fracture strength, ductile and relatively low cost of products and good glass-forming ability [1 – 6].

The conventional methods of fabrication of amorphous materials include casting methods e.g.: melt spinning or pressure die casting method. Mechanical alloying (MA) seems to be an alternative method for preparation of metallic amorphous alloys from high purity powders in high-energy mills. During the MA process particles are subjected to multiple cold welding, cracking and rewelding. Preparation of amorphous alloy by using this method is dependent on many factors. The most important factors are: determination of the appropriate weight ratio of grinding media to the mass of powders, selection of the proper milling time and length of interruptions, provide a protective atmosphere and cleanliness of grinding media and the reactor. The selection of these factors for different materials is carried out on an experimental basis, and it is time consuming [7].

Depending on the plastic properties of starting powder the MA process can take place in different ways. Titanium is brittle metal and copper is ductile. In this case the stages of the MA process illustrates Fig. 1.

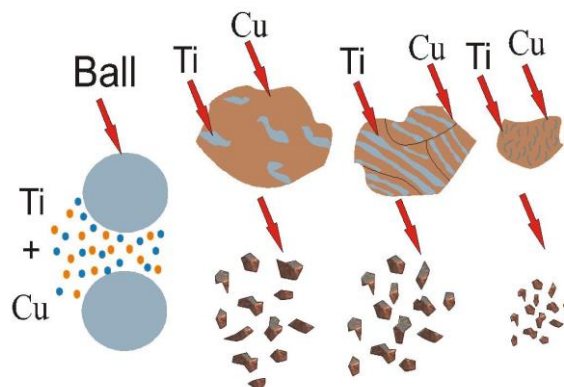


Fig. 1. MA steps for brittle and ductile elements [7]

2. Material and research methodology

Nine samples (Table 1) with composition of $\text{Cu}_{50}\text{Ti}_{50}$ (at.%) were prepared using commercially pure powders of copper (99,5 % purity, < 325 mesh) and titanium (99,5 % purity, < 325 mesh). Final weight of each sample was 8 grams with 4,5629 g of copper and 3,4371 g of titanium.

Tab. 1. Identification of prepared samples

Interruption time [min] / Milling time [min]	Time of mechanical alloying		
	6 h	8 h	10 h
0/60	sample 1	sample 2	sample 3
10/60	sample 4	sample 5	sample 6
30/30	sample 7	sample 8	sample 9

The experiments were conducted with three different milling times: 6 h, 8 h, 10 h. MA process was interrupted every 60 min (interval lasted 10 min) for samples 4 – 6 and every 30 min (interval lasted 30 min) for samples 7 – 9. Specimens 1 – 3 were milled incessantly. The long break during milling did not allow to overheating crucible and powders. Low temperature favours amorphization process. Powder composition was weighed on an analytical high precision balance AS/X. Cr steel balls of 13 mm diameter were used. The ball to powders weight ratio was 5:1. The powder mixture together with Cr steel balls were placed in austenitic crucible under argon atmosphere within a glove bag.

The mechanical alloying was performed in a high energy ball mill SPEX 8000 CertiPrep Mixer/Mill “shaker” type. The mill generated vibrations of the balls and the material inside the container [8-11].

X-ray diffractometer X'Pert Pro Panalytical with $\text{Cu K}\alpha$ radiation ($\lambda=0.15418$ nm) was used to structure verification of powders in as-prepared state. The data of diffraction lines were recorded by “step-scanning” method in 2θ range from 20° to 80° and $0,05^\circ$ step.

Particles size and shape of studied powders were characterized by using the Scanning Electron Microscopy (SEM) SUPRA 35 ZEISS with magnification up to 500x.

Chemical characterization of prepared samples were analysed by Energy Dispersive X-ray Spectroscopy (EDS). EDS provides surface chemical analysis of the field of view, linear or spot. Values of the characteristic radiation energy permit to qualitative analysis in the test sample, and the intensity (peaks height) allows for quantitative analysis.

3. Results and discussion

X-ray diffraction analysis has revealed that the samples after 8 h milling with 30 min interruptions was amorphous. The diffraction pattern shows a single broad diffraction halo with the 2θ range of $37^\circ - 47^\circ$ from the amorphous phase only (Fig. 2). The diffraction patterns show the broadening of diffraction lines for each milled samples. The lowest intensities were recorded for samples, which were milled 6h and 8h with 30 min intervals. Amorphization process favour short milling times and long intervals used during the cycle. Therefore the amorphization must be proceed carefully at the early stages of mechanical alloying.

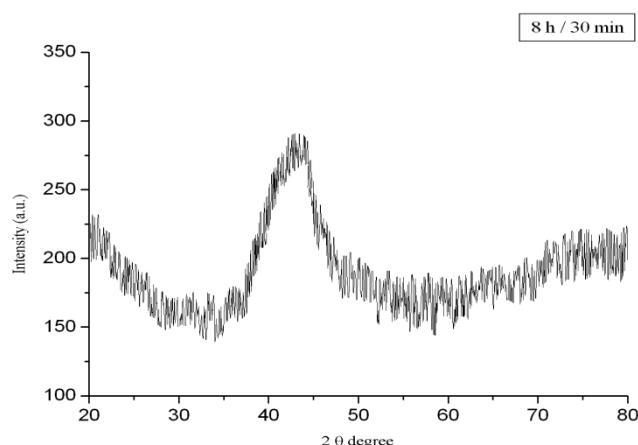


Fig. 2. X-ray diffraction pattern of $Cu_{50}Ti_{50}$ powders after 8 h of mechanical alloying with 30 min interruptions

The initial size of the powders was about $44\ \mu\text{m}$. The increasing of particle size was observed after each mechanical alloying process. Average particle size of the powders is presented in Table 2. Several relationship was observed on the basis of powders measurements. The increasing of milling time caused that the particle size also increased. The largest particles were obtained after 10 h mechanical alloying with intervals of 30 min. The particle size was five times larger than the initial powder (increase from $44\ \mu\text{m}$ to $200\ \mu\text{m}$). In samples 1 – 7 was observed variety of particles (small and large), whereas powders in samples 8 and 9 were homogeneous (of similar size).

The powders after milling without interruption and with 10 min intervals characterize very heterogeneous shape. In two cases (samples 3 and 5), the particles look like small sponges. Particles after milling with intervals of 30 min resemble the shape of very similar to spherical.

Tab. 2. Average particle size [μm] of the powders after MA

Interruption time [min]/ Milling time [min]	Time of mechanical alloying		
	6 h	8 h	10 h
0/60	70x89	123x138	128x163
10/60	113x133	152x176	170x189
30/30	140x135	160x165	150x190

Tab. 3. Results of chemical analysis from the surface of powder

Sample	Element	At. [%]
0	Cu	50
	Ti	50
1	Cu	51,04
	Ti	48,96
2	Cu	52,39
	Ti	47,61
3	Cu	53,76
	Ti	46,24
4	Cu	51,07
	Ti	48,93
5	Cu	51,91
	Ti	48,09
6	Cu	50,45
	Ti	49,55
7	Cu	48,82
	Ti	51,18
8	Cu	49,33
	Ti	50,67
9	Cu	51,15
	Ti	48,85

Figure 3 shows microanalysis of $\text{Cu}_{50}\text{Ti}_{50}$ powders after 8 h milling with 10 min interruptions with marked area from whole area of the sample. EDS results confirmed an existence of copper and titanium elements in studied sample. The chemical composition analysis was only a qualitative test and confirmed existing of main elements in studied alloy. The amount of atomic share of Cu and Ti depends on the time of milling. Table 3 presented detailed results of the chemical analysis for every sample. Each particle consisted only basic components (Ti and Cu). The initial atomic percentages of Cu equals 50 % and Ti 50 %. The investigation result have shown that the obtained powder particles after alloying process have very similar atomic composition in comparison with starting composition.

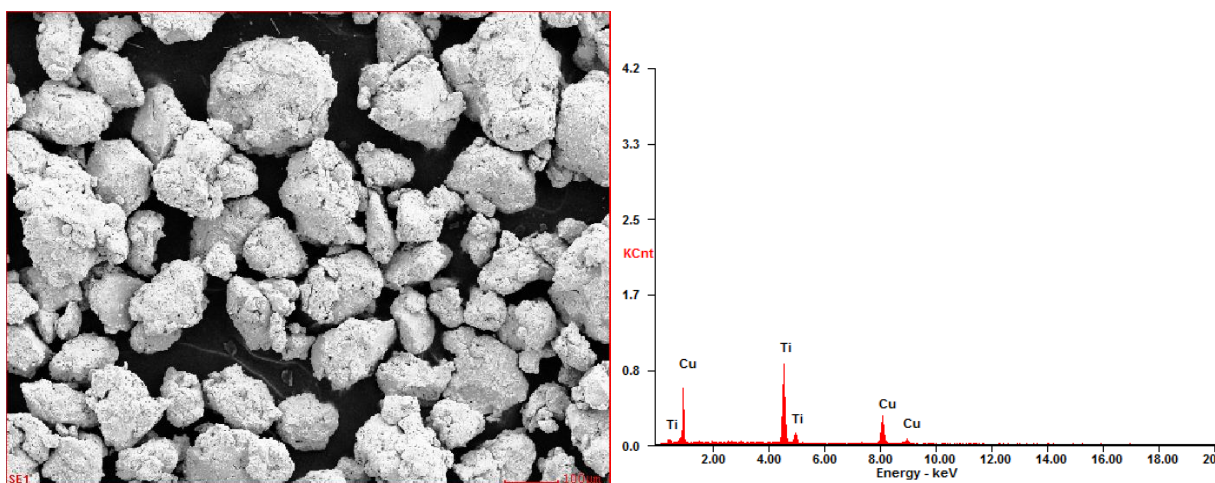


Fig. 3. The micrograph of $\text{Cu}_{50}\text{Ti}_{50}$ powders after 8 h mechanical alloying with 10 min interruption with marked area for which energy dispersive X-ray analysis (EDS) was performed from all area of sample

4. Conclusion

The obtained results after fabrication and testing of $\text{Cu}_{50}\text{Ti}_{50}$ powders allowed to state the following conclusions:

- It is possible to produce amorphous alloy by mechanical alloying method in a very short time (about 8 h),
- Both the milling time and the time of intervals have an influence on the forming of powders structure, its dimension and shape,
- The X-ray diffraction results showed that the most adequate conditions for amorphization is 8h milling with 30 min interruptions,
- In each case, regardless of the interruption length used during milling, particles size increased. The largest particles were observed after the longest milling time (10 h) and by using the longest intervals (30 min),
- Energy dispersive X-ray analysis demonstrated an occurrence of copper and titanium elements in studied powders. Each particle is characterized by a different content of copper and titanium, but very close to the initial powders.

Acknowledgements

Aleksandra Guwer is scholarship from project “SWIFT (Scholarships Supporting Innovative Technology Forum)” POKL.08.02.01-24-005/10 co-financed by the European Union under the European Social Fund.

References

1. P. Lee, C. Yao, J. Chen, L. Wang, R. Jeng, Y. Lin: Preparation and thermal stability of mechanically alloyed Cu–Zr–Ti–Y amorphous powders, “Materials Science and Engineering” 2004, Vol. A 375–377, pp. 829–833.

2. C. Suryanarayana, A. Inoue, *Bulk Metallic Glasses*, Boca Raton, CRC Press, 2011.
3. H. Kim, K. Sumiyama, K. Suzuki: Formation and thermal stability of nanocrystalline Cu-Ti-Ni prepared by mechanical alloying, "Journal of Alloys and Compounds", 1996, Vol. 239, pp. 88-93.
4. C. Hu, H. Wu, Formation of Cu-Zr-Ti amorphous powders with B and Si additions by mechanical alloying technique, "Journal of Alloys and Compounds", 2007, Vol. 434-435, pp. 390-393.
5. A. Inoue, B. Shen, A. Takeuchi, Fabrication, properties and applications of bulk glassy alloys in late transition metal-based systems, "Materials Science and Engineering", 2006, Vol. A 441, pp. 18-25.
6. A. Pusz, A. Januszka, S. Lesz, R. Nowosielski, Thermal conductivity measuring station for metallic glasses, "Achievements in Materials and Manufacturing Engineering", 2011, Vol. 47, pp. 95-102.
7. M. Jurczyk, *Mechanical alloying*, Poznań University of Technology Press, 2003 (in Polish).
8. R. Nowosielski, R. Babilas, G. Dercz, L. Pająk, J. Wrona, Barium ferrite powders prepared by milling and annealing, "Journal of Achievements in Materials and Manufacturing Engineering", 2007, Vol. 22, pp. 45-48.
9. R. Nowosielski, R. Babilas, G. Dercz, L. Pająk, Microstructure of composite material with powders of barium ferrite, "Journal of Achievements in Materials and Manufacturing Engineering", 2006, Vol. 17, pp. 117-120.
10. R. Nowosielski, R. Babilas, G. Dercz, L. Pająk, J. Wrona, Structure and properties of barium ferrite powders prepared by milling and annealing, "Archives of Materials Science and Engineering", 2007, Vol. 28, pp. 735-742.
11. G. Dercz, J. Rymarczyk, A. Hanc, K. Prusik, R. Babilas, L. Pająk, J. Ilczuk, Structural studies by XRD and Mössbauer spectroscopy on nanocrystalline substrates prepared using high-energy ball milling for $\text{Bi}_5\text{Ti}_3\text{FeO}_{15}$ synthesis, "Acta Physica Polonica", 2008, Vol. 114, pp. 1623-1629.

SELECTED ENGINEERING PROBLEMS

NUMBER 5

INSTITUTE OF ENGINEERING PROCESSES AUTOMATION
AND INTEGRATED MANUFACTURING SYSTEMS

Witold JANIK¹, Cezary GRABOWIK^{1*}, Grzegorz ĆWIKŁA¹, Krzysztof KALINOWSKI¹

¹ Silesian University of Technology, Faculty of Mechanical Engineering,
Institute of Engineering Processes Automation and Integrated Manufacturing Systems
Konarskiego 18A Str., 44-100 Gliwice, Poland
*cezary.grabowik@polsl.pl

MANUFACTURING PROCESSES OPTIMIZATION WITH APPLICATION OF GRIP NC PROGRAMMING LANGUAGE

Abstract: This paper presents the possible application of GRIP NC programming language in order to optimise a manufacturing process. The possible optimization could be provided in Siemens NX Software with use of .Net programming language, SNAP libraries or GRIP NC language supported up to current version. Simplicity of use is a main advantage especially in situation when industrial company starts applying automated optimization in a technological process preparation. Automation should be considered also in order to manage with multi machine processes. In the proposed solution there is an algorithm that executes the loop until parameters, trajectory and strategy of cutting satisfy the set ranges. The software application could be extended for other types of manufacturing. Simultaneously the result of manufacturing process is important according to quality of surface, and chip removal process.

1. Introduction

The Siemens NX routine tasks can be automated with software that is prepared by a user. The Siemens NX programming environment tools are MS Visual Studio and GRADE (Graphics Advanced Development Environment) [3]. GRADE is easy to operate (text menu) and GRIP/GRIP NC language is easy to learn and applying in practice. The important advantage of GRIP NC programs is their compatibility with all Siemens NX versions (also with current NX9.0) in opposite to .Net languages which are compiled with specific version of libraries. If software is created with current version of NX, the program is incompatible backwards (obsolete library objects definitions). In result the proper selection of environment has an major impact to the future adaptation of a prepared tool. The GRIP NC functions (procedural language) are oriented to prepare operations like: inner and outer surfaces turning (rough, finish, threading, cut, drilling), milling (blind shape pockets, planar surfaces according to contour, multi-axial, plane surfacing according to contour, sequence, cavitation based, drilling, electro wired). The environment is also supported with Siemens NX manufacturing module with already implemented tools, especially the simulation tool that helps to analyse the result of cutting in particular operation.

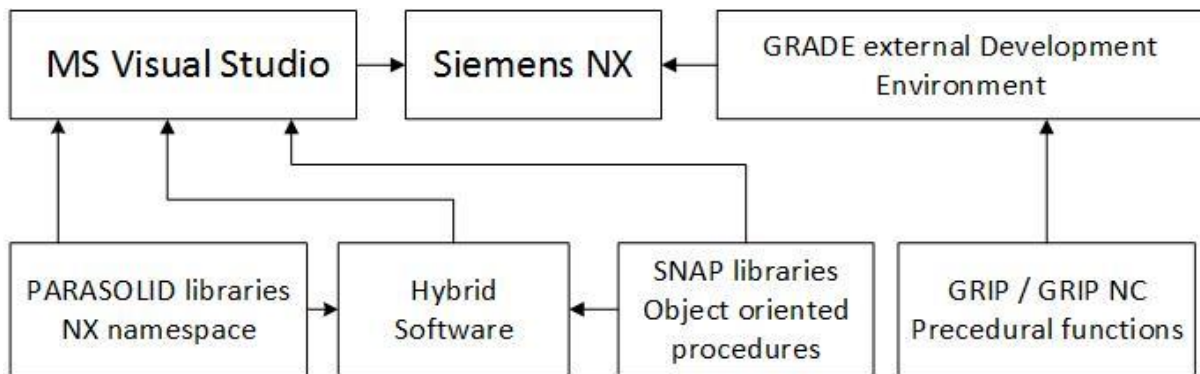


Fig.1. The programming tools environments bounded with Siemens NX software

2. Solution of optimization process automation

The preparation of technological process operation could be automated in various ranges. According to existing already defined operations or with simultaneously it creation the prepared operation could be automatically corrected in order to optimize cut parameters, trajectory of tools etc.. Furthermore the GPA symbols are used to set all main operations parameters and with additionally bounded code fragment with labels there is possibility to prepare iterative algorithm in order to generate operations with optimized cut parameters or a trajectory distribution points set.

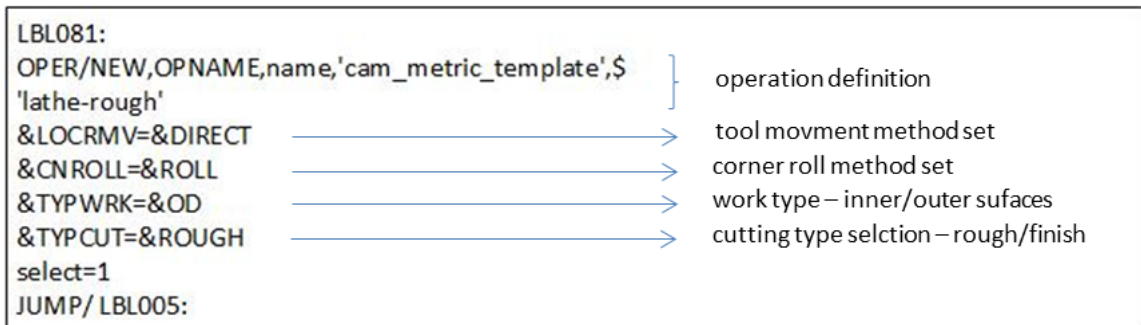


Fig.2. Example of operation generation code with standard set of parameters

For proper optimizations main parameters should not be considered as adjustable with algorithm, except &CNROLL GPA symbol. This parameter can be optimized, but with awareness of possible inaccuracy result of final machined surfaces. &CNROLL could be set as:

- a) &ROLL – roll around corner GPA set,
- b) &CLEAR – cut around corner using extended tangent.

In order to optimize technological operation algorithm should be implemented, according to schema presented in fig 3. The general algorithm is prepared in the loops that iteratively analyse the efficiency of proposed paths and parameters. When the primary set of parameters is prepared, the general algorithm start the loop until comparator confirms optimal values (technological operation selected data like: total time, path, parameters) according to an estimated range. The other possibility is an expert estimation of a generated machining

simulation, but it is not as fast as the previous method. The method could be also used for manufacturing based on models gained from 3D scanning [1].

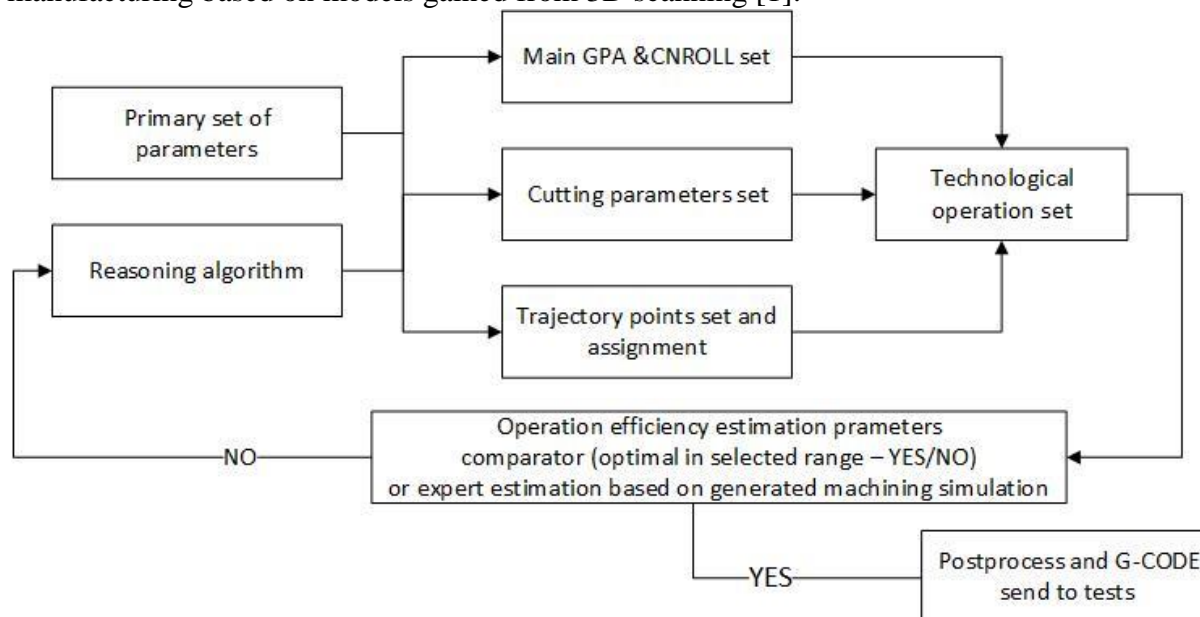


Fig.3. Solution for operation generation code with standard set of parameters

If the parameters fulfil rules stored in comparator algorithm according to technological data the post processing should be executed.

In order to ensure that the process is correctly optimized the practical verification should be always executed. Important aspect is that the practical verification can bring knowledge needed to adjust additional set of parameters or path manually or automatically. The automatically generated path is presented on fig. 4 where the path is optimized with the practical verification and the chip removal check. In example the chip removal during cutting process have a significant impact to a possible need of parameters optimization and path correction. The used local return point (LRT) for instance, brings possibility to avoid chip jam between tool and material, as well as cool down tool in order to prevent surface melting of the turned PA material. Disadvantage of a LRT use is an operation main time extension, which is worth to trade off in specific circumstances. All data modification made according to practical verification, should be saved in data base and described in order to modify existing algorithms or to modify a comparator values set. The additional development of program should bring the proper results that are also repeatable in similar cases. In other approach the optimization algorithm could be set in order to achieve a specified quality of surface, especially when technological operation is prepared with a share of cost effective analysis. If surface of specific manufactured element has similar surfaces quality to other it surfaces, the set of parameter of quality for each one should be assigned. The algorithm should adapt other parameters to reach specific level of other surface layer roughness [5].

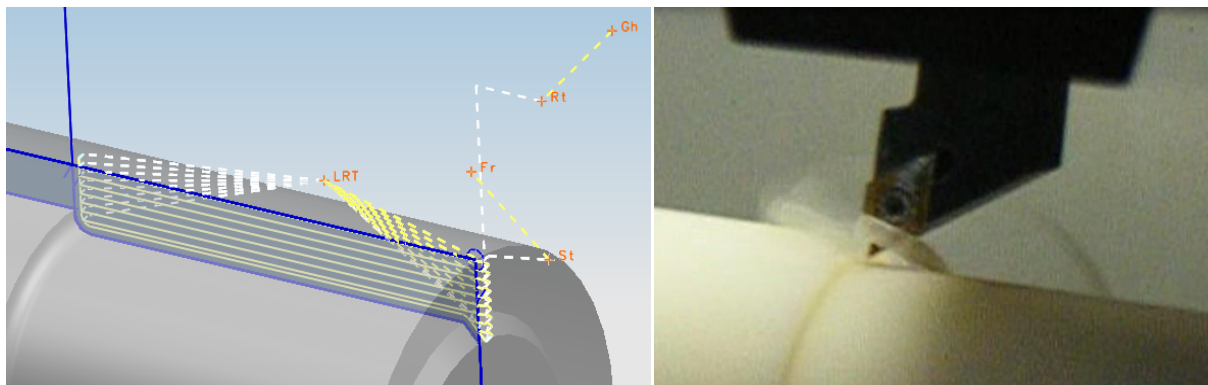


Fig.4. Automatically generated tool trajectory according to point-set distribution generated with algorithm and practical verification of chip removal

3. Summary

The software development environment like MS Visual Studio or GRADE, gives possibility to prepare software that can optimise: a trajectory, cutting parameters and a strategy of cutting. The balance of surface quality and operation time is a major problem to solve with the optimization algorithm. Furthermore the optimization algorithm can be bounded with data stored in a database which contains empirical data gathered during tests. Each solution of an optimized operation should be well described and gathered according to similar type of operations, for future use without need of additional research and tests, with only proper adjustment.

References

1. Grabowik C., Janik W.: The concrete casting matrixes inserts design preparation based on the master models, *Advanced Materials Research, Advanced Material Science and Mechanics*, 2013 vol. 702, p. 259-262.
2. Grabowik C., Kalinowski K.: Object-oriented models in an integration of CAD/CAPP/CAP systems. *Lecture Notes in Computer Science (including subseries Lecture Notes in Artificial Intelligence and Lecture Notes in Bioinformatics)*, 6679 LNAI (PART 2), (2011) p. 405-412.
3. Grabowik C., Janik W.: *NX GRIP – CAD*, Wyd. Pol. Śl., 2012
4. Grabowik C., Janik W.: Zastosowanie języka GRIP w technicznym przygotowaniu produkcji, *Komputerowo Zintegrowane Zarządzanie*, T. 1. Pod redakcją Ryszarda Knosali, Oficyna Wydawnicza Polskiego Towarzystwa Zarządzania Produkcją, 2009 p. 373-381.
5. Janik W.: The method of a material loss detection for cylindrical shape parts of elements with a 3D scanning application, *International Journal of Modern Manufacturing Technologies*, 2013 vol. 5 no. 2, p. 58-64.

SELECTED ENGINEERING PROBLEMS

NUMBER 5

INSTITUTE OF ENGINEERING PROCESSES AUTOMATION
AND INTEGRATED MANUFACTURING SYSTEMS

Adrian KAMPA^{1*}, Grzegorz GOŁDA¹

¹ Institute of Engineering Processes Automation and Integrated Manufacturing Systems Department,
The Faculty Of Mechanical Engineering, Silesian University of Technology, Gliwice

* adrian.kampa@polsl.pl

RAPID MACHINING WITH INDUSTRIAL ROBOT

Abstract: Industrial robots are used for many tasks, mainly for material handling and welding. Robots can be also equipped with other tools and used for machining. Nowadays small numbers of robots are used mainly for machining of soft materials, such as plastic, wood, foam and aluminium. This technique is used mainly for rapid prototyping. In this article an example of computer modelling of robotic cell for machining is shown. Some problems related with robot programming, accuracy, repeatability and calibration are discussed. An example of machining in polystyrene is presented.

1. Introduction

Industrial robots are now becoming wider use. It is estimated that around the world is already over one million industrial robots and a systematic increase in their numbers is observed. Most applications of robots include manipulation of cargoes and welding services. In such tasks, industrial robots have proven themselves very well. But robots are characterized by their high versatility and can be also equipped with cutting and grinding tools and used for some machining tasks. Because industrial robots are built similar to human arm and shows a high flexibility of movement, they are predestined to the tasks associated with manual work, such as e.g.: deburring and chamfering of sharp edges or grinding and polishing the surfaces [6].

Due to the low stiffness of robot arm and cutting forces arising during operation, previous application of robots is limited primarily to machining of relatively soft materials such as wood, plastics, aluminum alloys and non-ferrous metals. At work [2], a model of a load of the robot arm during machining is presented and predicted value of cutting force for different materials were compared. In the case of hard materials such as steels and cast iron, it is followed by a significant increase in cutting forces that result in unfavourable load of robot arm. Machining of soft materials can be classified as rapid prototyping techniques [3]. The resulting prototypes can serve as models for the implementation of the molds or as a temporary enclosure and insulation [4].

2. Robot programming

Robots can be programmed on-line directly at the workcell (teaching by operator) or off-line using a dedicated computer systems. Directly teaching by operator in the case of common handling task is relatively easy. However, in the case of machining tasks, there are some complications, because of a collision trajectory of the robot. Because the tool delves into the material and must move after specific trajectories associated with the geometry of the part.

This causes complications while programming, which is why the off-line programming with dedicated programs, such as, DELMIA, RobotMaster, RoboGuide and others, are used. These are the advanced CAD/CAM systems, which enables to build three-dimensional virtual model of the robot and workcell. Virtual robot can be controlled with virtual teach pendant similar to real robot. Generation and simulation of robot program is possible, which allows testing the robot work before implementation. Robot motion path can be generated based on the geometry of the workpiece (CAD to PATH). Then developed programs can be sent to the robot control system and executed. Developed model of robotic workcell for machining is shown in figure 1.

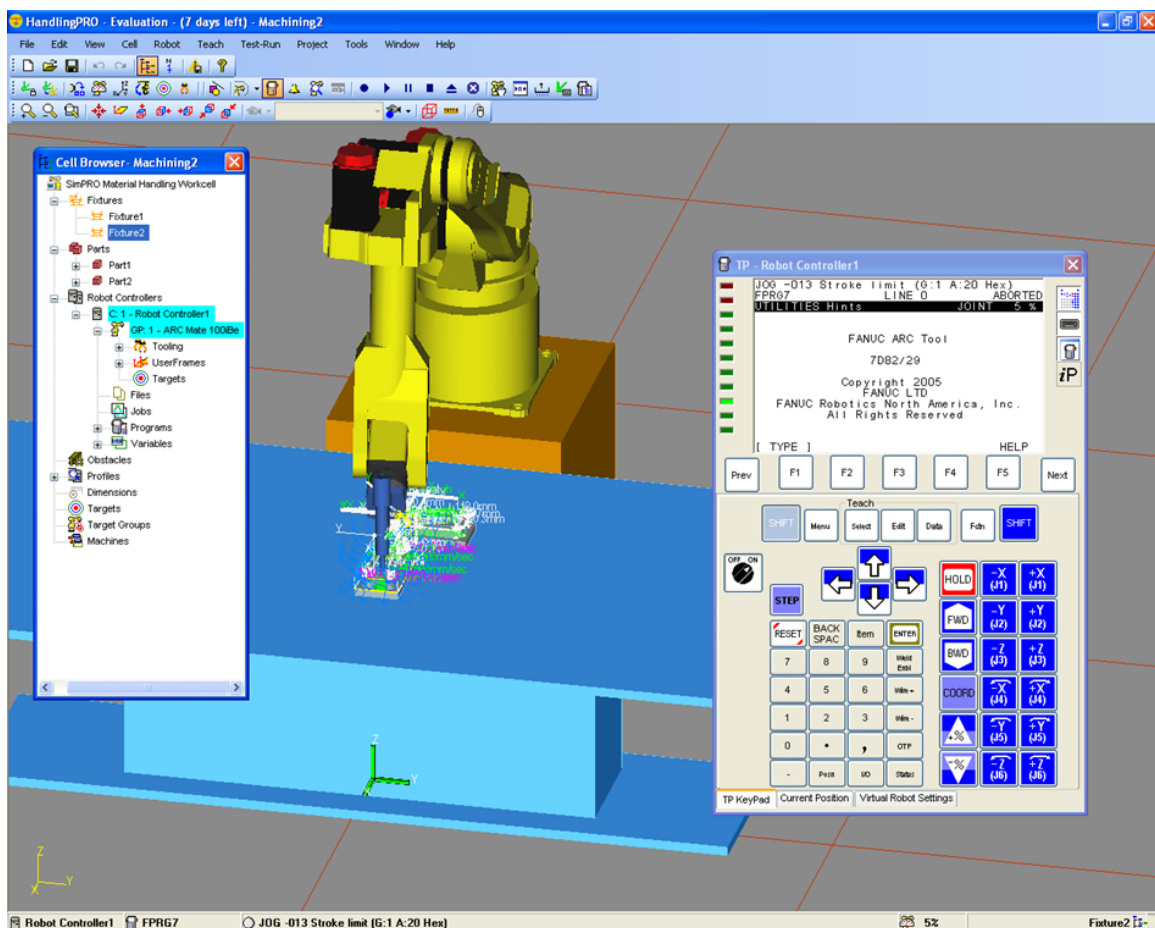


Fig. 1. Virtual model of robotic workcell for machining in RoboGuide

3. Robot accuracy, repeatability and calibration

Robot manufacturers, as an industry standard, publish the accuracy and repeatability of each machine. These specifications are determined in accordance with ISO standards 9283 [9]. Typical robots achieve the accuracy of positions and repeatability about ± 0.1 mm. High precision robots are possible to obtain accuracy about $\pm 0,01-0,05$ mm [6]. For high positioning precision a calibration of robot is needed. Calibration is the process of determining the actual values of kinematic and dynamic parameters of an industrial robot and is usually done by manufacturers.

In the case of computer-generated programs prior to running the robot a cell calibration is also required, i.e. determination of reference points between the computer model and position of elements in the real world. This is related, inter alia, with the dimensional inaccuracy between the computer model and the real workcell.

The robot's control system uses several coordinate systems (Fig. 2) that can be assigned to the various elements of the workcell and can be modified if necessary. The control system automatically recalculates coordinates expressed in different frames and adjusts the motion path. In typical applications the robot movement is done by non-collision trajectories and position accuracy is required only in certain positions. However, in the case of machining tasks there are some collision trajectories and precision robot movement is required. Each deviation has a direct reflection of the workpiece surface.

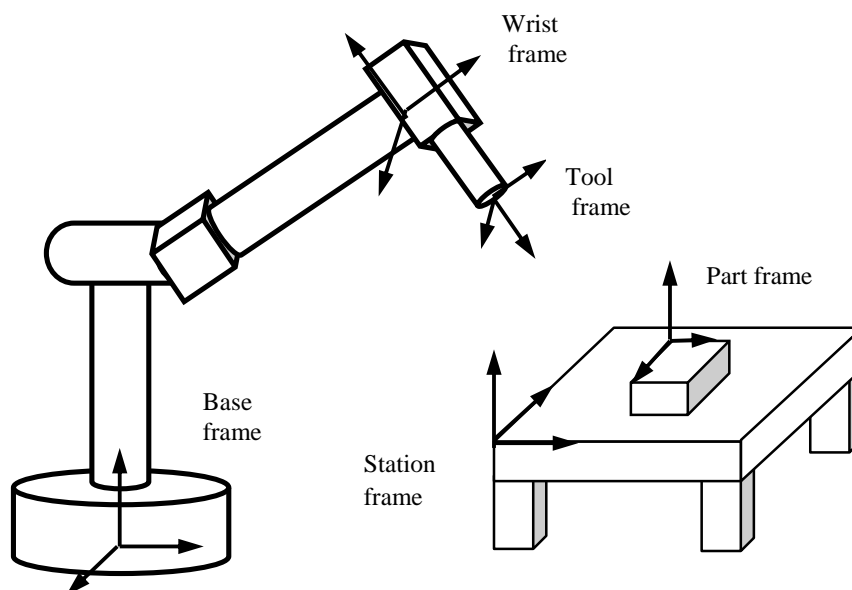


Fig. 2. Robotic workcell coordinate system

Positioning accuracy of robot is determined by a number of errors related to deviation in representation of the robot structure and kinematics and the dynamic influence [1]. It depends upon many different factors that include: friction, temperature, loading, manufacturing tolerances etc.

Robot positioning errors to a large degree are dependent on the arm configuration settings. At a constant setting of arm some tools errors ($+\delta-\delta$) are compensated, while at the opposite arm configuration the tool error is doubled (-2δ). (Fig. 3).

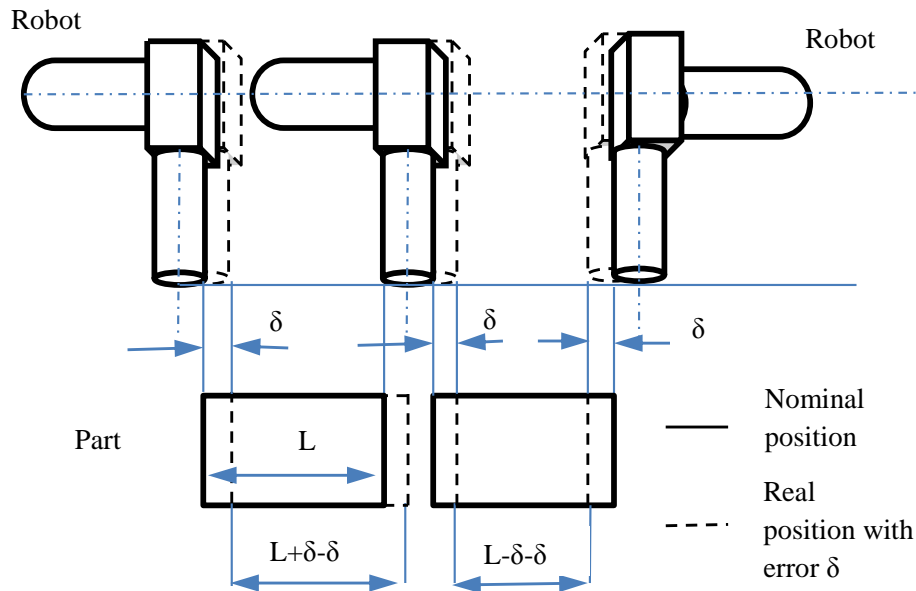


Fig. 3. Robot tool error δ and part accuracy

In the case of machining operation the uncertainty of robot motion is reflected in the uncertainty of the workpiece, therefore by measuring inaccuracies of the workpiece, it can be determined whether the robot was well calibrated. The most accurate method of robot calibration is the use of special laser trackers [7].

4. Robot machining

There are some examples of machining with robots described in bibliography [6] and presented in Internet [8]. The figure 4 shows the machining example of polystyrene cover. Robot program has been generated on the basis of the 3D model shown in Figure 1. The operation was carried out using a robot Fanuc ArcMate 100iB equipped with pneumatic spindle 2000 rpm with a mill cutter from HSS with diameter 12 mm. The treatment was successful and the desired accuracy $\pm 0,5$ mm has been achieved. Obtained part can be used as insulation cover. The processing was very fast, therefore it can be denominated as rapid machining.

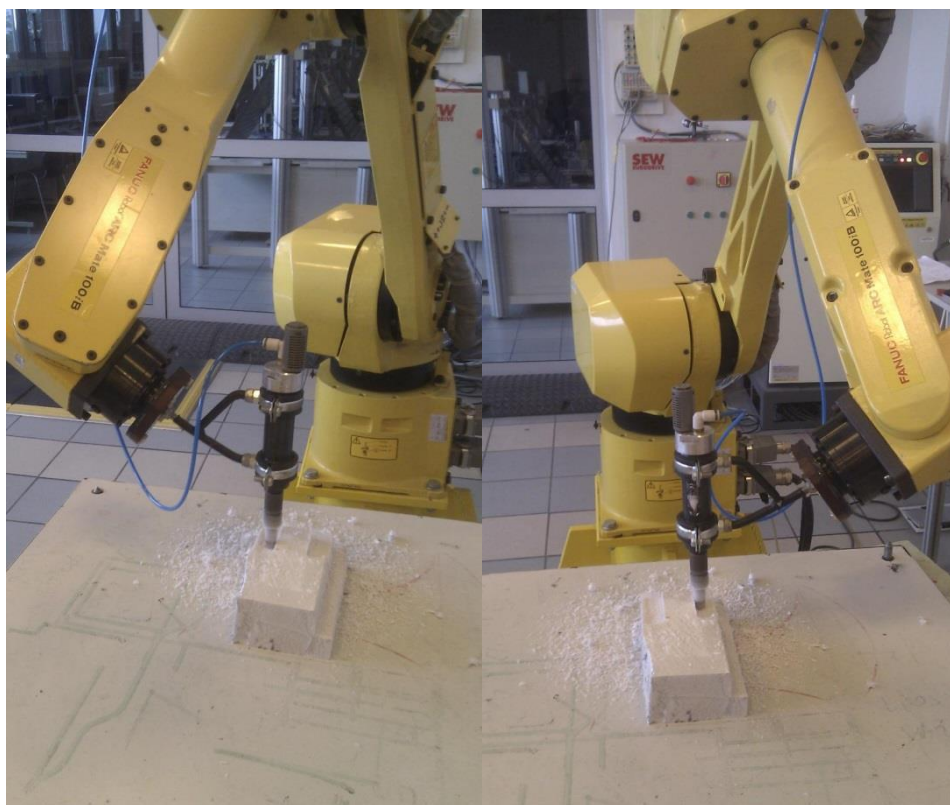


Fig. 4. Example of machining of workpiece from polystyrene

5. Conclusion

The use of industrial robot for the machining shows a number of advantages. Industrial robot can replace a worker while performing the tasks associated with manual processing and some machinery tasks. Compared to the classic machine tools, industrial robots have a much smaller mass and a lower stiffness. According to the work [5] rigidity of heavy-duty robots falls within the scope of about 200-700 N/mm. These values are about ten times lower than the typical rigidity of machine tools. As a result, positioning accuracy obtained by robots is much lower than the accuracy of the machine tools. However, for many of the machining tasks the accuracy is sufficient. Robots advantages are large workspace and faster speed of movement. The use of additional axes controlled as positioners or contact tracks allows enlarging the working space and handling of bulky workpieces. There are potentially large possibilities of use of robots in machining tasks, however, it is related with high cost of investment in robotization.

References

1. Conrad, K. L., Shiakolas, P. S., & Yih, T. C. (2000, July). Robotic calibration issues: Accuracy, repeatability and calibration. In Proceedings of the 8th Mediterranean Conference on Control and Automation (MED2000), Rio, Patras, Greece. p. 6
2. Gołda G., Kampa A.: Modelling of Cutting Force and Robot Load During Machining. Advanced Materials Research Vol. 1036 (2014) pp 715-720

3. Gołda G., Kampa A.: The use of industrial robots in rapid prototyping processes. Postępy robotyki T. 2, pod red. K. Tchoń, C. Zieliński. Oficyna Wydawnicza Politechniki Warszawskiej, Warszawa 2014, s.579-586. (in polish)
4. Kampa A.: Impact of rapid prototyping techniques for the manufacturing of new products. SELECTED ENGINEERING PROBLEMS No 3, Gliwice, 2012, p. 93-96
5. Lehmann Ch., Halbauer M., Euhus D., Overbeck D. (2012). Milling with industrial robots: Strategies to reduce and compensate process force induced accuracy influences. http://www.cometproject.eu/publications/etfa2012_a34.pdf
6. Yonghua Ch., Fenghua D.: Robot machining: recent development and future reaserch issues. The International Journal of Advanced Manufacturing Technology, June 2013, Volume 66, Issue 9-12, pp 1489-1497.
7. FARO – <http://www.faro.com/en-us/solutions/applications/robot-calibration> (access 7.10.2014)
8. Kuka Milling : <http://www.kuka-robotics.com/usa/en/products/systems/milling/start.htm> (access 7.10.2014)
9. ISO 9283 Manipulating Industrial Robots – Performance criteria and Related Test Methods”. International Standards Organization, 2003.

SELECTED ENGINEERING PROBLEMS

NUMBER 5

INSTITUTE OF ENGINEERING PROCESSES AUTOMATION
AND INTEGRATED MANUFACTURING SYSTEMS

Klaudiusz KLARECKI¹, Dominik RABSZTYN², Mariusz Piotr HETMAŃCZYK³

^{1,2,3}Institute of Engineering Processes Automation and Integrated Manufacturing Systems,
Faculty of Mechanical Engineering, Gliwice, Poland

*kladiusz.klarecki@polsl.pl

THE EFFECT OF BACKGROUND CURRENT INTENSITY ON THE HYSTERESIS OF PROPORTIONAL VALVES

Abstract: The article presents the results of experimental studies focused on effect of setting background current on the hysteresis of the proportional directional control valve (D1FB series, manufactured by the Parker Hannifin). Described tests were performed according to the Fractional-Factorial Experiment Method (FFEM). In presented experiment influence of the background current, vibrations and the positioning accuracy of hydraulic receivers on pressure pulsations have been omitted.

1. Introduction

Proportional valves are widely used in modern electrohydraulic systems [7], especially in hydrostatic systems. In spite of that fact many users do not fully understand the rules of their actions, what causes limitation of the quality of designed systems.

One of the major drawbacks of proportional directional control valves without internal feedback system is a large hysteresis, resulting mainly from the frictional resistance of moving parts (valve head or slider located in the sleeve) [1,2,4]. This may cause problems with the positioning [3,5,6] of a hydraulic drive controlled by the valve or other objectionable effects. Manufacturers reduced the hysteresis of valves by equipping electromechanical transducers with control systems allowing adjustment of a variable DC component, so-called background current (named also like the Dither current intensity) [8]. For described case the movable parts of valves are triggering in vibrations what apparently reduces the influence of friction.

Parameters of the background current intensity have an impact not only on the value of the hysteresis but also on [2]: pressure pulsations, vibration level, lifetime of the proportional valve subassemblies (wear of slider and bushing) and reliability of the hydraulic devices (eg. an appearance of leakages between the valve chambers).

2. Description of the experimental studies

The study was carried out on the basis of hydraulic system consisting of: the proportional directional control valve (D1FBB32FC0NJW0 Parker Hannifin [8]) powered with the

PWD00A-400 amplifier, a rotary hydraulic motor (PGM511A0060B54D3N series) and hydraulic power feeder. An evaluation of an influence of the Dither current intensity on hysteresis of the proportional valve has been realized on the basis of the test stand built according to the hydraulic diagram presented in the figure 1a.

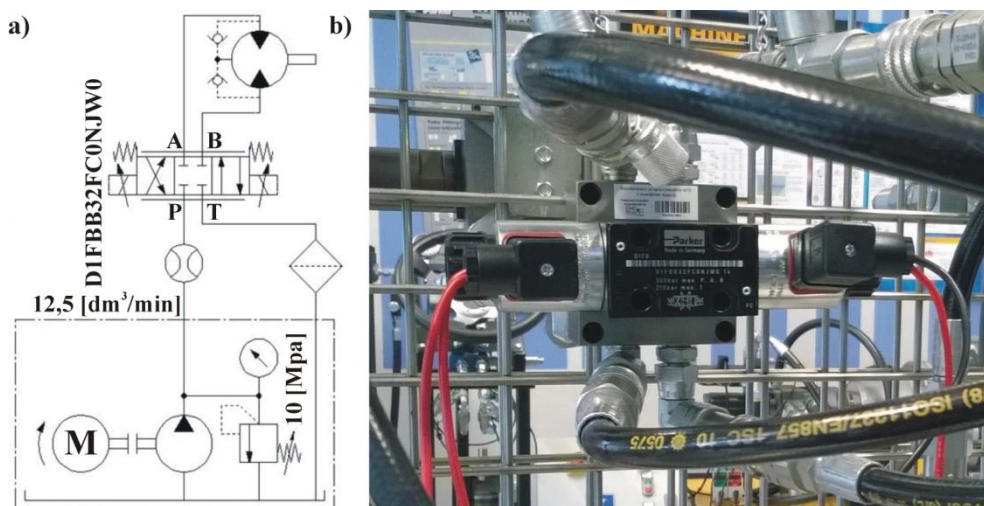


Fig. 1. The test stand: a) the hydraulic diagram, b) view of tested valve

During experiments parameters of the background current intensity were changed within the following ranges:

- frequency - $20 \div 80$ [Hz] (range recommended by the manufacturer $30 \div 60$ [Hz]),
- oscillation amplitude - $0 \div 8\%$ of the constant component C_C (range recommended by the manufacturer $3 \div 6\%$ of the C_C value).

3. The effect of Dither current on the valve hysteresis

Measurements were carried out for several Dither current parameter settings, including set points compatible with default manufacturer and without a Dither current intensity modulation.

Figure 2a shows example characteristics obtained as a result of the static test of the D1FB proportional directional control valve without Dither control. In the presented case the largest apparent value of the hysteresis occurs in the control voltage values about $|4|V$. This is due to the insensitivity of a turbine flow meter used for measuring the flow rate.

The hysteresis value for the linear part of characteristics has been determined at the absolute value of control voltage equal $|6| V$. In order to eliminate fluctuations of recorded hysteresis values, the following procedure was adopted:

- regression lines were determined for various runs (ascending and descending) in terms of the control signal $5 \div 7V$ (a flow from P to B direction) and $-7 \div -5V$ (the flow from P to A direction),
- on the basis of obtained regression equations a flow rate or rotational speed of the receiver were determined ($6V$ - the flow from P to B and $-6V$ - the flow from P to A),
- the hysteresis value is defined as the difference between regression equations (of the flow or rotation of the receiver) divided by the maximum value of the recorded value.

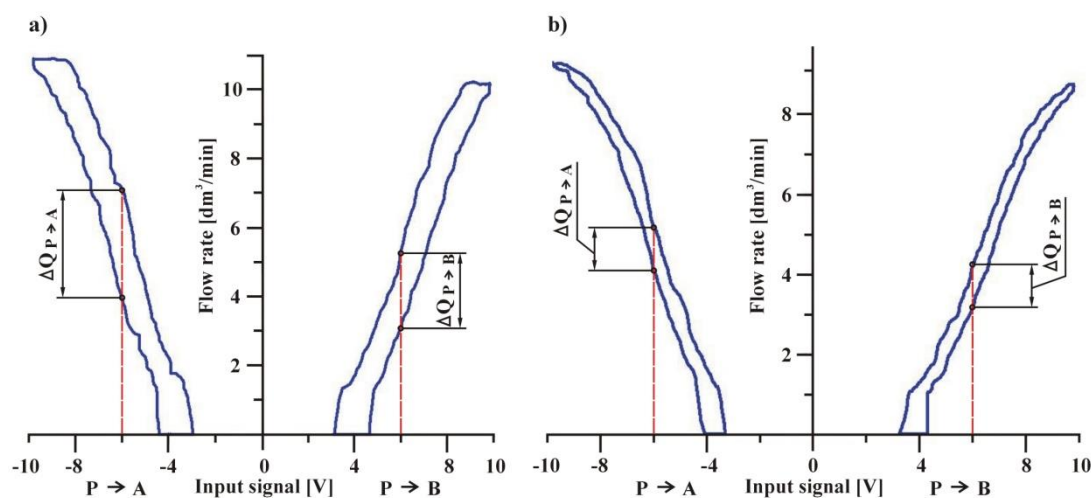


Fig. 2. Static characteristics of the proportional directional control valve (type D1FB): a) without Dither control, b) with the Dither control

The obtained experimental results for selected valve control settings and partial scores (S_c) for accepted Dither current settings are shown in Table 1.

Tab. 1. Results of performed laboratory tests with partial scoring ($S_c=0\div 5$, maximum value means best meet the requirements)

FFEM indexes				Hysteresis at 6 V input signal				Standard deviation of hysteresis				S_c
x_1	x_2	f_r [Hz]	A [%]	Δn P-B	ΔQ P-B	Δn P-A	ΔQ P-A	$s(\Delta n)$ P-B	$s(\Delta Q)$ P-B	$s(\Delta n)$ P-A	$s(\Delta Q)$ P-A	
-1	-1	29	1,2	12,3%	13,6%	15,7%	17,7%	1,70%	1,73%	1,68%	2,03%	2
-1	1	29	6,8	7,4%	8,9%	8,4%	9,8%	0,09%	0,71%	0,56%	1,25%	4
1	-1	71	1,2	16,7%	18,1%	19,8%	21,3%	2,38%	1,66%	1,53%	1,58%	1
1	1	71	6,8	8,7%	9,9%	9,8%	10,8%	0,60%	0,14%	0,97%	0,89%	3
-1,41	0	20	4	7,6%	9,0%	8,3%	9,4%	1,46%	1,68%	0,94%	0,99%	3
1,41	0	80	4	10,9%	12,0%	14,5%	15,8%	1,10%	1,38%	1,20%	1,59%	2
0	-1,41	50	0	18,8%	19,6%	21,9%	23,8%	1,55%	1,65%	1,74%	1,51%	0
0	1,41	50	8	7,2%	8,1%	7,6%	9,3%	0,55%	0,31%	0,83%	1,25%	4
0	0	50	4	9,2%	10,2%	8,9%	10,9%	0,77%	0,99%	0,48%	0,95%	3

It is noted that tested proportional directional control valve is characterized by a certain asymmetry in operation:

- flow in the direction P→A is characterized by a noticeably bigger hysteresis (smaller backlash of slider in the sleeve),
- differences in the maximum values of flows (directions A→P and P→B) result from unsymmetrical grooves made on the edges of the slider (A:B→2:1 version).

5. Conclusions

Presented results of experimental studies focused on the impact of Dither current settings (especially frequency and amplitude) on the hysteresis of proportional valve lead to the following conclusions:

- hysteresis of proportional directional control valves is much more sensitive to the Dither amplitude than its frequency, therefore the correct setting of the valve in order to minimization of the hysteresis should take into account in the first instance the Dither amplitude,
- control with the low frequency of Dither current (below the limit frequency of the valve) may result in adverse pressure pulsations and this may cause rising resonance in the driven machine and in consequence to its failure or damage.
- exist the need to optimize the setting holding current (chosen by the producers of proportional valves according to the general principles of tuning without considering the impact of the external loads).

Additionally it must be taken into consideration the characteristics of the receiver (hydraulic cylinder), which affects at the accuracy of the entire system. The next step will be connected with investigations including dependence of the control parameters and valve lifetime (in terms of vibration and amplitude of valve slider).

References

1. Barbachowski E., Klarecki K.: Methods for Correcting The Characteristics of Proportional Valves "Selected Engineering Problems" 2011, No. 2, pp. 29–34(in Polish).
2. Klarecki K., Hetmańczyk M., Rabsztyń D.: Multi-Criteria Optimization of The Dither Current Intensity in The Case of Proportional Valve. "Vibroengineering Procedia" 2014, Vol. 3, pp. 82-87.
3. Klarecki K., Hetmańczyk M., Rabsztyń D.: Influence of The Controller Settings on The Behaviour of The Hydraulic Servo Drive. "Mechatronics-Ideas for Industrial Application. Advances in Intelligent Systems and Computing" 2015, Vol. 317, pp. 91-100.
4. Kudźma Z.: Test Stand for Estimation of Static and Dynamic Characteristic of Proportional Hydraulic Valves. "Measurements Automation and Robotics" 2014, Vol. 3, pp. 112-119 (in Polish).
5. Milecki A.: Linear Electro Hydraulic Servo Drives. Poznan: Poznan University of Technology Publishing, 2003 (in Polish).
6. Pizoń A.: Electro Hydraulic Analog and Digital Automation Systems. Warsaw: WNT Publishing House, 1995 (in Polish).
7. Tomasiak E., Klarecki K., Barbachowski E.: Servo Drives in Machine Construction. "Hydraulics and Pneumatics" 2009, No. 1, pp. 16-20 (in Polish).
8. Materials developed by Parker Hannifin: Direct Operated Proportional DC Valve Series D1FB.www.parker.com/literature/Hydraulic%20Controls%20Europe/HY113500UK/PDF_2013/D1FB%20UK.pdf.

SELECTED ENGINEERING PROBLEMS

NUMBER 5

INSTITUTE OF ENGINEERING PROCESSES AUTOMATION
AND INTEGRATED MANUFACTURING SYSTEMS

Damian KRENCZYK^{1*}

¹ Institute Of Engineering Processes Automation And Integrated Manufacturing Systems,
Faculty of Mechanical Engineering, Silesian University of Technology, Gliwice, Poland

*damian.krenczyk@polsl.pl

THE AUTOMATED PROCESS OF CREATING SIMULATION MODELS

Abstract: In the paper the method of data transformation to a scripting language code creating the simulation model objects used in the implementation of the methodology of production planning and control with discrete simulation systems integration has been presented. For this purpose the so-called transformation templates containing the code of the templates, without a specified value, but together with the placement of the input data have been used. The examples of transformation template notation and the result code generated by the XSLT processor have been shown.

1. Introduction

Increasing the efficiency of the production planning and scheduling process, which in today's enterprises is one of the main areas where on a large scale computer support applications are used, is made possible by the integration of production planning and control (PPC) systems and systems of computer modeling, simulation and visualization of production processes flow [1, 2, 6, 7].

In the previous papers [2, 3, 4, 5], the methodology of integration of production planning and control systems with discrete event simulation systems (DES), based on the methods of data mapping and data transformation has been presented. The main advantage of the proposed approach is the ability to generate the simulation models automatically regardless of the production system structure, which depends on the actual type of production flow.

The structure of the production flow can be changed depending on the produced assortment in the production system, resulting from a package of orders for the planning period. Another distinguishing feature of the proposed method from the solutions available on the market is the flexibility in adapting the proposed solutions to computer aided planning systems and discrete-event simulation systems through the use of the neutral data formats and the neutral intermediate data model. Generated simulation models are given the opportunity to use the data obtained from conducted simulation experiments to support decision-making process in the planning area and should be a very effective tool for verification of production plans and the possibility of order execution.

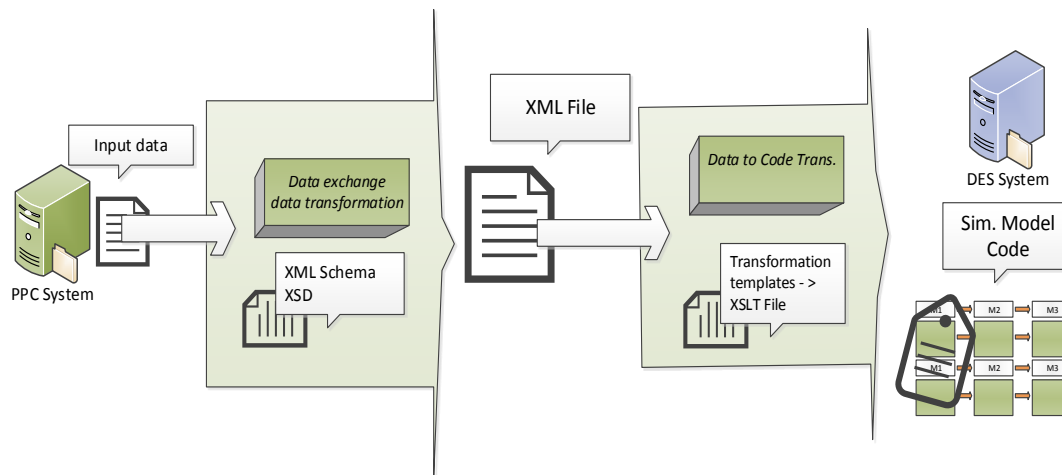


Fig.1. The method of integration of production planning and control systems with discrete event simulation systems

The implementation of the proposed methodology (Fig. 1) requires the identification of data mapping and transformation methods for specific, chosen production planning and simulation systems. The implementation process requires to carry out the process of the data schema mapping between source and target schema for the intermediate data model. Then the process of data transforming between the intermediate model and the target model is performed for the data required in the transformation template process to script code of simulation system internal language. The results of the mapping in the form of logical formulas, so called depending formulas, are the basis to generate a transformation code in extensible style sheet language transformations (XSLT). In this paper the stage of data transformation to script code using a *transformation template* for the two commercial simulation systems has been presented.

2. Transformation template

Generating a script code in the internal simulation system language is a sequential process and must be performed in the order of the individual layers to a defined simulation model. It is not possible, for example, to generate the parameterization code of the cycle-times for manufacturing resources without previous generating the code to create the appropriate amount of production resources resulting from the input data. Data transformation process to the internal code of the simulation system programming language is implemented based on the defined *transformation template* - templates containing code with a specific location of the input data (either directly or using a transformation function). The developed functions correspond to individual layers of code of creation of a simulation model.

The transformation template is defined as three [4]: $TS_i <[tmp(\#1...\#n)]; A_j; m>$;
where:

TS_i – i -th numer of the transformation template; this number determines the location of the transformation in the sequence,

$tmp(\#1...\#n)$ – the template which is a text string containing the lines of the code of internal simulation system programming language with tags $\#1...\#n$, specifying

the place of entry to a data template; tags can be used to implement arithmetical operations on the data, which correspond to (e.g. #2-#1, #2*#11),

A_j – data corresponding to the tags in the template, j = 1...n,

m – the number of repetitions in the template code.

The transformations templates are defined at the stage of implementation of the methodology, because the templates necessarily correspond with syntax of the internal programming language of the simulation system.

a. Practical example

An example of the transformation which uses 4dScript language of Enterprise Dynamics system that creates an instance of the production resource in the manufacturing simulation model is shown below:

```
TS10 <[Sets(CreateAtom(AtomByName([Server], Library), Model, [M#1])),
setloc(_(4+7*(#1 - round((#1-1)/#2))*#2)_ , _(round((#1-1)/#2+1)*3)_ ,0),
SetChannels (_(count(#3))_ , _(count(#3))_ ,s)], Id, y_pos,
No_of_Processes, 1>
```

The example of the transformation template, using FlexScript language of FlexSim simulation system, which, like the above, it creates an instance of the manufacturing resource in the simulation model is:

```
TS10 <[createinstance(node("/Processor", library()), model());
setname(last(model()), "M#1"); setloc(last(model()), _(4+7*(#1 - round((#1-
1)/#2))*#2)_ , _(round((#1-1)/#2+1)*3)_ ,0);], Id, y_pos, No_of_Processes,
1>
```

For prepared transformation template may then be generated the resulting code in the data transformation language selected by the user: XSLT, SQL, XQuery, Java, or C++. Generated XSLT code for the above example (for Enterprise Dynamics system) is as follows:

```
<xsl:for-each select="Production_System/Resources/Resource">
  Sets(CreateAtom(AtomByName([Server], Library), Model, [M<xsl:value-
of select="Id"/>])),
  setloc(<xsl:value-of select="4 + 7 * (Id - ((round((Id - 1) div
$rzad)) * $rzad))"/>, <xsl:value-of select="(round((Id - 1) div $rzad) + 1)
* 3"/>, 0),
  SetChannels (<xsl:value-of
select="count(/Production_System/Processes/Process)"/>, <xsl:value-of
select="count(/Production_System/Processes/Process)"/>, s),
</xsl:for-each>
```

For the other simulation systems creation of transformation templates is carried out in a similar manner, and its content is also dependent on the adopted neutral data model.

b. Simulation model objects code

By using data, describing the production system and manufacturing processes, stored in the intermediate data model and above transformations templates and generated on the basis of their XSLT code, program code containing instructions for creating a fully functional

simulation model can be generated. For this purpose, it can be used on any XSLT processor software, eg. XMLSpy, Sablotron for C++, XSLT for PHP, etc. The following is a fragment of the generated 4DScript code for creating objects in the simulation model:

```

Sets(CreateAtom(AtomByName([Server], Library), Model, [M2])),
setloc(18,3,0),
SetChannels(5,5,s),

SetExprAtt(1,[czasy(Value(StripString(Name(First(c)),[P])),Value(StripString(Name(c),[M])))],s),
SetExprAtt(2,[Value(StripString(Name(First(c)),[P]))],s),

SetExprAtt(18,[openic(lrrkz(Value(StripString(Name(c),[M])),+(mod(input(c),lrrkz(Value(StripString(Name(c),[M])),299)),1)),c)],s),
OnReset(s):=[Do(Inherit,CloseAllIc(c),InStrategy)]

```

The full versions of the models and files presented in this article, can be found on the website: imms.home.pl/RapidSim.

3. Conclusion

Approach and software tools presented in this paper make it possible to directly generate the simulation models of production systems. The implementation of the methodology of PPC and DES systems integration, which uses the presented methods is applicable to data acquired from PPC systems, regardless of the structures of the production system, the topology of the processes flow in the system or the amount of resources and production orders. Further research on the methodology presented in the article addresses issues related to the area of the development of the concept of virtual enterprises and dynamic manufacturing networks.

References

1. Drake G. R., Smith J. S., Peters B. A.: Simulation as a planning and scheduling tool for flexible manufacturing systems. Proceedings of the WSC 1995, pp. 805–812.
2. Krenczyk D.: Data-driven modelling and simulation for integration of production planning and simulation systems. Selected Engineering Problems, no. 3, 2012, pp. 119–122.
3. Krenczyk D.: RapidSim – software for supporting PPC and DES systems integration. Selected Engineering Problems, no. 4, 2013, pp. 119–122.
4. Krenczyk D.: Integration of production planning and discrete event simulation systems (in polish), Wydawnictwo Politechniki Śląskiej, Gliwice, 2013.
5. Krenczyk D., Skołud B.: Production preparation and order verification systems integration using method based on data transformation and data mapping. Lecture Notes in Computer Science, vol. 6697 2011, part II, 297-404.
6. Lee S., Son Y.-J., Wysk R. A.: Simulation-based planning and control: From shop floor to top floor. Journal of Manufacturing Systems, vol. 26, no. 2, 2007, pp. 85–98.
7. Sihm W.: Simulation-based configuration, animation and simulation of manufacturing systems. Progress in Virtual Manufacturing Systems, pp. 215–218, 2003.

SELECTED ENGINEERING PROBLEMS

NUMBER 5

INSTITUTE OF ENGINEERING PROCESSES AUTOMATION
AND INTEGRATED MANUFACTURING SYSTEMS

Łukasz MANDLA, Edyta KRZYSTAŁA

Department of Theoretical and Applied Mechanics, Faculty of Mechanical Engineering,
Silesian University of Technology, Gliwice, Poland
lukasz.mandla@gmail.com, Edyta.Krzystala@polsl.pl

THE USE OF BIOMECHANICAL INDEX TO ESTIMATE SOLDIER'S LEVEL OF THREAT

Abstract: The aim of the article was to characterize the biomechanical indicators for assessing the severity of the crew of special vehicles. Defined parameters affecting obtainable value of indicator, their the method of determining and interpretation. In addition, the author developed a original computer program to determine the biomechanical indicators. The examples of the results of the indicators obtained on the basis of experimental studies are presented as well.

1. Introduction

An explosion of land mine under a military vehicle has a great influence on the vehicle itself but also, and first of all, on the people inside it. All factors like temperature, pressure or acceleration have a measurable impact on a person's physical and mental health. A branch of science dealing with mechanical overload on a human body is called biomechanics. Each part of the body, any organ reacts in a different way to a given overload. To understand the threats biomechanical index has been elaborated for their estimation [2, 3].

The scale of crew's danger in a moment of explosion depends on the distance from the source of explosion as well as the direction of the shock wave. A proper vehicle construction is able to cushion some of the overloads or at best level them completely. To parts of the body most prone to injury we include a head, a spine, lower limbs and internal organs. The explosion is connected with many factors which influence the body in many various ways [2, 3].

2. Head Injury Criterion

A head is the most injury-prone part of a body. It often happens that passengers of military vehicles experience serious injuries, lameness or even death. Such injuries are common in car crashes that's why the parameter is often tested in crash-tests to evaluate the vehicle's safety [2].

Overload tolerance is individual for every person and depends on such factors like age, sex, health condition. The degree of injury is dependent on maximum parameter value but also the direction of acceleration and time [1,2].

To set a factor Head Injury Criterion the formula beneath is applied [2,3]:

$$\text{HIC} = \max \left[(t_2 - t_1) \left(\frac{1}{t_2 - t_1} \int_{t_1}^{t_2} a(t) dt \right)^{2,5} \right] \quad (1)$$

where:

$a(t)$ - acceleration of the center of mass of the head [m/s^2],

g - gravity acceleration [m/s^2],

$(t_2 - t_1)$ - interval of maximum acceleration [s].

For the factor HIC36 critical value was taken 1000. The research is done within 36 ms. Exceeding the value can result in serious head injuries or even a loss of life. The value was used regardless of sex, age, or weight of a person. The latest research suggests lowering critical value HIC 15 to 700 (examined max within 15 ms) as a barrier between the lack of injuries and the appearance of medium injuries. The value would be right for men, women and children over the 6th year of age. For 3 year old children the value would be 570 and for babies/infants 390. The values were examined due to a fact that the factor is also used to check car safety, airbags or in designing extreme sport helmets. Head Injury Criterion is the basic criterion used in designing soldier's helmet too [2, 3, 1].

3. Neck Injury Criterion

The mechanism which reduces overload affecting head is neck spinal column. In the moment of acceleration the head moves backwards. The move gives a beginning to forces affecting cervical vertebrae which results in injuries. Very often along with head injuries, the spine is endangered too. Biomechanical factor describing the relation of acceleration impact and speed over the probability of injury is called Neck Injury Criterion [2, 3].

$$\text{NIC} = 0,2a_{rel} + v_{rel}^2 \quad (2)$$

where:

a_{rel} - the relative acceleration between the first thoracic vertebra (T1), and the first cervical vertebra (C1) [m/s^2],

v_{rel} - the relative velocity between the first thoracic vertebra (T1), and the first cervical vertebra (C1) [m/s],

0,2 – constant that specifies the length of the cervical spine.

The critical value index is assumed NIC 50 -15 m^2/s^2 . After exceeding the value there is a change in the natural shape of spinal column what in consequence results in breakage of vertebra and other and other serious injuries. All spine injuries lead mostly to lameness and death at worst [2, 3].

The acceleration exerted on the spine turns into certain squeezing and stretching forces as well as bending moments affecting the cervical part of the spine. There is a criterion including the parameters called N_{ij} . Beneath the formula is presented [2, 1, 8]:

$$N_{ij} = \frac{F_z}{F_{int}} + \frac{M_y}{M_{int}} \quad (3)$$

where:

F_z – compression force [N],

M_y – extension or flexion bending moment [Nm],

F_{int} – critical value for extension or flexion [N],

M_{int} – critical value for extension [Nm].

The parameter in the formula depends on type of overload. The force in the axle can squeeze vertebra or cause their stretching. Critical value of axle force is independent on the direction of its action. A slightly different situation occurs during bending moments. For N_{ij} criterion, index border value equals 1.0. Exceeding the value means 15% probability that serious injuries will occur. The probability rises proportionally to the rise of index value. The most common injuries of cervical part are breakage, grinding or twisting [2, 1, 8].

Table 1. Critical value of parameters for N_{ij} criterion [2, 8]

Human body type	Compression force [N]	Flexion force [N]	Bending moment to front [Nm]	Bending moment to back [Nm]
1 year -old baby	1465	1465	43	17
3 year-old toddler	2120	2120	68	27
6 year- old child	2800	2800	93	39
Woman	3370	3370	155	62
Average man	4500	4500	310	125
Big man	5440	5440	415	166

4. Combined Thoracic Index

Thoracolumbar part of the spine like the cervical is prone to serious injuries evoked by explosion. At the highest level there are inner organs namely a heart or lungs, absolutely essential for life. The organs are protected by ribs which nonetheless under pressure of shock wave bend or even break leading finally to their complete damage. Too big chest indentation results in crushing the inner organs. Moreover the organs are hurt by bits of breaking ribs. High pressure can lead to disturbance of natural heart electromechanical impulses that stimulate its action (Fig. 1). There is a danger of arrhythmia, atrial fibrillation or heart attack [8].

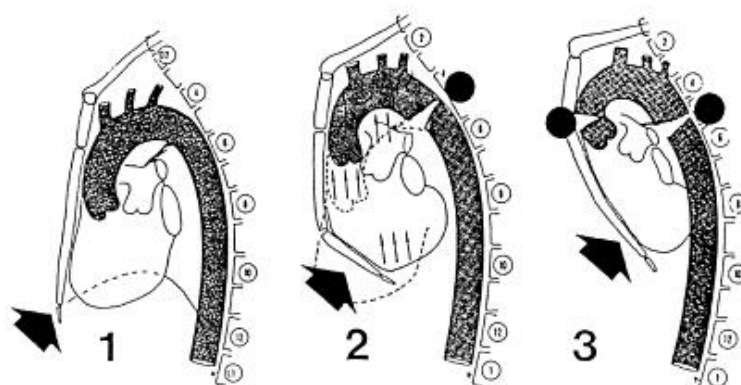


Fig. 1. The consequences of excessive chest pressure load [8]

$$CTI = \frac{A_{max}}{A_{int}} + \frac{D_{max}}{D_{int}} \quad (4)$$

where:

A_{max} - the maximum value of the acceleration acting on the chest [m/s^2],

D_{max} - the maximum deflection of the chest [mm],

A_{int} - maximum allowable values of the acceleration acting on the chest [m/s^2],

D_{int} - maximum allowable deflection of the chest [mm].

CTI index value should not exceed 1.0. Each man is different in height, weight, age and sex. It applies to inner organs too which are able to cushion the explosion overload on the chest [1].

Table 2. The critical values of the parameters for the criterion CTI [3]

Human body type	Large Male	Mid - sized Male	Female	6 year- old child	3 year – old toddler	1 year - old baby
D_{int}	114	103	84	64	57	50
A_{int}	83	90	90	90	74	57

5. Dynamic Response Index

Another biomechanical index connected with thoracolumbar part of spine is Dynamic Response Index (DRI). This criterion can help to estimate spine compression as a result of charge explosion under a multi-purpose vehicle. The index was borrowed from the aircraft industry where it is used for pilot seats' examination. The criterion is nothing but an analysis of simple mechanical set with one latitude (Fig. 2). The set does not correspond with the human body and its dynamic reaction to sudden overload in the direction of an axle (hence the index is often defined as DRI) [2, 3].

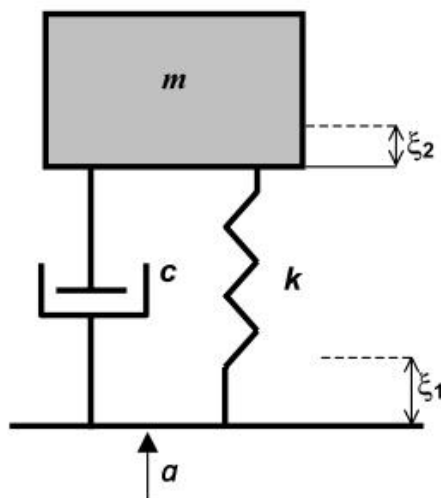


Fig. 2. Model DRIZ [1,2]

Using simple dynamic mechanical systems dependence, the following equation of motion for this model is [2, 3]:

$$a(t) = \frac{d^2\delta}{dt^2} + 2\varphi\omega_n \frac{d\delta}{dt} + (\omega_n)^2\delta \quad (5)$$

where:

$a(t)$ – is the acceleration in the vertical direction measured at the position of initiation;

δ – is the relative displacement of the system with,

$$\delta = \xi_1 - \xi_2 \quad , \delta > 0 \quad (6)$$

φ – is the dumping coefficient,

$$\varphi = \frac{c}{2 \cdot m \cdot \omega_n} \quad (7)$$

ω_n – is the natural frequency with,

$$\omega_n = \sqrt{\frac{k}{m}} \quad (8)$$

The Dynamic Response Index is calculated by the maximum relative displacement δ_{\max} , natural frequency ω_n and the gravity acceleration g [1,2].

$$DRI = \frac{\omega_n^2 \cdot \delta_{\max}}{g} \quad (9)$$

where:

ω_n - 52,9 rad/s = 8,4 Hz,

φ - 0,224.

The above parameter values were assigned in the aircraft industry research. Border value of DRI index equals 17.7. Exceeding the value according to AIS scale means 10 % probability of serious spine injuries. DRI index analysis enables technical development of military vehicle's seats [2, 3].

6. Tibia Index

Reactions acting in the vertical axle create a great danger for lower limbs. In the time of explosion under a military vehicle feet are located on the bottom. As a result of local explosion the floor of the vehicle gets distorted and the same forces affect directly the lower limbs. The most prone to injury is tibia. To estimate danger we apply Tibia Index [3, 1].

$$TI = \frac{F_z}{(F_z)_{int}} + \frac{M_g}{(M_g)_{int}} \quad (10)$$

where:

F_z – axial compression force [kN],

M_g – resultant bending moment [Nm],

$(F_z)_{int}$ – critical axial compression force [kN],

$(M_g)_{int}$ – critical bending moment [Nm].

Table 3. The critical values of the parameters for the criterion TI [1]

Human body type	Large female	Mid – sized female	Male
$(M_g)_{int}$	307	225	115
$(F_z)_{int}$	44,2	35,9	22,9

7. Traumatic Brain Injury

Biomechanical index which estimates the level of brain injury is Traumatic Brain Injury (TBI). The injuries which seem to be harmless in the very first moment often end in serious complications leading to disability or death. The injury is caused by a rapid and strong head impact into an object. Brain injury is caused by acceleration parameter affecting the brain along with making it move in a braincase (brain ricochet or brain injuries caused by broken skull bones). Biomechanical index TBI, unlike the other indexes, is not defined by a formula. The essential thing is the right recognition of brain injuries as a result of accidents. That's why the symptoms connected with TBI index can be divided into: light, mild and hard [7, 6].

8. Chest Wall Velocity Predictor

Another index referring to inner organs placed in the thoracolumbar part of the spine is Chest Wall Velocity Predictor (CWVP). Like in the DRI case, chest is perceived as a simple dynamic and mechanical structure (Fig. 3).

The essential parameter is the pressure affecting the rib cage. While the chest sinks deeper into the body, the internal organs such as a heart and lungs and ribs are crushed. The structure of the chest is able to cushion the pressure by acting like a spring. A measurable affect onto the parameter's harmfulness is the direction and time of action [2, 3, 5].

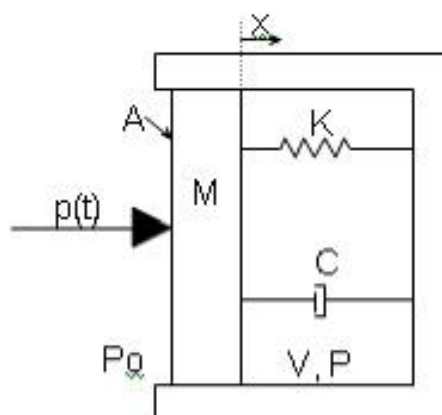


Fig. 3. Thorax Model [2]

The action of presented structure in fig. 3 can finalize in the formula beneath [3]:

$$M \cdot \frac{d^2x}{dt^2} + C \cdot \frac{dx}{dt} + K \cdot x = A \cdot \left[p(t) + P_0 - \left(\frac{V}{V - A \cdot x} \right)^\gamma \cdot P_0 \right] \quad (11)$$

where:

A – effective area [m²],

M – effective mass [kg],

V – initial gaseous volume of the lungs [m³],

x - displacement [mm],

C – damping factor [Ns/m],

K – elasticity pressure [N/m],

P₀ – ambient pressure [Pa],

p(t) - overpressure [Pa],

γ – polytropic exponent for gas in lungs.

Most parameters are dependent on the type of human body. The values have been checked by Axelsson and put in a chart (4) for medium human (about 70 kg) [3]:

Table 4. The parameter values for a medium-sized man [3]

Parameter	Unit	Value
M	kg	2.03
C	Ns/m	696
K	N/m	989
A	m ²	0,082
V	m ³	0,00182
γ	-	1,2

Exceeding the values of 3.6 ms speed onto the chest given a risk of injuries. The higher the speed, the greater the injury [3, 5].

9. An original computer program for determining the biomechanical indicators

Within a project an authorial computer program was elaborated which is used to appoint selected biomechanical indexes to estimate the danger of the crew. Matlab program was used to carry out the task. The idea helps to perform complicated calculations and simulations. Moreover it is possible to design dedicated graphic interface (GUI) which enables to move around intuitively as well as to operate easily. The program allows to appoint indexes described before (Fig. 4).

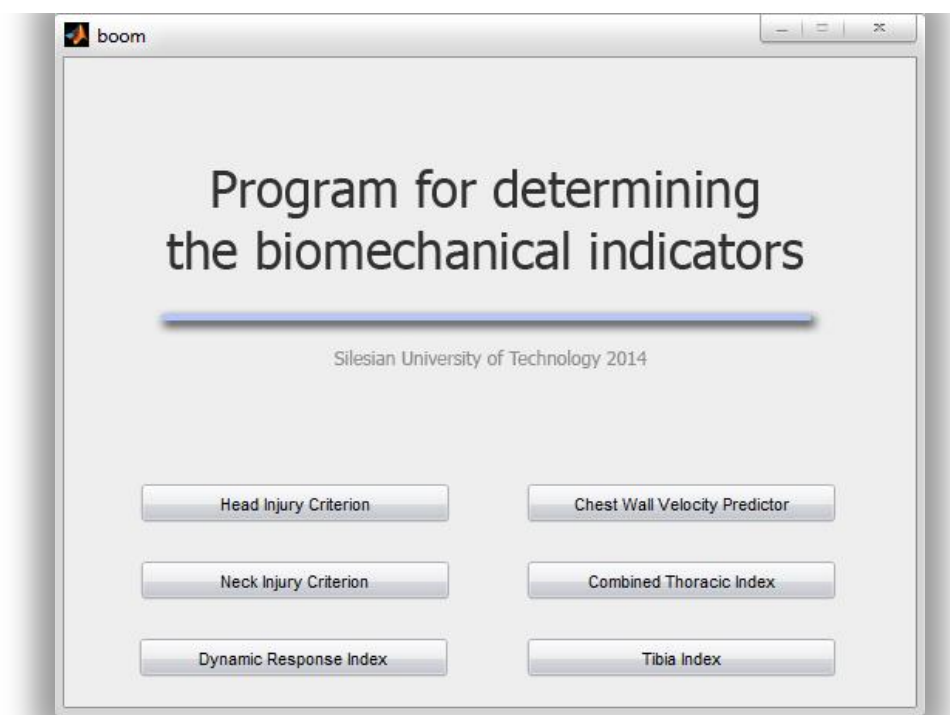


Fig. 4. Graphic User Interface

The program allows to become familiar with basic information about the selected indicator, such as the formula and the critical value (Fig. 5).

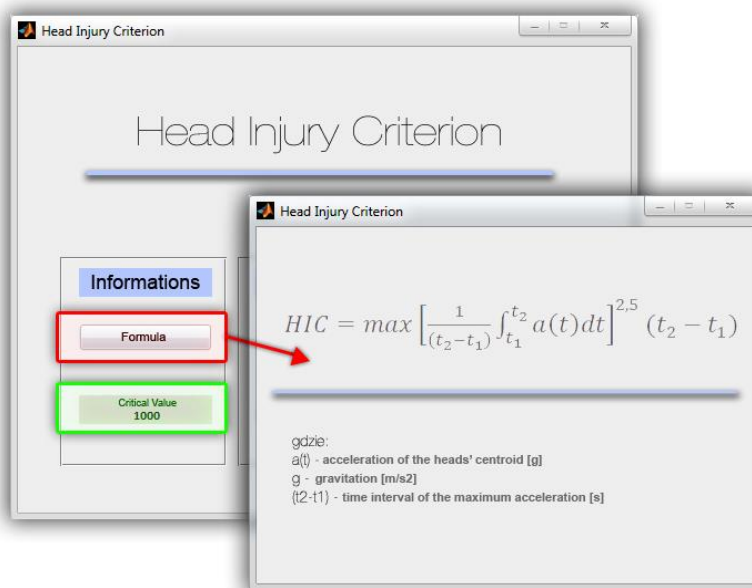


Fig. 5. Window containing the formula for calculating the sample rate of HIC indicator

It is possible to perform calculations using the downloaded file measurement data obtained during the tests. The result appears on the right side of the window and the corresponding color indicates a possible critical value is exceeded. Moreover, the results are displayed as a graph of the resulting value changes over time and saved to a separate file so that it is possible to analyze them next (Fig. 6).

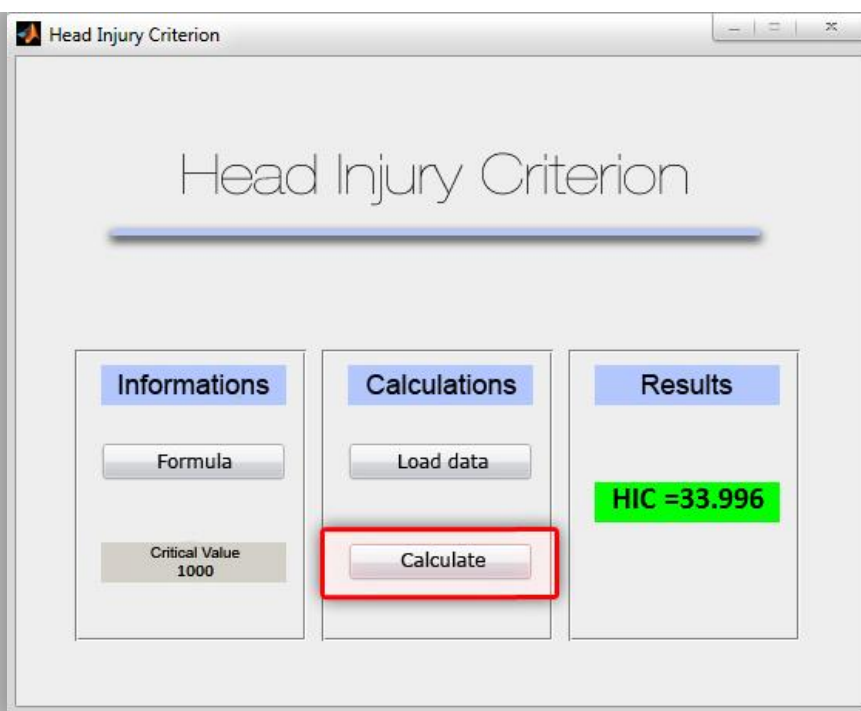


Fig. 6. Window program after completing the calculation

10. Conclusion

Biomechanics is an interdisciplinary science dealing with the examination of living organisms and their behavior influenced by external forces. It can be applied to many branches of science such as medicine, sport or even military. By means of biomechanical indexes it is possible to estimate the level of danger resulting from exceeding of critical values to organism. For many years they have been applied in car industry e.g. Crash tests through which the car's safety is examined. Nowadays biomechanical index is a part of technological development in military vehicles or as a means of soldiers' personal security used by modern armies.

References

1. Development of Improved Injury Criteria for the Assessment of Advanced Automotive Restraint Systems. Eppinger R. NHTSA. 1999.
2. Krzystała E., Kciuk S., Mężyk A.: Identification threat of a crew of special vehicles during explosion (in English), Publishing House of the Institute for Sustainable Technologies, Gliwice 2012.
3. RTO Technical Report TR-HJN-090 TECHNICAL REPORT TR-HFM-090 Test Methodology for Protection of Vehicle Occupants against Anti-Vehicular Landmine Effects.
4. Schmitt K., Nieder P. F., Muser M. H., Walz F.: Trauma Biomechanics: Accidental injury in traffic and sports, Springer 2009
5. Teland A. J.: Review of blast injury prediction models. Norwegian Defence Research Establishment (FFI-rapport), 2012.
6. http://en.wikipedia.org/wiki/Traumatic_brain_injury [date of access: 23.10.2014]
7. <http://www.ninds.nih.gov/disorders/tbi/tbi.htm> [date of access: 23.10.2014]
8. http://zone.ni.com/reference/en-XX/help/370859J-01/crash/neck_nij/ [date of access: 22.10.2014]

SELECTED ENGINEERING PROBLEMS

NUMBER 5

INSTITUTE OF ENGINEERING PROCESSES AUTOMATION
AND INTEGRATED MANUFACTURING SYSTEMS

Piotr MICHALSKI¹, Krzysztof TKOCZ¹

¹Institute of Engineering Processes Automation and Integrated Manufacturing Systems,
Faculty of Mechanical Engineering, Silesian University of Technology, Gliwice
*piotr.michalski@polsl.pl

THE ALGORITHMS SUPPORT FOR VISUALISATION OF INDUSTRIAL ROBOT MOVEMENTS

Abstract: This paper presents a practical implementation of algorithms for correctly visualize the movements of an industrial robot in the SCADA type visualization. As an example, the authors chose the three-arm robot with end effector.

1. Introduction

Modern industrial process visualization systems allow you to view images with high resolution. With processors for high performance computing, it is possible to implement algorithms to support accurate visualization of selected elements of the process. This article describes the algorithms necessary to perform professional visualization of an industrial robot, consisting of 3 arms and gripper. As a sample SCADA system the CodeSys 3S has been chosen.

2. Industrial robot movements

The movement of the robot will be controlled by forcing the displacement of one of the four arms. Authors created a model of an industrial robot shown in Figure 1a, just to perform the visualization. When modeling a robot arms, users should pay attention to the pivot point of the arm, it has to be located in the same position as the center of rotation axis. One of example robot arm in Figure 2b has been presented. Assuming that for the changes in the rotation angle will be responsible such a variable as: rRR1 up to rRR4, as well as taking the RX1 up to X4 and RY1 up to RY4 as auxiliary variables to determine the displacement, simple function code has been developed:

```
(* position point – axis no 2, arm 2 *)  
rX1:=rRR1*0.01745329; (* conversion of an angle *)  
rX2:=SIN(rX1)*126; (* determine the horizontal position X *)  
rY1:=COS(rX1)*126; (* additional help variable *)  
rY2:=126-rY1; (* determine the vertical position Y *)
```

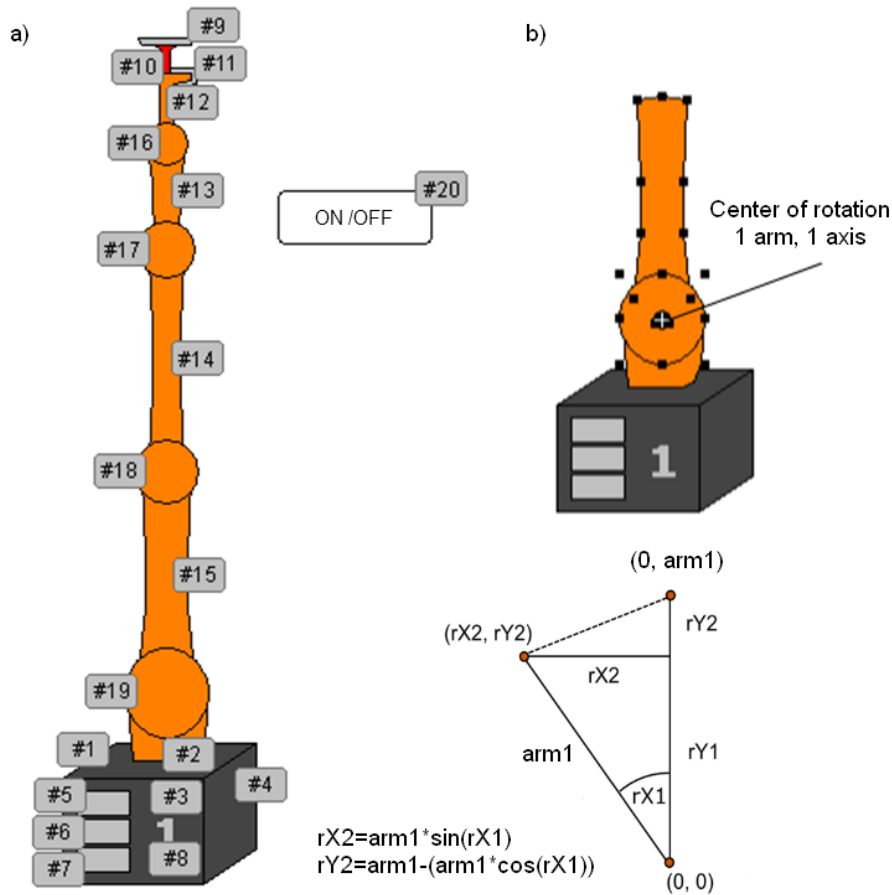


Fig. 1. Model of industrial robot: a) view with part numbers, b)

In the CoDeSys software the function of SIN and COS are calculated in radian measure, therefore, is required for the conversion. The length of the first arm (126 pix) measured from the pivot point to the last point of the upper - see Figure 1b. The moving parts are at the end of the first arm (# 14, # 18) is required to determine the position of X and Y as changing its angle of rotation. For this purpose, the function using simple trigonometric transformations determines the value of the displacement in the vertical and horizontal axes – see the equation on Figure 1b. The moving parts at the ends of the arm of the second and third proceed similarly, add additional displacement determined by means of further parts of programs.

```

(* position point – axis no 3, arm 3 *)
rX3:=rRR2*0.01745329;
rX4:=SIN(rX3)*126;
rY3:=COS(rX3)*126;
rY4:=126-rY3;

(* position point – axis no 4, arm 4, and additional elements *)
rX5:=rRR3*0.01745329;
rX6:=SIN(rX5)*58;
rY5:=COS(rX5)*58;
rY6:=58-rY5;
    
```

Transformation of the trigonometric functions used to designate the position of subsequent visualization elements of an industrial robot shown on Figure 2.

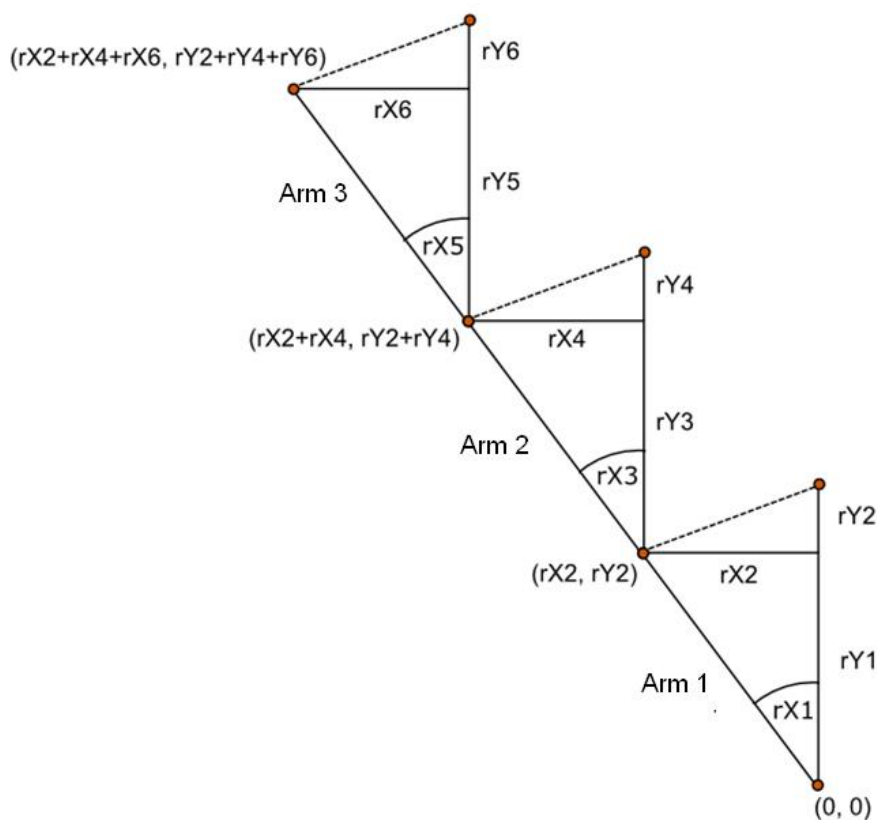


Fig. 2. Determination of the position of the items placed on the end of the third arm

The algorithm of the control program is based on forcing the successive movements of the arms of an industrial robot in order to reach the set-point position. In the example shown in this article, a program responsible for the movement of the robot from base position, in which the values of the angles are equal to zero to the position of pickup the item detail (movement of each arm mowing sequence: 20, -100, -150, -180). Global variable defined in the program and used by the robot are as follows:

(* main program variables *)

bStartRobot1:BOOL:=FALSE; (* START/STOP of the robot *)

(* robot status variables *)

bWlaczonyRobot1:BOOL:=TRUE; (* robot is ON *)

bPracaRobot1:BOOL:=FALSE; (* robot is BUSY *)

bCzekaRobot1:BOOL:=FALSE; (* robot is WHITING FOR A JOB *)

(* robot speed control variables *)

rPredkoscRobot1Ramie1:REAL:=2; (* speed of arm 1 *)

rPredkoscRobot1Ramie2:REAL:=2; (* speed of arm 2 *)

rPredkoscRobot1Ramie3:REAL:=2; (* speed of arm 3 *)

rPredkoscRobot1Ramie4:REAL:=2; (* speed of arm 4 *)

rPredkoscRobot1Dojazd:REAL:=1; (* additional speed of base *)

Creation of an additional movement simulation program for proper operation of the visualization has been required. In our example, as the PLC programming language the ST language has been selected. The code automatically forces the variables, so we are able to see the robot movements in the visualization. The proper code looks like:

```
PROGRAM VARIABLE_GEN
VAR
    blinkGen: BLINK;
    ctuLicznik: CTU;
    rSygnal: REAL;
END_VAR
    blinkGen(ENABLE:=bWylacznikAwaryjny, TIMELOW:=T#50ms, TIMEHIGH:=T#50ms);
    ctuLicznik(CU:=blinkGen.OUT, RESET:=rSygnal=1);
    rSygnal:=ctuLicznik.CV;
```

The motion simulation used a pulse generator (Blink-like element located inside the Util.lib), which in defined intervals gives on the output the high logical state (BOOL variable). Since the simulation will need variable of type REAL, in addition to the output of the generator the up counter CTU (library Standard.lib) has been connected, which reset condition was set as CV> 1. RSygnal variable defined at the output of the counter. Thus prepared, the system allows you to generate a variable of REAL type in equal to 1 specified intervals.

The next step is to create a robot motion control program, including to insert a new module called Robot_1 (as the PLC language we choose SFC), then declare local variables used in the control program. The code looks like:

```
PROGRAM Robot_1

VAR
    (* Condition to pass step 1 to 8 *)
    bWarunek1: BOOL;
    ...
    bWarunek8: BOOL;

    (* variable of displacement *)
    rX1: REAL; rX2: REAL;
    rX3: REAL; rX4: REAL;
    rX5: REAL; rX6: REAL;
    rY1: REAL; rY2: REAL;
    rY3: REAL; rY4: REAL;
    rY5: REAL; rY6: REAL;

    (* variables responsible for movements of each arm *)
    rRR1: REAL;
    rRR4: REAL;
    rRR3: REAL;
    rRR2: REAL;
END_VAR
```

In order to achieve smooth motion simulation function of displacement of the robot to be placed in each block of shares, which are associated with the movement instructions. You should also be aware of the negation of the previous transition conditions placed on top of all the blocks. Below are the contents of each block of shares robot control program. Boot (the INIT) block is the first element of the program, which provides condition for the start of the robot and the control variables statuses.

Start:

```

bWarunek8:=FALSE;
IF bStartRobot1=TRUE THEN      (* condition of starting *)

    (* statuses variables *)
    bWlaczonyRobot1:=FALSE;
    bPracaRobot1:=FALSE;
    bCzekaRobot1:=TRUE;

    bWarunek1:=TRUE; (* transition condition = open the gate *)
END_IF

```

In the next container block (Akcja_1) provided instructions for changing the displacement of each robot arms. The principle of operation is the addition of a variable pulse motion simulation variables corresponding to the displacement of each of the arms. The condition of leaving the block is the movement of the first arm by an angle of 20 degrees. Conditions for the other arms ensure you do not exceed the target values.

```

Akcja_1:
    bWarunek1:=FALSE; (* transition condition = close the gate *)

    (* variables for movements *)
    rRR1:=rRR1+rPredkoscRobot1Ramie1*Variable_gen.rSygnal;
    rRR2:=rRR2-rPredkoscRobot1Ramie2*Variable_gen.rSygnal;
    rRR3:=rRR3-rPredkoscRobot1Ramie3*Variable_gen.rSygnal;
    rRR4:=rRR4-rPredkoscRobot1Ramie4*Variable_gen.rSygnal;

    (* function of displacements *)
    rX1:=rRR1*0.01745329;
    rX2:=SIN(rX1)*126;
    rY1:=COS(rX1)*126;
    rY2:=126-rY1;
    rX3:=rRR2*0.01745329;
    rX4:=SIN(rX3)*126;
    rY3:=COS(rX3)*126;
    rY4:=126-rY3;
    rX5:=rRR3*0.01745329;
    rX6:=SIN(rX5)*58;
    rY5:=COS(rX5)*58;
    rY6:=58-rY5;

    (* END conditions *)
    IF rRR4<=-180 THEN rRR4:=-180; END_IF
    IF rRR3<=-150 THEN rRR3:=-150; END_IF
    IF rRR2<=-100 THEN rRR2:=-100; END_IF
    IF rRR1>=20 THEN bWarunek2:=TRUE; END_IF

```

Instructions for enabling positioning of the other arms are located in action blocks Akcja_2 up to Akcja_4. Terms transitions are fulfilled by reaching preset positions for the next industrial robot arms.

```

Akcja_2:
    bWarunek2:=FALSE;
    rRR2:=rRR2-rPredkoscRobot1Ramie2*Variable_gen.rSygnal;

```

```
rRR3:=rRR3-rPredkoscRobot1Ramie3*Variable_gen.rSygnal;
rRR4:=rRR4-rPredkoscRobot1Ramie4*Variable_gen.rSygnal;
```

```
(*function of displacements *)
```

```
IF rRuchRamie4<=-180 THEN rRR4:=-180; END_IF
IF rRuchRamie3<=-150 THEN rRR3:=-150; END_IF
IF rRuchRamie2<=-100 THEN bWarunek3:=TRUE; END_IF
```

```
Akcja_3
```

```
bWarunek3:=FALSE;
rRR3:=rRR3-rPredkoscRobot1Ramie3*Variable_gen.rSygnal;
rRR4:=rRR4-rPredkoscRobot1Ramie4*Variable_gen.rSygnal;
```

```
(*function of displacements *)
```

```
IF rRuchRamie4<=-180 THEN rRR4:=-180; END_IF
IF rRuchRamie3<=-150 THEN bWarunek4:=TRUE; END_IF
```

```
Akcja_4:
```

```
bWarunek4:=FALSE;
rRR4:=rRR4-rPredkoscRobot1Ramie4*Variable_gen.rSygnal;
```

```
(*function of displacements *)
```

```
IF rRuchRamie4<=-180 THEN bWarunek5:=TRUE; END_IF
```

On the screen we should be able to see the visualization of fluid motion robot moving to the target position.

3. Conclusion

The example can be freely expanded by adding the value of movements for each arm in successive blocks of control. After we create the control program we should assign a variable displacement to each arm, also keeping in mind the account of the previous arms movements, as shown in Figure 2. The final result visualization looks very realistic.

References

1. Legierski T., Kasprzyk J.: Programowanie sterowników PLC, WNT, Gliwice, 2008.
2. Sałat R., Korpysz K., Obstawski P.: Wstęp do programowania sterowników PLC, WNT, Warszawa, 2010.
3. Kasprzyk J.: Programowanie sterowników przemysłowych, WNT, Warszawa, 2006.
4. Programing manual for CoDeSys, Warszawa, 2010.

SELECTED ENGINEERING PROBLEMS

NUMBER 5

INSTITUTE OF ENGINEERING PROCESSES AUTOMATION
AND INTEGRATED MANUFACTURING SYSTEMS

Magdalena MIKOŁAJCZAK, Krzysztof KALINOWSKI^{1*}, Cezary GRABOWIK^{1*},
Grzegorz ĆWIKŁA^{1*}, Witold JANIK^{1*}

¹ Institute of Engineering Processes Automation and Integrated Manufacturing Systems,
Faculty of Mechanical Engineering, Silesian University of Technology, Gliwice
*{krzysztof.kalinowski, cezary.grabowik, grzegorz.cwikla, witold.janik}@polsl.pl,

THE REORGANIZATION OF THE INPUT STORE OF STEEL RAW MATERIALS IN THE MANUFACTURING SYSTEM - CASE STUDY

Abstract: The proper warehouse management strongly affects the condition of the company. The paper describes a way to reorganize the input storage layout of steel raw materials of the company that specializes in manufacturing large-size products. In particular, the existing state of the store and next three new conceptions were presented. Attention was paid to the storage area intended for the steel sheets. Some alternative variants of horizontal and vertical steel sheets storing and means of the internal transport were considered in these new solutions. The most important criteria for choosing a solution for implementation were also presented. The designed layout of the magazine, compared to the existing state, enables the elimination of waste associated with the available capacity, reduce time and cost associated with the involvement of the means of production and human resources.

1. Introduction

The proper stock management is essential for the efficiency of production, but in many companies it is not paid the sufficient attention to this issue. As a result, the company may incur significantly higher costs of production and lose competitiveness [1]. Therefore, the storage space should be well thought and organized in a way that minimizes costs associated with available space and as well as in such a way that allows reducing and simplifying manipulation of materials and transport processes. The storage methodology and problems of space design has been widely presented in [2,4].

For storing metallurgical raw materials in the form of sheets, rods and others, dedicated and adapted storage areas are used. Due to the often large weight and dimensions, these materials are often stored in the open space, close to the manufacturing shop. The roles of such magazine often perform storage areas located in such a way that the transport of input materials for production was carried at the shortest possible distance. Small-size items can be stored in the enclosed spaces, on shelves, in transport boxes, etc. In fact, the manner of storage of these materials depends on the availability of space allocated for storing, available means of transport and maximum loads allowable for storage surface (safe stack height on the

ground, racks, platforms, etc.). Selected practical guidance on the storage of various types of materials are presented in [3,6].

This work is the part of scientific research work on the organization of production in the local enterprise that specializes in manufacturing large-size products conducted in the Institute of Automation Processes Engineering and Integrated Manufacturing Systems of Silesian University of Technology.

2. The existing layout of the input store

Steel sheets storage is located in the immediate vicinity of the production system (figure 1). Storage area is restricted by the operating range of the crane. By technological reasons, delivery of raw materials from store to manufacturing area is carried out only through the one, entry gate. Three output gates located at the side of store are used occasionally, but storage of material in this area is not allowed. Due to the limited capacity of the crane the transportation of the largest sheets is performed one by one, which greatly increases the time of the transport process – the total delivery time from identifying the proper sheet by the worker, through manipulation, transportation, loading on the rail truck up to delivery to the manufacturing department is approximately 3h.

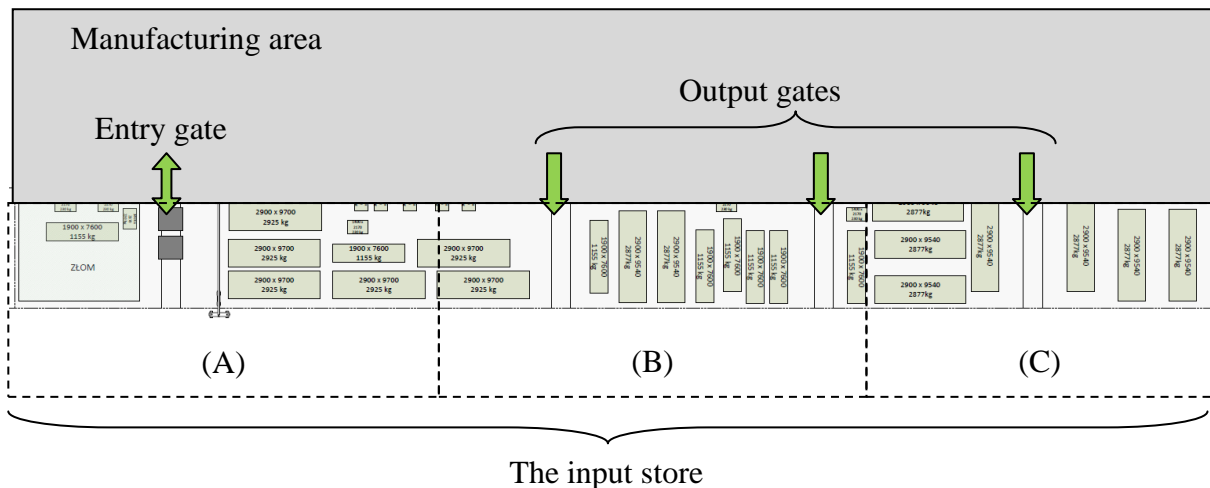


Fig. 1. The location of the input steel sheets store

Currently, the steel sheets are stored horizontally in available free space based on the individual preferences of workers, without clearly defined rules. Very often sheets with different sizes are stacked in the same pile (figure 2). Such random arrangement of sheets causes difficulties in finding suitable sheets for production and often significantly increases delivery time and workload, when putting sheets from one stack to another.

In figures 3-5 the existing layout of the input store is presented. Current material storage areas, with the dimensions of the sheets, transportation, gates areas and scrapping area were marked.



Fig. 2. Storing sheets of different sizes - random arrangement of sheets in stocks

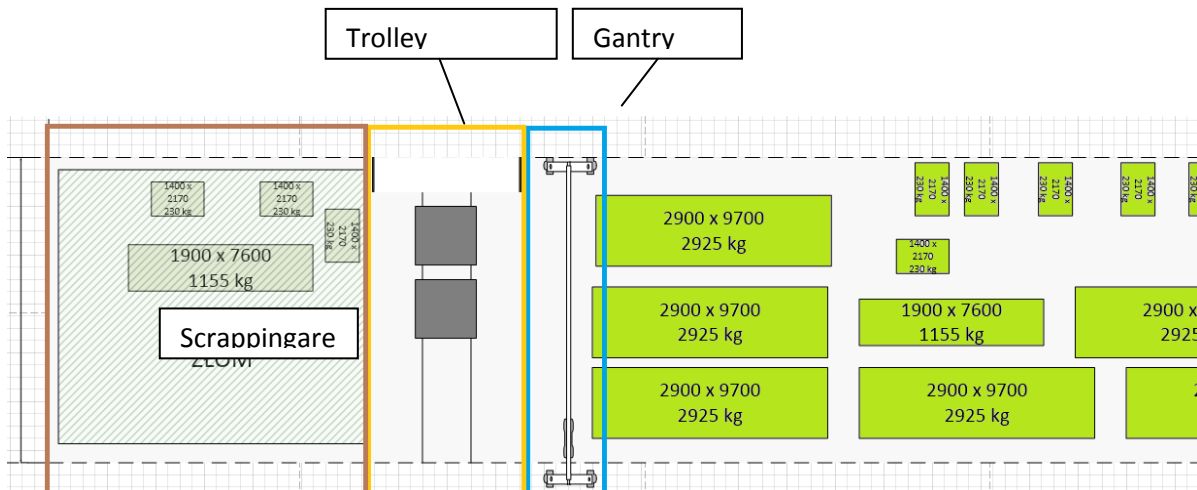


Fig. 3. The existing layout of the input storage, part A

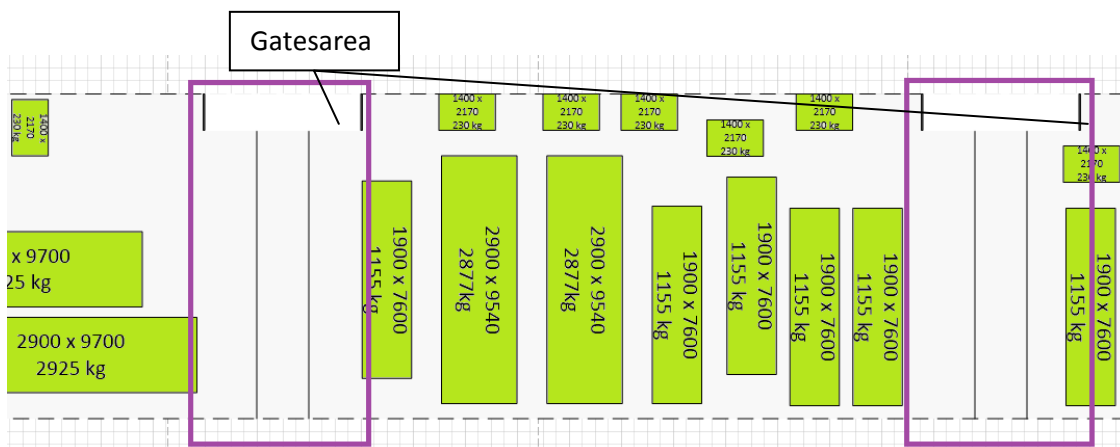


Fig. 4. The existing layout of the input storage, part B

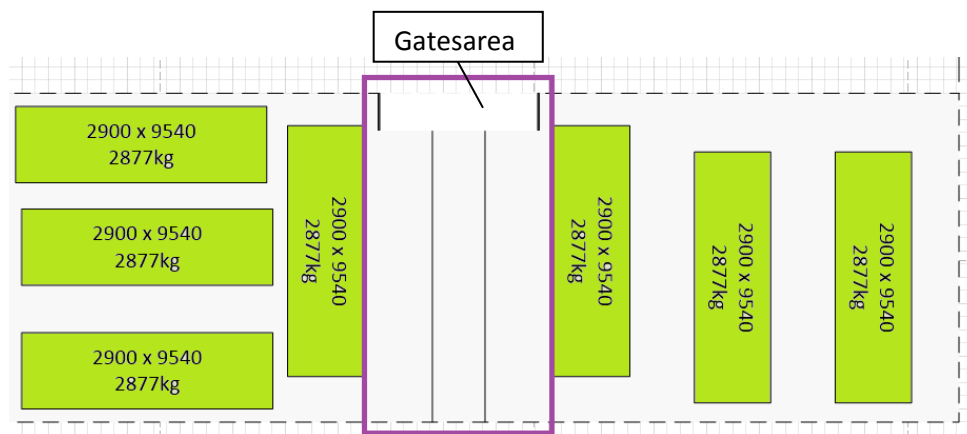


Fig. 5. The existing layout of the input storage, part C

3. The proposed variants of the layout arrangement

On the base of analysis of possible configuration changes in the input store layout described in [5] three variants of the steel sheets arrangement were proposed. The following criteria were assumed:

1. The ability to use an alternative means of transport – e.g. in case of the crane breakdown.
2. Minimizing the transport time of the raw materials from the storage to the production area.
3. Simplicity of the layout and clearly marked storage area in order to avoid mistakes and reduce the searching time for the right material by workers.
4. Easiness of manipulation of materials in the storage.
5. Easiness of unloading materials from the means of transport.
6. Ability to handle the increased supplies of materials.
7. Minimizing the investment and operational costs of storage.

The steel sheets are classified by their dimensions into 4 groups:

- S1: 9540 mm x 2900 mm x 13 mm (2877 kg),
- S2: 9700 mm x 2900 mm x 13 mm (2925 kg),
- S3: 7600 mm x 1900 mm x 10 mm (1155 kg),
- S4: 2170 mm x 1400 mm x 9,5 mm (230 kg),
- S5: other remaining sizes.

The combination of horizontal and vertical stacking sheets was proposed. Stored sheets will be handled mainly by the crane. For transportation of large-size sheets stored vertically ropes/hooks or dedicated magnetic gripper can be used. In order to improve the operation of the horizontally stored sheets an additional mean of transport in the form of a forklift truck was proposed. For easier handling by a forklift sheets stacked in piles should be stored on pallets. In all variants the scrapping area was placed in the opposite side of the raw material entry gate – on the right side of the store (figures 7-9).

In the variant 1 (figure 7), S1 group of sheets are arranged in stacks of up to 10 pieces. Within this area the transportation will run so far – using a gantry crane. S1 sheets are

arranged in the close vicinity of trolley conveyors used for transport sheets to the production system. S2 type sheets are partially stacked and also stored vertically. Stacks of them are up to 8 pieces, which covers the needs of production system for one day.

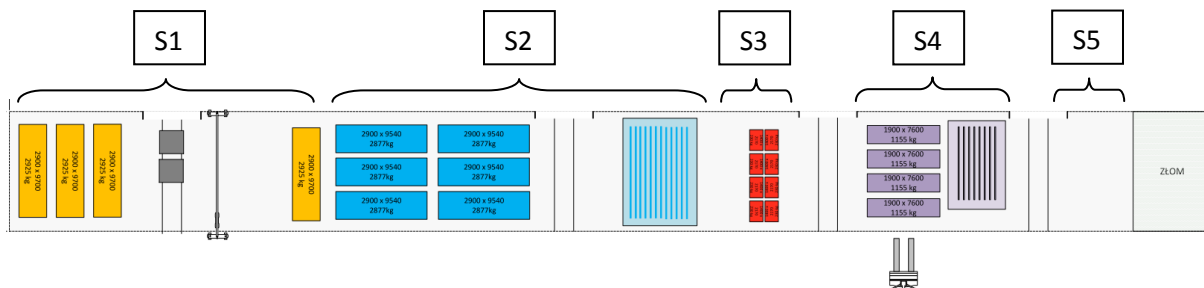


Fig. 6. The arrangement of the steel sheets in the store – variant 1

For covering periodically increased demand and reducing required space a vertical position of storing material sheets was also proposed. Transportation of S2 type sheets can be carried out in two ways – overhead crane and a forklift truck with a high load capacity. The combination of horizontal and vertical storage has also been proposed for storing sheets of S4 group of sheets. S4 sheets are stored up to 9 pieces in a pile, which covers demand for 2 days. Sheets of S3 group, with the smallest size, were placed in stacks of up to 20 pieces in the place that allows easy access and operation of the truck.

The variant 2 (figure 8) considered no vertical storages for large size sheets, so sheets from group 1,2 and 3 are stored in a horizontal position, in stacks. The expected number of sheets in stacks is as follows: for sheets of S1 up to 10, for sheets of S2 up to 8, for S4 up to 9 pieces. S3 sheets were placed at 15 shelves of the rack; each of them can hold up to 10 sheets.

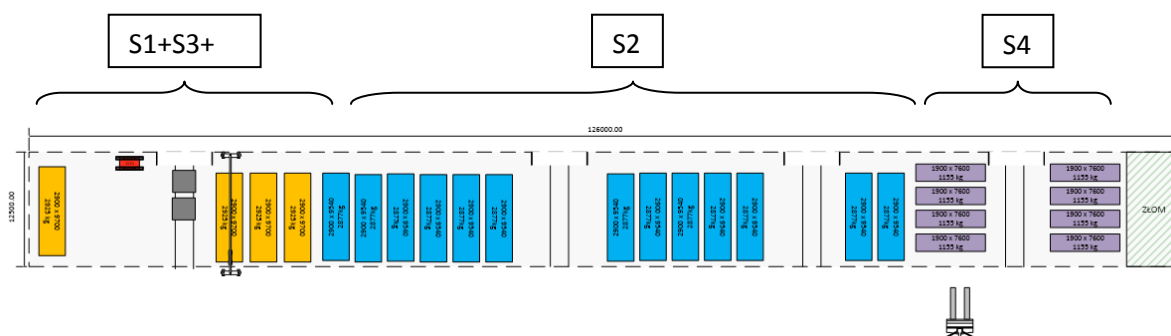


Fig. 7. The arrangement of the steel sheets in the store – variant 2

In the variant 3 (figure 9) storing of S1 sheets mostly in a vertical position is proposed. S2 sheets are stored in stacks of 8 pieces. For S3 sheets the same rack as in variant 2 was proposed.

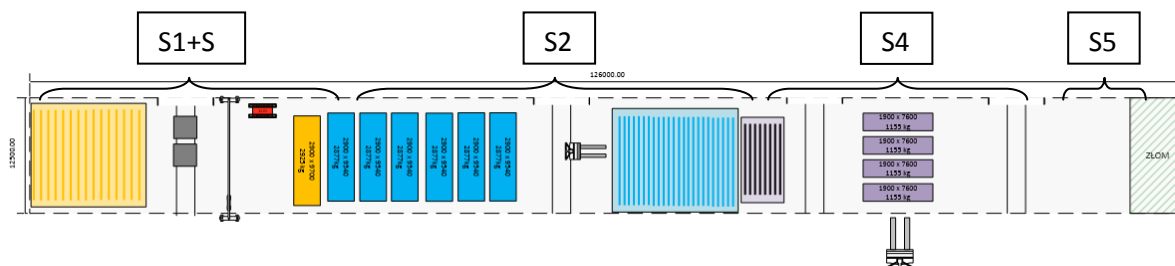


Fig. 8. The arrangement of the steel sheets in the store – variant 3

The conducted multi-criteria analysis, based on set of criteria presented above, showed that the most preferred option is variant 3 but the final decision on the choice of variant has not been made yet.

4. Conclusions

The proposed solution of the input storage layout reorganisation is one of the first steps to improving production organization in the company. The main result of the new layout arrangement is reduction of waste associated with time and cost of the means of production and human resources and possibility of calculation available capacities.

Determination of the maximum storage capacity within the operation area of the crane for the separated groups of raw materials allows for rational stocks management and optimal supply planning. Described changes to the rearrangement are related to location of specific raw materials but also the general improvement of storage operation is provided in further work. The most important are the solutions that enable rapid and clear identification of the place of the sheet storage (localisation) by workers.

References

1. Grzybowska K. „Inventory management and warehouse” (in Polish), part 2. Dyfin, Warsaw 2010.
2. Hiregoudar Ch.: Facility Planning and Layout Design. An industrial Perspective. Technical Publications, Pune 2007.
3. Krzyżaniak S.: Fundamentals of inventory management in the examples (in Polish). Logistics Library (Biblioteka Logistyczna), Poznań 2005.
4. Langevin A., Riopel D.: Logistics Systems: Design and Optimization. Springer Science & Business Media, 2005.
5. Mikołajczak M. Reorganization of the steel products warehouse on the example of the selected large-size products manufacturing company (in Polish). Master's thesis. Institute of Engineering Processes Automation and Integrated Manufacturing Systems, Faculty of Mechanical Engineering, Silesian University of Technology, Gliwice 2014.
6. Stephens M.P., Meyers F.E.: Manufacturing Facilities Design and Material Handling. Pearson Prentice Hall, 2005.

SELECTED ENGINEERING PROBLEMS

NUMBER 5

INSTITUTE OF ENGINEERING PROCESSES AUTOMATION
AND INTEGRATED MANUFACTURING SYSTEMS

Marcin MOCZAŁA¹, Mariusz Piotr HETMAŃCZYK^{2*}

^{1,2}Institute of Engineering Processes Automation and Integrated Manufacturing Systems,
Faculty of Mechanical Engineering, Gliwice, Poland

*mariusz.hetmanczyk@polsl.pl

THE MINIATURE PHOTOVOLTAIC SYSTEM WITH SUN-TRACKING ALGORITHM

Abstract: To the non-renewable energy sources belongs each source which is not subjected to a process of renewal in a short time. This means that their consumption is much faster than the replenishment of the stock. According to the laws of power engineering departments the conventional energy source mostly is obtained by the combustion of organic fossil fuels. Due to the limitation of resources appears the necessity of looking for new alternative energy sources, among others wind, solar, hydro, etc. The article presents the model of the miniature photovoltaic system with the Sun-Tracking algorithm. The authors also described the designed mechanical structure, control system, selection of sensory elements, security devices and wiring diagrams.

1. Introduction

The noticeable increase in prices of energy derived from fossil fuels and simultaneous growing environmental demands have contributed to an intensification of work focused on improving usage of renewable energy sources [1].

Advanced systems for converting solar energy into electricity are likely to prevail also in Poland, provided that the technology development will be accompanied by a marked decline in their prices [2]. This effect will allow for significantly increase the profitability of investment in this area [3]. It is estimated that over the next ten years the price of energy produced in the traditional way and by photovoltaic systems will be equal.

The simplest devices used for converting solar into electrical energy are photovoltaic cells. The increase of interest in the world market is caused by first of all by a direct conversion of solar energy into electricity without noise and pollution.

Photovoltaic systems are divided at two basic types, in terms of the energy storage and its conversions, as follows [4-6]:

- OFF-GRID (also called stand-alone or island systems) - photovoltaic systems without direct connection to the electric grid,
- ON-GRID (systems fully integrated with electric grids) - designed to produce alternating current with simultaneous transmission of excess power to the electric grid.

In case of the difference at orientation methods, solar photovoltaic systems are divided into two main groups [7-9]:

- stationary - working at constant, fixed angles of azimuth and inclination to the horizontal direction,
- movable (the Sun-Tracking systems) - enable movement with respect to the horizontal axis (azimuth change, assuming that the module is inclined to the horizontal at a constant angle equals to the latitude of the place where it is installed), about a fixed vertical axis (with elevation changes) and both axes.

2. Structure of designed Sun-Tracking photovoltaic system

The basic premise was realization of structural design of biaxial system allowing positioning of photovoltaic panel surface at right angle to the axis of sunlight (regardless to the time of day and the weather conditions). To the development of a 3D model (Fig. 1) the Solid Edge was used.

The turntable consists of three basic elements:

- supporting structure with housing for mounting of drives and control devices,
- the movable platform for changing orientation of the moving elements (seated on vertical axis) by wheel rim with internal toothing driven by electric motor,
- rail with connector to mounting a photovoltaic panel and toothed bar with external toothing (a movement control in the horizontal axis).

The kinematic structure of designed device (with required mobility of axes at ranges of rotation about the vertical axis 70° and the horizontal axis 355°) allows obtaining high efficiency and (additionally with combination of implemented Sun-Tracking algorithm) an optimum positioning in respect to a direction of sun radiation.

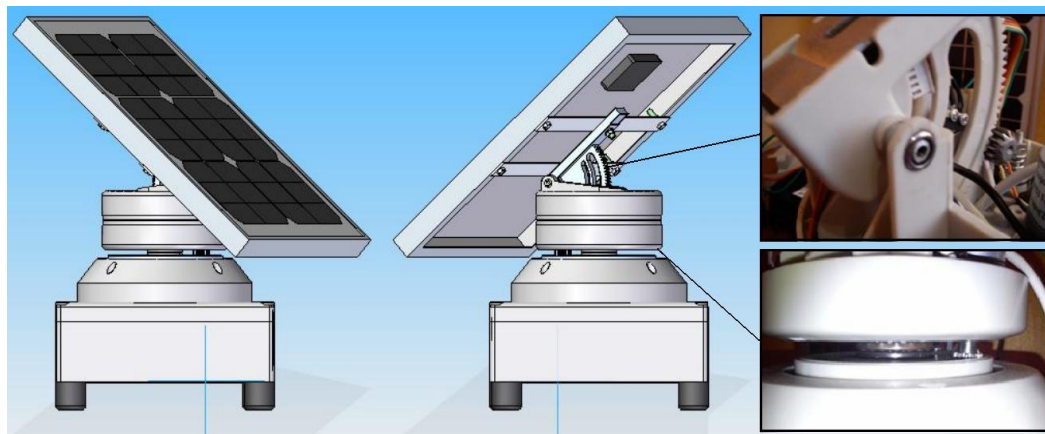


Fig.1. The 3D model view of the mini photovoltaic system with the Sun-Tracking algorithm

For the manual operation the control panel was made. The panel consists of an enclosure, two three-position switches (mono-stable), LED indicators (the voltage emergence at terminals of analog outputs), a two-position switch (selection of automatic or manual modes) and output terminal blocks.

After switching to the automatic mode, the PLC is powered up. An axis control is based on the input values (phototransistors placed on a surface of the photovoltaic module) processed by the algorithm.

All phototransistors were arranged on the circumference of the backplane at 90° . Additionally phototransistors located opposite each other are inclined at angle of 5° to each other.

3. The structure of the sensory subsystem

Sensors (Fig. 2) are powered by the 12 Volts battery, but analog inputs of the PLC unit require voltage in the range between $0 \div 10$ V. In order to protection the voltage regulator was used. By reducing the voltage elaborated system uses almost the whole measuring range of analog inputs of the PLC controller.

Resolution of the PLC controller equals 10-bits, which means that the PLC is able to recognize voltage level greater than or equal to 9.77 millivolts.

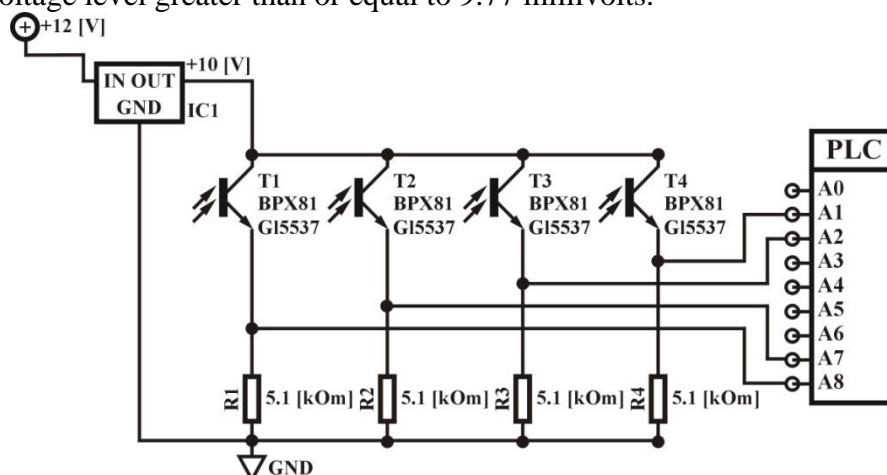


Fig.2. Wiring diagram of the sensory system with the PLC controller

To the analog inputs of the PLC controller four phototransistors have been connected. Other inputs were connected to limit switches which indicate exceeding of permissible values for rotational moves (Fig. 3).

As a result the user can select three methods for control of the orientation of the photovoltaic panel:

- an open system - positioning based on the calculated position of the sun, i.e., the clock algorithm (change in the position takes place at predetermined intervals of time),
- a closed system - positioning based on information from the sensors and the measured position of the photovoltaic cell,
- a hybrid system - a combination of open and closed systems.

For power generation the mono-crystalline solar MH10-10W was used. Selected photovoltaic cell is made up of thirty-six mono-crystalline units placed on a rigid and lightweight composite substrate, protected against damage by the hard antireflective glass. Electric contacts are terminated in a waterproof junction box.

The panels can be connected in parallel (to increase the current intensity) or in series (to increase the voltage). Efficiency of panels drops after 10 years up to 90% power, and after 25 years up to 80% nominal power.

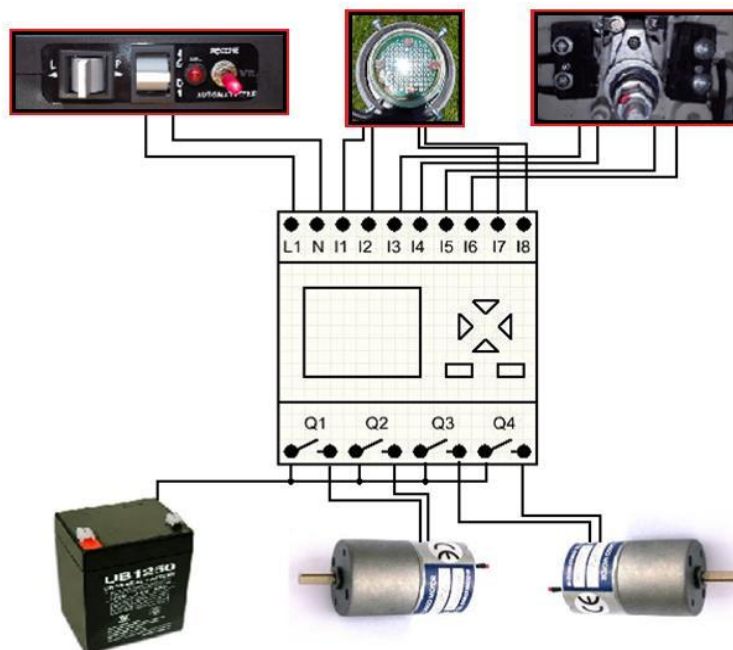


Fig.3. The schematic connection diagram of the PLC controller

The main selection criteria of axis drives can be described in few points: low power consumption, 12 Volts power supply, small overall dimensions and build-in self-locking gear. As the drives were chosen gear motors equipped with DC motors with permanent magnet (type SG-27123000-610k). Small values of the input current intensity caused that control can be realized using low-power transistors, directly from the TTL output as well as with usage operational amplifiers.

4. Practical verification of system operation

The ability to control in automatic and manual modes allows comparison the power yield with usage of stationary and movable (with the Sun-Tracking algorithm) systems (Fig. 4).

In the case of the stationary system the authors adopted the optimum location in a southerly direction at an angle of 35° above the plane of the horizon. Selection of the optimum angle was made by using the interactive PVGIS software (Photovoltaic Geographical Information System). Selected value of angle for the studied geographical coordinates allows for obtaining the greatest efficiency.

On the basis of obtained results the authors elaborate a plot (Fig. 5) illustrating the difference in received power in case of stationary and movable system with the Sun-Tracking algorithm. The difficulties associated with the use of solar energy in Poland are as follows:

- low density of the daily flux of solar radiation, which in Poland does not exceed $100\text{W}/\text{m}^2$ and its value approximately equals $1000\text{kWh}/\text{m}^2$ per year,
- existing seasonal and daily variations of solar energy radiation,

- high prices of additional and basic equipment (very high cost of producing photovoltaic cells and batteries).

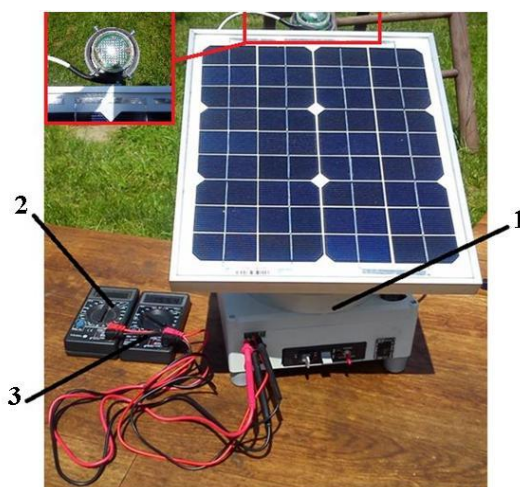


Fig.4. View of measuring stand, where: 1 - tested photovoltaic system, 2 - voltmeter, 3 - ammeter

An additional problem is the operating range, so in the winter the whole control and energy storage systems (batteries) should be kept in a positive temperature. Another important problem is icing of moving parts and stiffening of lubricants manifesting in increased motion resistance of gears.

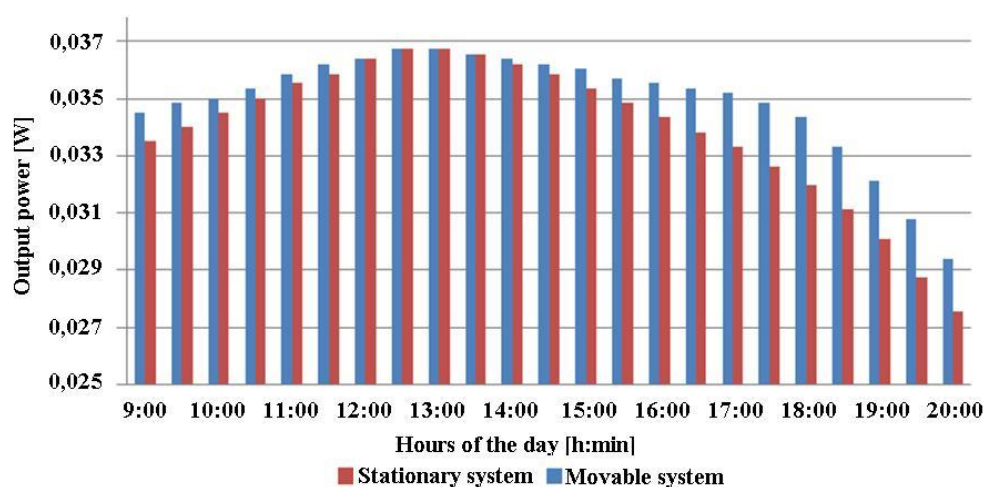


Fig.5. Comparison of results of investigated photovoltaic systems (stationary and movable)

In practice only between 12:30÷13:00 conversion results of the two systems are identical. In other cases values of energy yield are higher in use of Sun-Tracking algorithm.

On the basis of presented case it is difficult to indicate incontestable premises to the use of the Sun-Tracking algorithm. Such situation arises from the fact that within the range of analysed geographic coordinates results of the measurements exhibit only the minimum energy yield. The practical use of solar energy requires estimation of the actual and potential solar energy resources in the area and taking into account the impact of meteorological conditions tailored to the needs of used energy conversion technology.

6. Conclusions

Designed installation despite the proved energy yield, it also has a number of drawbacks in the form of: higher investment costs and the complexity as well as a high failure rate.

The advantages of photovoltaic power plant may include: the autonomous work and the lack of need for an external power supply (production of sufficient energy amount used for reorientation of photovoltaic cell and supply of external devices).

Additionally the installation with the Sun-Tracking algorithm does not require precise alignment of starting position and is characterized by a quick response to changing angle of sunlight incidence [10].

The measured values were obtained during the summer without taking into account the power consumption of other types of electric drives. In the next step should be defined characteristics in negative temperatures, which would determine the efficiency of the system in relation to the entire annual cycle.

References

1. Klugmann-Radziemska E.: Photovoltaics in theory and practice, BTC Publishing House, Legionowo 2010 (in Polish).
2. El Chaar L., Lamont L.A., El Zein N.: Review of photovoltaic technologies. „Renewable and Sustainable Energy Reviews” 2011, Vol. 15 Issue 3, pp. 2165–2175.
3. Wang, J., Jing, Y., Zhang, C., & Zhao, J.: Review on multi-criteria decision analysis aid in sustainable energy. „Renewable and Sustainable Energy Reviews” 2009, Vol.13, pp. 2263-2278.
4. Chong K.K., Wong C.W.: General formula for on-axis sun tracking system and its application in improving tracking accuracy of solar collector. „Solar Energy 2009, Vol. 83 Issue 3, pp. 298–305.
5. Chong K.K., Siaw F.L., Wong C.W., Wong G.S.: Design and construction of non-imaging planar concentrator for concentrator photovoltaic system. „Renewable Energy” 2009, Vol. 34, pp.1364–1370.
6. Yazidil A., Betin F., Notton G., Capolinol G.A.: Low cost two-axis solar tracker with high precision positioning. „Environment Identities and Mediterranean Area ISEIMA '06” 2010, pp. 211-216.
7. Roth P., Georgiev A., Boudinov H.: Design and construction of a system for sun-tracking, „Renewable Energy” 2004, pp. 393-402.
8. Salem Farhan A.: Mechatronics Design of Solar Tracking System. „International Journal of Current Engineering and Technology” 2013, Vol. 3, pp. 417-429.
9. Tudorache T., Kreindler L.: Design of a Solar Tracker System for PV Power. „Acta Polytechnica Hungarica” 2010, pp. 23-39.
10. Tao Y., Guo W.: Study on tracking strategy of automatic sun-tracking system based on CPV Generation. „Intelligent System Design and Engineering Application (ISDEA)” 2010, Vol. 2, pp. 506-509.

SELECTED ENGINEERING PROBLEMS

NUMBER 5

INSTITUTE OF ENGINEERING PROCESSES AUTOMATION
AND INTEGRATED MANUFACTURING SYSTEMS

Zbigniew MONICA^{1*}, Aleksander GWIAZDA¹

¹ Institute of Engineering Processes Automation and Integrated Manufacturing Systems,
Faculty of Mechanical Engineering, Silesian University of Technology,
Konarskiego 18a Street, 44-100 Gliwice, Poland
*zbiegniew.monica@polsl.pl

OPTIMIZATION OF A PRODUCTION SYSTEMS USING VIRTUAL MODELS OF WORKPLACES

Abstract: Optimization of conducted operations in a production system is one of the most important element of production process designing. It is particularly important for the lean production process. The papers presents a concept of an optimizing process basing on application of virtual models of element constituting the analysed system. Modern CAE system allows to build and investigate any technical systems in a virtual environment. The analysis of a cooperation process between all elements of the investigated system let to improve the project of future system or the design of an existing one. Moreover in the paper are presented virtual models of created and investigated technical system. Also the basic relation between mentioned systems are discussed.

1. Introduction

Lean Production is a method of production manufacturing basing on the Toyota production System [1]. The main objective of this method is to create the value for the customer. Other, non-value creating, activities are eliminated (“slimmed”) as the wasteful ones. To describe the Lean Production approach one could use the concept of 7 or 8 wasted introduced by Toyota production engineers. According the TIMWOOD model this wastes are detected in next processes and places, or they are caused by [2]: transportation, inventory, motion, waiting, over-processing, over-production and defects. In the case of transportation the waste is considered either with unnecessary movements of products or products damaging during transportation operations. The inventory waste refers to the excessed inventory of materials or products in relation to the real production and market demand. The next waste, motion, describes the situation in which damaged is production equipment or injured are workers as a result of non-planned moves. This waste is also considered with time loses which are caused by not needed moves of production staff. Waiting, the next waste, is related with the harmony of the production cycle. If it is wrong scheduled produced element must wait for the next operation what generate increasing of the total production time. Over-processing or in other words extra-processing is a definition of the situation when product is manufacture in more complicated operation or when too high quality level is required (higher than required by the

customer). Generally it means that it is not recommended to exceed any customer requirements (e.g. complexity, quality, functionality, precision). To this is related the waste considered with over-production. In Lean Production it means that the production level could be determined only by real market demand. Also the production before the demand is diagnosed is treated as over-production. This waste is considered as the worst one. The defects waste is considered both with manufactured products and with manufacturing processes. This waste results in doubling the cost of one single product. It should be noted that this waste are often called *muda* (from Japanese). The additional, 8 waste, is non-utilized talent. It is important, in any production system, to best utilize the skills of employees.

The whole Lean Production system could be based on some basic assumptions. To this assumptions one could include [1]:

- 5S method,
- Total production Maintenance (TPM),
- added valued definition,
- wastes reduction,
- pull-system.

Main objectives of Lean Production are gained using innovative approach to the production system management. Firstly it is needed to change the way of employees thinking. Secondly one should introduce the new tool of production analysis like value stream mapping (VSM). Thirdly it is important to properly delegate the responsibilities in the management layer of the production system. It should be a one-man. Moreover production process should be continuously monitored.

2. Optimization problems in Lean Production systems

Optimization problems considered with Lean Production systems are mainly considered with their structure. In Fig.1 is presented an exemplar production system forming a workcell. It consists of machine tools, an industrial robot and a conveyor. The system is supervised by a control computer. Machine tools are responsible for production tasks. The robot and conveyor are responsible for transportation task. One of the main objective considered with controlling such production system is to ensure the smooth cooperation of all units.

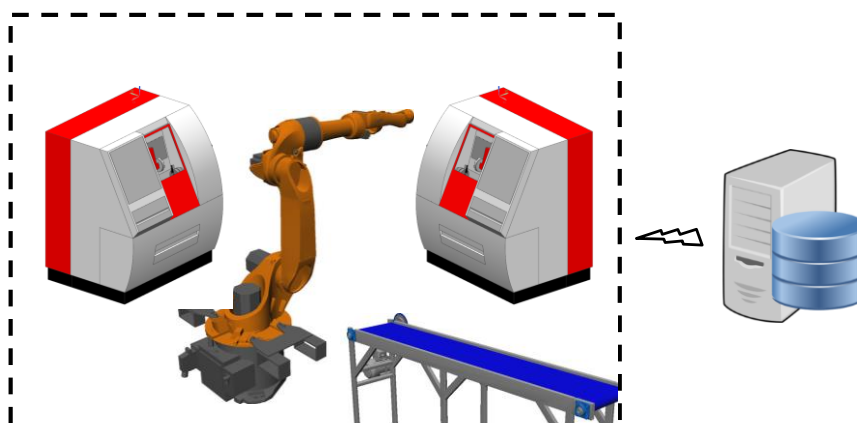


Fig.1. Model of a production system

The main problem considered with optimization task is the balanced cooperation between elements of a production system realizing its control programs. Investigation of a real system are related with the risk of damages or other dangerous situations that could affect the work of a system. In that case the solution is to use a virtual model of system elements.

3. Exemplar virtual model of a machine tool as the system element

The most popular production system are configured in workcells grouping technological, transport and auxiliary equipment. The representative of technological equipment is a numerically controlled lathe (Fig.2). This model was created in the Siemens NX program basing on the real EMCO Concept Turn 155 lathe.

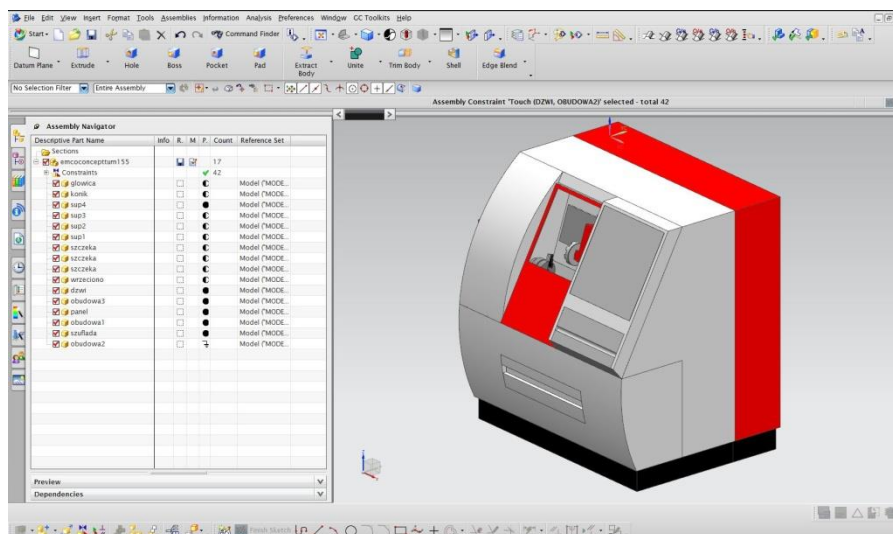


Fig.2. Model of a virtual lathe

The elaborated model could simulate the work of a real one. It could also realize task introduced using standard G-code (Fig.3).

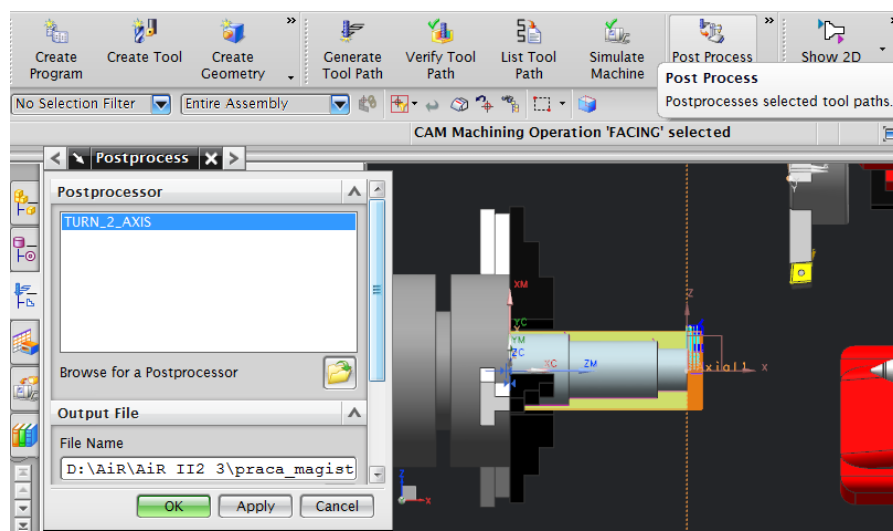


Fig.3. Model of a virtual lathe

Such a virtual model of a system element could be used to create the whole model of a analysed production system, not only a workcell. The other elements that could be realized are: transport units (robots, conveyors) and auxiliary units (reorientation stands, buffers, magazines). All these units could work controlled by the G-code programs and could be supervised by the system host computer. It could be responsible for coordination of a system work and for system state monitoring.

4. Conclusion

Presented solution is the initial phase of virtual production system building. It could help to introduce the rules of Lean Production to the practice of production systems designing. Such virtual environment allows also to link engineering programs with information ones [3]. The last are particularly important at task like production scheduling. The representative of this class of computer systems are programs of computer aided process planning (CAPP) that help to automatize tasks considered with production engineering [4].

Secondly, to develop the virtual environment of running production systems, it is needed to expand the functionality and possibilities of designing and simulating informatics tools [5,6]. They could let to integrate informatics tools representing different areas of production systems modelling. Moreover the virtual environment allow conducting investigations considered with analysis of an occurrence of particular *mudas* (wastes) and tracking results of chosen their elimination methods.

References

1. Womack J. P., Jones D. T., Roos D.: The Machine That Changed the World: The Story of Lean Production. New York:Free Press 1990.
2. Rother M, Shook J.: Learning to See: Value Stream Mapping to Add Value and Eliminate MUDA. Cambridge: Lean Enterprise Institute 2008.
3. Ćwikła G.: The methodology of development of the Manufacturing Information Acquisition System (MIAS) for production management. "Applied Mechanics and Materials" 2014, Vol. 474, pp. 27-32.
4. Grabowik C., Kalinowski K., Kempa W., Paprocka I.: A survey on CAPP systems development methods. "Advanced Materials Research" 2014, Vol. 837, pp. 387-392.
5. Gwiazda A.: System of Designing Complex Technical Means Using Fuzzy Analysis. "Applied Mechanics and Materials" 2014, Vol. 474, pp. 147-152.
6. Banaś W., Herbuś K., Kost G., Nierychlok A., Ociepka P., Reclik D.: Simulation of the Stewart platform carried out using the Siemens NX and NI LabVIEW programs. "Advanced Materials Research" 2014, Vol. 837, pp. 537-542.

SELECTED ENGINEERING PROBLEMS

NUMBER 5

INSTITUTE OF ENGINEERING PROCESSES AUTOMATION
AND INTEGRATED MANUFACTURING SYSTEMS

Ryszard NOWOSIELSKI, Anna KILJAN*, Aleksandra GUWER, Rafał BABILAS

Institute of Engineering Materials and Biomaterials, Faculty of Mechanical Engineering,
Silesian University of Technology, Gliwice, Poland

* anna.lebuda@polsl.pl

CHARACTERIZATION OF SELECTED MG-BASED AMORPHOUS ALLOY

Abstract: This paper describes results of chosen investigations of Mg-based amorphous alloy. The amorphous structure has been verified by X-ray diffraction method, SEM observations and thermal analysis. The investigations have been done on the glassy alloy $Mg_{65}Cu_{25}Y_{10}$ in the form of plate which was obtained by copper mould pressure casting.

1. Introduction

Bulk metallic glass is an alloy of metals or metals with metalloid, which has an amorphous structure, resulting from the high rate of cooling during the casting process (transition from the liquid to the solid state without the step of crystallization).

Metallic glasses can be divided into conventional and bulk forms. Characteristic structure of crystal materials (Fig. 1a) is a repeatable arrangement of atoms in three main directions, while amorphous materials (Fig. 1b) are characterized with random distribution [1].

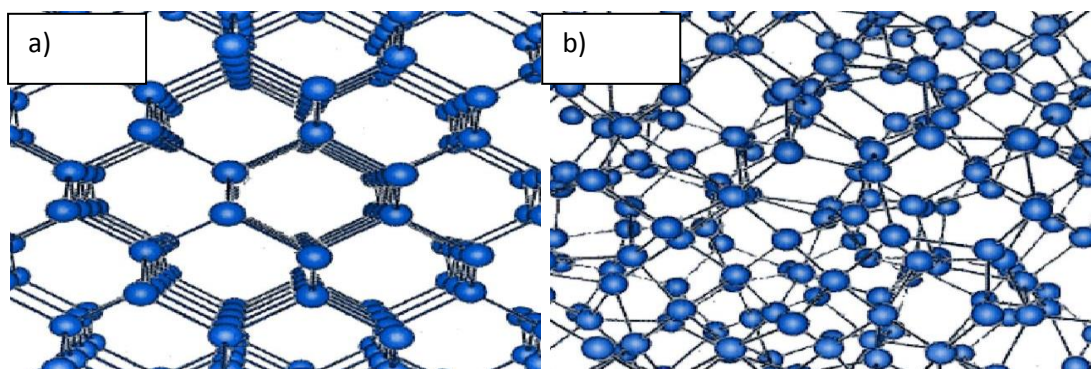


Fig. 1 Crystalline structure (a) and amorphous structure (b) [1]

The Mg-based amorphous alloys are the new group of materials, which are characterized by a high glass-forming ability, low crystallization temperature and low density.

Most of the researches were conducted using Mg-Cu-Y alloys with different alloying elements like Zn, Ni or Ag [2].

The main problem is to obtain the amorphous structure. In order to prove that the obtained structure is amorphous - XRD, microscope and calorimetric examinations are carried out.

2. Useful experimental methods

Constant knowledge development in range of materials has caused the widening and improving investigation methods. At the moment the scientists are able to examine phenomenons concerning phases occurring in alloys, atomic lattice structure, structure, revealing defects and to determine mechanical, corrosive, physical and technological properties. Used methods can be divided with regard to type of obtained results, chemical analysis, physical research, mechanical properties examination, non-destructive testing, corrosion testing, metallographic examination, X-ray crystallography. Those methods are used for structure analysis and engineering materials properties with crystalline structure.

Those research can be used also for testing the structure and amorphous material properties.

Amorphous structure research includes [3,4,5]:

X-ray examination

X-ray diffraction (XRD) concerns crystalline, polycrystalline and amorphous substances and to determine phase structure composition which occur in tested samples. This is the basic method of structure and defect material analysis. Diffraction data are obtained in form of diffractograms which depict relationship between diffraction reflection intensity and spacing between the planes d or Bragg's reflective angle 2θ . Diffractogram composes specific and unique diffraction picture of specific substance. This picture always looks the same for specific substance. Diffraction testing is carried out by the diffractometer or goniometer [6].

Scanning electron microscopy

Scanning electron microscope (SEM) is used to examine microstructure and sample analysis. This microscope has unusual resolution ability in range from 2,5 up to 5,0 nm during examination of cast samples. Additional advantage is the depth of focus which is used to examine strongly developed surfaces. Materials tests done with help of the electron microscope can be divided into three basic areas with regards to degree of sample's surface topography development. The first group are the investigations related to material decohesion and analysis of strongly developed material surfaces. Those are fractographic tests allowing to link the fracture structure with damage mechanism and material properties. Second area contains analysis of medium developed surfaces. Those are surfaces subjected to corrosion process. Third group uses high resolution ability of scanning microscope. In this case the flat surfaces are the subject of examination which correspond to surfaces of optical microscope metallographic specimens [7,8].

Thermal analysis

Thermal analysis describes changes which occur in material during temperature impact. Material under the test can undergo physical changes, like: glass-transition (vitrification), devitrification, crystallization, melting, sublimation, vaporization or boiling as well as chemical changes like: decay reaction, reduction, oxidation. These thermo-analytic investigation consist of [9,10,11]:

- TGA – Thermogravimetric Analysis, which records material mass changes,
- DTA – Differential Thermal Analysis, which bases on gradual and precisely determined heating and cooling of the sample, recording different temperatures

between test sample and a reference material where both are in the same conditions. The result of this test is the curve showing relationship between thermocouple voltage difference and temperature.

- DSC – Differential Scanning Calorimetry, which determines changes of heat stream difference of reference material during enforced temperature changes. The result of this test is the curve showing relationship between delivered heat energy into the sample and temperature.

3. Results and discussion

The investigations have been carried out on the received $Mg_{65}Cu_{25}Y_{10}$ alloy of in the form of plate (Fig. 2a) with thickness of 1 mm and width of 5 mm. This sample has been obtained by the pressure casting method of molten alloy into copper mould cooled by water. The casting process was done in the argon atmosphere.

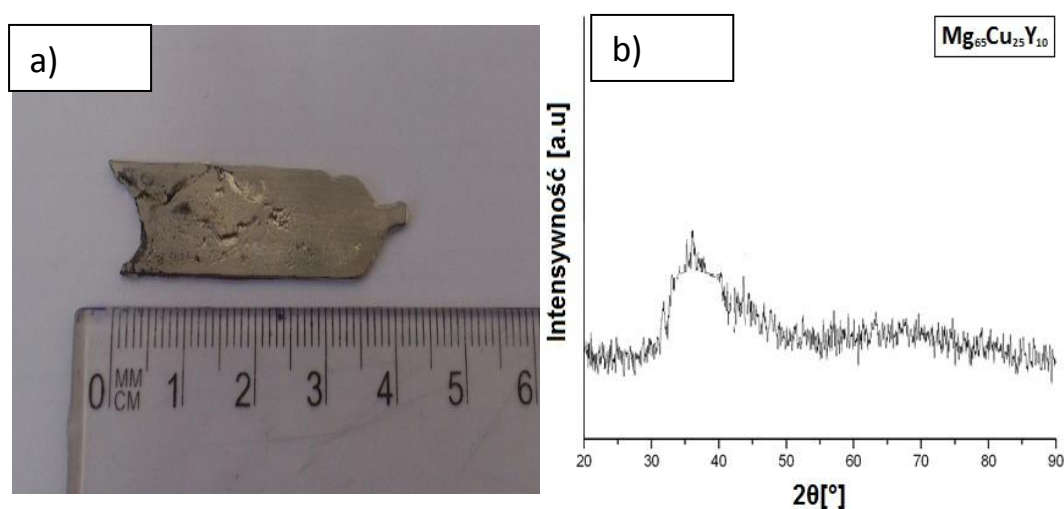


Fig. 2 External morphology (a) and XRD pattern (b) of $Mg_{65}Cu_{25}Y_{10}$ metallic glass in the form of plate

X-ray diffraction tests have been carried out by the X-ray diffractometer X'Pert Pro with cobalt anode. and showed that the test sample of $Mg_{65}Cu_{25}Y_{10}$ alloy has the amorphous structure. XRD pattern shows broad halo between 30-50° which is typical for amorphous structure of magnesium alloys (Fig 2b). What is more, single diffraction peak could be observed on the amorphous halo which may probably suggest a beginning of oxidation of prepared sample.

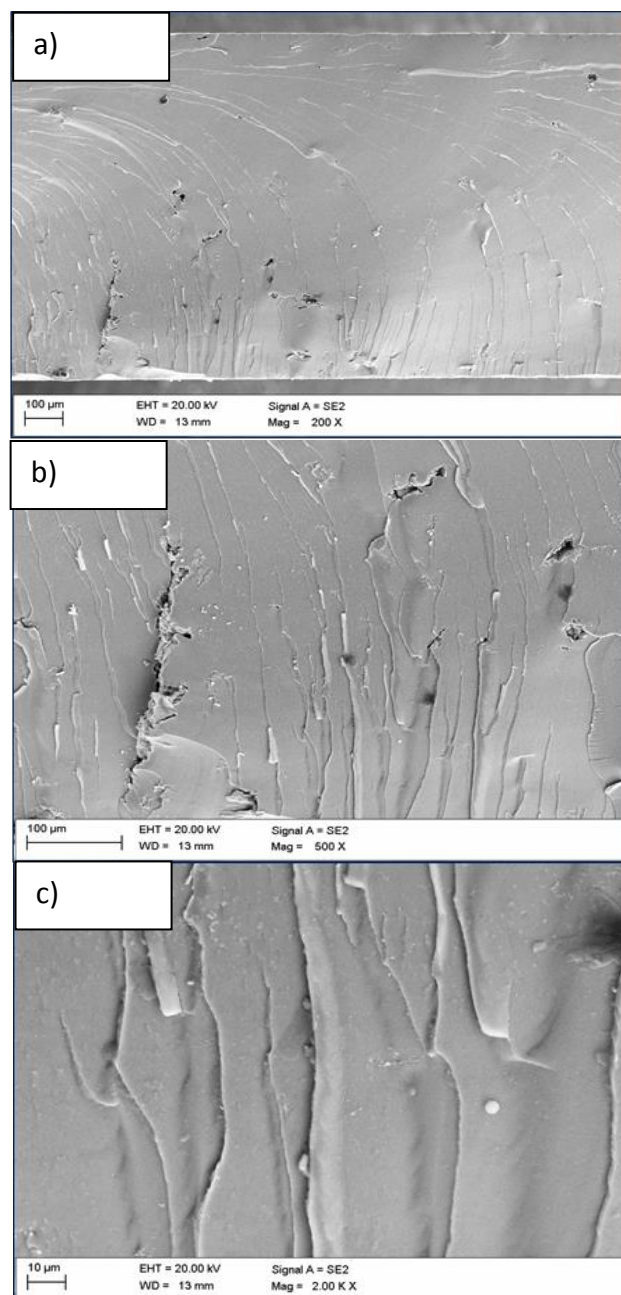


Fig. 3 Fracture morphology of $Mg_{65}Cu_{25}Y_{10}$ glassy alloy – SEM images with magnification of: a) 200x, b) 500x, c) 2000x

Figure 3 shows fracture morphology of the amorphous plates obtained by SEM observations with magnification of 200x, 500x i 2000x. On the chosen areas one can see mixed fractures as well as scaly. The scaly fractures are typical for brittle bulk metallic glasses.

DTA method was used to determine the onset (T_m) and end (T_L) of melting temperature of $Mg_{65}Cu_{25}Y_{10}$ master alloy (Fig. 4). Tests have been carried out with using Netzsch DSC 404C calorimeter in temperature range of 200 - 800 °C with heating rate of 10 K/min and an

argon protective atmosphere. The T_m temperature was 441°C and the T_L temperature was 583°C.

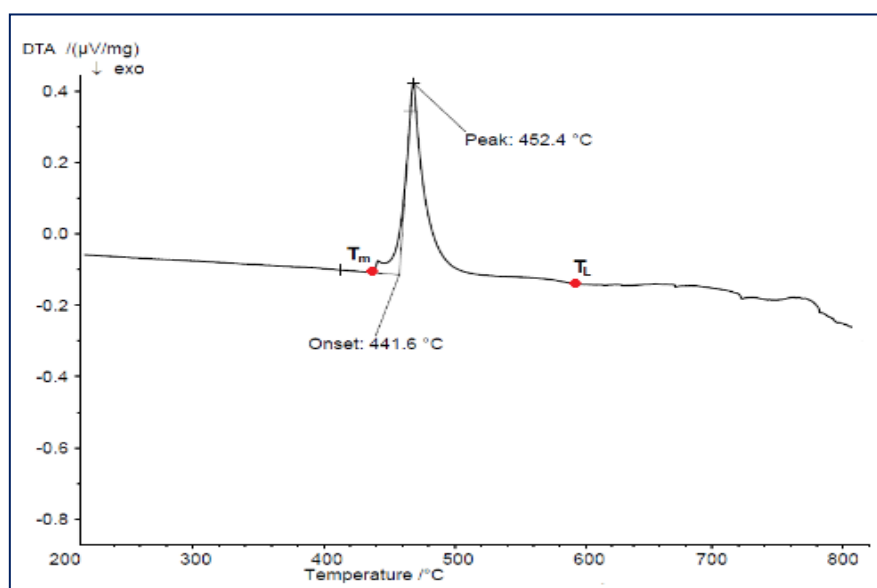


Fig. 4 DTA curve of Mg65Cu25Y10 master alloy

Similarly, DSC method (Fig. 5) method was used to determine the glass-transition (T_g), onset crystallization (T_x) and peak crystallization temperature (T_p). The investigations were carried out using the Netzsch DSC 404C calorimeter in temperature range of 100-400°C. Measurements have been carried out in argon protective atmosphere and heating rate of 10 K/min. The T_g was 122°C, the T_x temperature was 180°C. The crystallization peak temperature equals to 188°C. Value of ΔT_x is 58°C and is similar to values showed in the literature for this alloy. ΔT_x is the difference between temperature T_x and T_g .

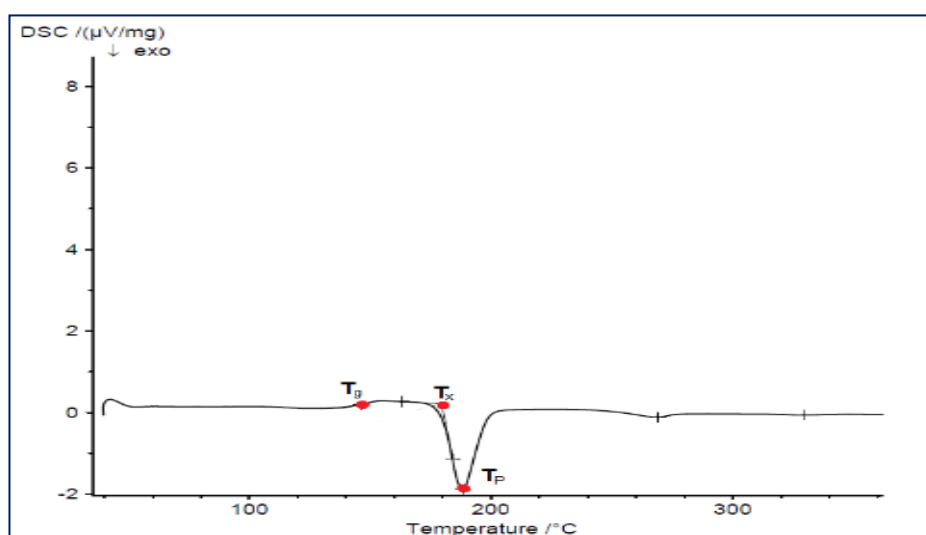


Fig. 5 DSC curve of Mg65Cu25Y10 glassy alloy

4. Conclusions

In this paper experimental methods used for verification of an amorphous structure and selected properties of $Mg_{65}Cu_{25}Y_{10}$ alloy have been described. X-ray analysis confirmed that the obtained alloy has amorphous structure. Analysis of fracture surfaces has showed the presence of scaly fractures which are typical for brittle metallic glasses. Calorimetric analysis allowed to determine the onset crystallization temperature ($T_x=184^{\circ}C$), crystallization temperature peak ($T_p=190^{\circ}C$) and the glass-transition temperature ($T_g=134^{\circ}C$).

References

1. L. Brindley, Fixing bones with dissolvable glass, <http://physicsworld.com>
2. Babilas R., Zajączkowski A., Głuchowski W., Nowosielski R., Preparation and glass-forming ability of Mg-based bulk amorphous alloys, "Archives of Materials Science and Engineering" 2013, vol. 62 (2), pp. 78-86.
3. Collective work edited by R. O. Wielgosza, S. M. Pytla, The laboratory of metallurgy, Cracow University of Technology publishing, Cracow 2003
4. J. Deputat, S. Mackiewicz, J. Szelażek, Problems and techniques of non-destructive testing of materials, Biuro Gamma publishing, Warsaw 2007
5. M. Wojtas, Product defects detected by non-destructive methods, Biuro Gamma publishing, Warsaw 2006
6. S. Mackiewicz, X-ray diffractometry in NDT - new European standards, National conference radiographic researches, 2005.
7. D. E. Newbury, D. C. Joy, Advanced Scanning Electron Microscopy and X-Ray Microanalysis, Plenum Publishing Corporation, New York 1986
8. X.L. Zhang, G. Chen, T. Bauer, Mg-based bulk metallic glass composite with bio-corrosion resistance and excellent mechanical properties, *Intermetallics* 29, 2012
9. M. Szechyńska-Hebda, M. Hebda, Thermal analysis studies of materials biological, *Technical Journal*, Cracow University of Technology publishing, 2-Ś/2011, pp. 227-234
10. T. Rydzkowski, Researches of the structure of polymers the degree of crystallinity, Koszalin University of Technology publishing, 2008, pp. 143-148
11. Ling-ling Shi, Hian Xu, Mg based bulk metallic glasses: Glass transition temperature and elastic properties versus toughness, *Journal of Non-Crystalline Solids*, 357, 2011, pp. 2

SELECTED ENGINEERING PROBLEMS

NUMBER 5

INSTITUTE OF ENGINEERING PROCESSES AUTOMATION
AND INTEGRATED MANUFACTURING SYSTEMS

Wirginia PILARCZYK, Magdalena MAJCHRZAK

Institute of Engineering Materials and Biomaterials, The Faculty of Mechanical Engineering, Silesian University of Technology, Gliwice 44-100, ul. Konarskiego 18a, Poland
Corresponding author: magdalena.majchrzak90@gmail.com, wirginia.pilarczyk@polsl.pl

THE IDENTIFICATION OF HAZARDS IN THE PROCESS OF PRODUCTION AND EXAMINATION OF BULK METALLIC GLASSES WITH FERROUS MATRIX

Abstract: In this article hazards connected with production and examination of bulk metallic glasses with ferrous matrix were described. Bulk metallic glasses were produced by the use of high-pressure casting to copper mould cooled with water. The sample structure examination was carried out with the use of X-ray analysis (XRD), light microscopy and scanning electron microscopy (SEM). Thermal properties were tested with scanning differential calorimeter (DSC). Test and casting stands underwent occupational risk assessment with the use of Risk Score method.

1. Introduction

Bulk metallic glasses show series of extraordinary properties connected with their structure. These are non-crystalline alloys formed because of high cooling speed (in the range of 10 K/s). The solidification speed decreases with the increase of cross-section width. The material of amorphous structure is considered as bulk, only when the cast cross-section width is at least 1 mm. Attractiveness of these materials, compared with typical crystalline alloys, makes that they are very useful and desirable. They are used apart from others for IT elements, sports or medical devices. In practice you can get metallic glasses using different methods of production. But using the equipment at test stands of these materials is connected with a slight hazard, which has to be assessed. The aim of occupational risk assessment is hazard effect prevention and risk reduction and elimination. Residual risk that cannot be eliminated should be controlled, but the knowledge of risk and hazard should be passed to the employees.

2. Fe-Co-B-Si-Nb alloy formation with the use of pressure casting

At the first stage the basic alloy of proper atom composition with Fe,Co, B,Si and Nb elements was formed. To homogenize the structure double induction remelting was used. Next, comminuted ingot was molten in a quartz crucible with the use of an induction heater. Molten material was cast under pressure into a copper mould. The material was cast in the form of two 20x10x1mm plates.

3. The examination of bulk metallic glasses in the form of plates

The experiment carried on the created plates allowed to draw unique conclusions. Both X-ray and calorimetric testing together with microscopic observations showed that the sample number 1 is crystalline, whereas the second one is amorphous and crystalline. Series of diffraction lines of such intermetallic components as Fe_2B , Co_3B , FeSi were discovered on diffraction pattern.

The observations with the use of light microscope revealed a lot of precipitates, crystallites, non-metallic inclusions and microcracks on the crystalline plate. On the other hand there is a small number of little precipitates and uniform area on the amorphous plate. SEM images show that in the amorphous plate sample cross-section two sections can be observed, those comprising "plain" areas and characteristic patterns (resembling rivulets). Exothermic peak on DSC curve for the second sample confirms the presence of crystallization process. The peak crystallization temperature equals 899.23K, whereas the temperature of vitrification is 830.08K.

4. Occupational risk assessment

Occupational risk assessment is connected first of all with work process risk and hazard establishment. The term hazard means any factor occurring in the work environment which can suddenly and violently create dangerous events causing accidents and potential accidents, failures and technical damages. Risk is the occurrence of harmful factors in work environment, which because of longer exposure on human organism can cause occupational diseases, semi-occupational diseases (occupational illness) or employee's temporary efficiency decrease.

According to PN80/Z08052 (Polish norm) dangerous and harmful factors are the physical, chemical, biological and psychophysical factors.

Occupational risk assessment means detailed hazard and risk identification at the work place. On its basis it is possible to assess occupational risk on a given position and compare risk assessment with risk acceptance criteria and define reduction actions.

The occupational risk assessment by Risk Score method was carried out on the following posts: sample preparation stand, stand equipped with X-ray diffractometer, to make microsections and observations with the use of light microscope and finally posts equipped with SEM and DSC. Risk Score is a popular method of risk indicator. In this method three-factor-formula is used:

- P- the probability of event occurrence,
- E- hazard exposure,
- S- the probable hazard effects.

Calculations of the final hazard index can be presented in the following way: $WR=P \cdot E \cdot S$. The carried out occupational risk assessment (Fig.1) showed that most hazards on research stands are on acceptable level.

The greatest danger on the alloy preparation stand is the induction heater, which not only emits harmful electromagnetic radiation, but can also be the source of burns or metal chips. A major hazard during the use of X-ray diffractometer is X-ray radiation. During microscopic observations the decrease of eyesight organ efficiency and bone-muscular system load used by a forced body position. These hazards are also applicable as far as the stand which is equipped with scanning differential calorimeter are concerned. What is more on the research

stands with light microscope and devices for making microsections, the caustic substances and moveable elements of machinery and devices create danger. The work with scanning electron microscope causes exposure to electromagnetic radiation. All stands (apart from the one for massive amorphous alloys casting) possess a computer which is the source of electromagnetic radiation and such hazards as: movement organ overloading and eyesight perception overloading.

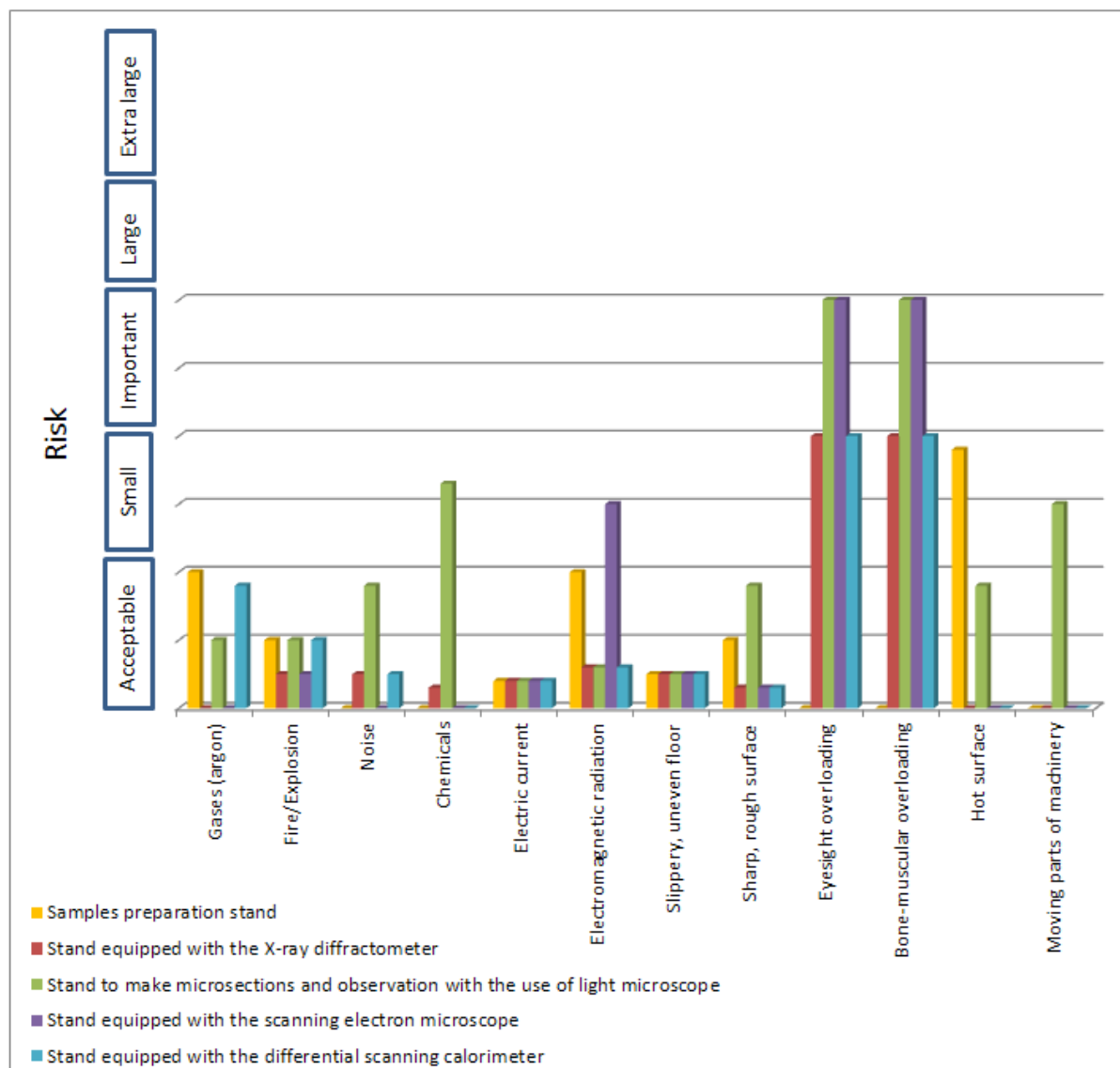


Fig.1 The result of Risk Score method occupational risk assessment on different research stands.

5. Summary

X-ray analysis, calorimetric research and microscopic observations showed that the first sample is crystalline whereas the second is amorphous-crystalline one.

Risk Score method occupational risk assessment proved that the majority of hazards occurring on research stands is on an acceptable level. So one should aim at minimizing the risk thanks to preventive measures.

On the microscopic observation stands an essential danger is eyesight and bone-muscular overloading. It is caused by a forced body position both during working with the computer and microscopic observations. Occupational risk assessment points at the elements creating hazardous situations or exposure during working process. Employers are obliged to obey Industrial Safety regulations and inform their employees about dangers. But the main aim of risk assessment is to allow the employer to take necessary measures to guarantee their employees safety and health protection such as:

- guarantee ergonomic workplace (chair, monitor, keyboard regulation, proper lighting, ventilation);
- equip in means of personal and collective protection (using protective gloves while working with hot surfaces and chips and using lead shields in the case of X-ray radiation);
- frequent measuring (using health physics membrane while working with X-ray diffractometer and measuring control);
- good work organization (good spatial organization, proper aisle width, order in the workplace, clean and non-slippery surfaces, cleanliness);
- the use of breaks at work (5 min. after each hour of work, employment contract guarantees 15-minute-break every 8 hours if the daily work time at the computer lasts at least 4 hours);
- good electrical system working condition.

Acknowledgment

This project was funded by the National Science Centre allocated on the basis of the decision number DEC-2011/01/D/ST8/07327

References

1. Krause M.: Risk assessment – requirements, guidelines, examples. Edition I, Higher Engineering School of Safety and Labour Organization in Radom, Radom 2008.
2. Rączkowski B.: Health and safety at work in practice. Edition XII, Advisory Centre and Staff Training Sp. z o. o., Gdańsk 2009.
3. Suryanarayana C., Inoue A., Bulk Metallic Glasses, CRC Press Is An Important Of The Taylor & Francis Group, An Informal Business, 2011.
4. http://www.pip.gov.pl/html/pl/prewencja/ocena_ryzyka_zawodowego/96000000.php.

SELECTED ENGINEERING PROBLEMS

NUMBER 5

INSTITUTE OF ENGINEERING PROCESSES AUTOMATION
AND INTEGRATED MANUFACTURING SYSTEMS

Marek PŁACZEK

Institute of Engineering Processes Automation and Integrated Manufacturing Systems,
Faculty of Mechanical Engineering, Silesian University of Technology, Gliwice, Poland
*marek.placzek@polsl.pl

A CONCEPT OF THE MECHATRONIC SYSTEM DESIGNED FOR FREIGHT CARS MANAGEMENT

Abstract: Paper presents assumptions of the mechatronic system designed for freight cars management during their exploitation. The system is based on the idea to use piezoelectric transducers for measuring dynamical response and inferred on its basis about the status of the wagon. Non-classical transducers such as Macro Fiber Composite or Polyvinylidene Fluoride piezoelectric foils are proposed to be used in the system as sensors. Those elements should be glued on surfaces of the freight car's elements and connected to the wireless transmitting system. The type 1415 A3 freight car is considered in this work.

1. Introduction

Nowadays railway transport is very important for the development of the modern economy. Many research works concerning with problems occurring in this way of transport and its development are being carried out all the time [1,3,7,9-11]. The main goals of those works are usually to develop the infrastructure that is used for transport of goods and people, make it more cost-effective, safe and less burdensome for the environment. Presented work is also a part of the research project that aim is to modernize freight cars during their renovation. It is continuation of the research works connected with modernization of freight cars [3,11]. The project is carried out by the consortium that consists of the scientific entity – the Institute of Engineering Processes Automation and Integrated Manufacturing Systems from the Silesian University of Technology and enterprises – DB Schenker and Germaz. The aim of this research project is to modernize the analysed wagon during its renovation using new composite materials. Effects that are to be achieved by the modernization are:

- better corrosion protection of the wagon elements,
- easier unloading of the wagon in winter conditions (no freezing of the cargo to the sides and floor of the wagon),
- reduction of the weight of the wagon while its load increases,
- easier management of freight cars during exploitation.

In this work main assumptions of the mechatronic system designed to fulfil the last proposed goal are presented. The idea of the system is to make possibility to infer about the status of the wagon on the basis of its vibration generated during driving. What is more the

system should be self-powered. Energy of vibrations will be also used for generate electric voltage using direct piezoelectric phenomena.

Applications growth of piezoelectric transducers is parallel to the process of piezoelectric materials development. New, more efficient transducers are searched all the time. Direct and reverse piezoelectric phenomena are very often used in new, innovative mechatronic systems. It is mostly caused because there is easy to transform mechanical energy into electrical energy and vice versa using piezoelectric transducers. It causes that they can be used both as sensors or actuators in mechatronic systems. Analysis and synthesis of the mechanical and mechatronic systems were presented in [2,4-6,8].

2. Object of considerations – the freight car type 1415 A3 and its models

As the object of considerations the freight car type 1415 A3 was selected. It is the 4-axle open wagon series EAOS and produced by BREC Belgium. It is one of the most popular types of wagons designed to unload with the use of tipplers. After consultations with employees of enterprise specialized in repairing of freight cars it can be noticed that the main problems during exploitation of this type of wagons are:

- corrosion of plating of the wagon's plating,
- mechanical damage of the wagon's plating - usually as a result of the improper unloading (using buckets and excavators instead of tipplers).

At the same time the type 1415 A3 wagon has a high strength of the supporting box (top girder, lateral reinforcing strip etc.). The considered type of freight wagon and its typical damages are presented in Fig. 1.



Fig.1. The considered freight wagon and damage of the body shell

As the first step of the whole research project CAD models of a few selected freight wagons were created using Siemens NX 8.5 software. Precision of the created models was verified by checking its mass after defining material properties of wagon components and juxtaposing it with the mass of the real wagon. After verification the models were used in strength analysis using the Finite Element Method in NX software. The CAD model is

presented in Fig. 2. The created 3D model is very detailed and obtained discrepancy is 5,34% of the real wagon mass. The difference is the result that the model does not include the braking system (pipes and pneumatic cylinders, brake pads etc.) After its verification the model was used in strength analysis using the Finite Element Method in NX software. Obtained results will be presented in others author's publications.



Fig.2. The CAD model of the considered type of freight car

In order to verify assumptions of the designed mechatronic system based on analysis of the dynamical response of the freight car a physical laboratory model of the supporting structure of the considered 1415 A3 freight wagon was built in scale. It is presented in Fig. 3. There are a lot of simplifications in the created model juxtaposed with the real object. The purpose is that the laboratory model was created only for initial verification of the possibility to measure the dynamical response of the wagon using piezoelectric films. In the future works measurements on the real object will be carried out.



Fig.3. The simplified laboratory model of the supporting structure

In Fig. 3 a pendulum that was used for vibration excitation is also presented.

3. Measurements and results

In carried out tests the piezoelectric PVDF film was used as a sensor and pendulum was used for vibration excitation. The PVDF film was glued on the frame of the laboratory model in the position of the second measuring point (see Fig. 4). Measuring points were chosen on the basis of the modal analysis carried out using CAx software and virtual model of the system. In carried out tests a model LDT1-028K of PVDF piezoelectric foil was used [12]. It is presented in Fig. 5.

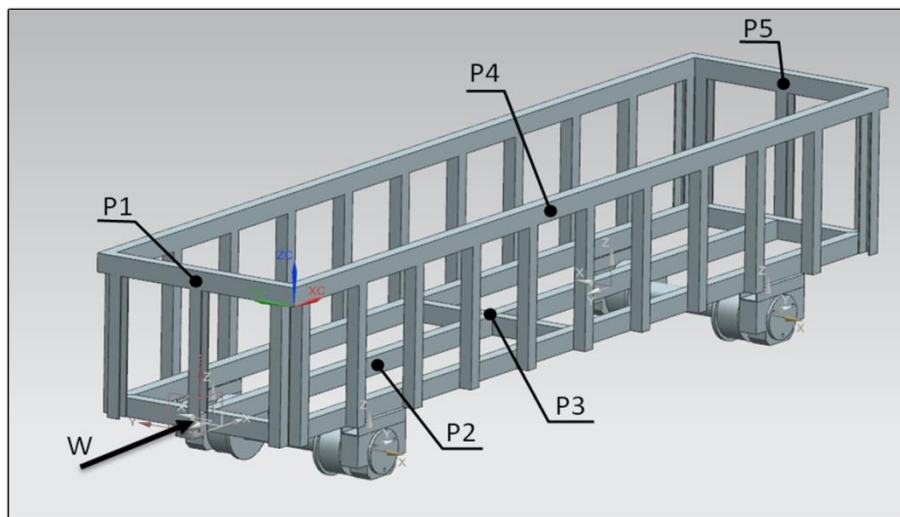


Fig.4. The CAD model of the laboratory stand with measuring points



Fig.5. The CAD model of the laboratory stand with measuring points

PVDF piezoelectric film, and more particularly the sensor LDT, which was used in this study consists of three layers: polyester laminate, a piezoelectric film and a protective coating. The PVDF piezoelectric film elements produce more than 10 mill volts per micro strain and about 60 dB higher than the voltage output of a foil strain gage. Their capacitance is proportional to the area and inversely proportional to the thickness of the element. Such kinds

of sensors are the simplest form of piezoelectric film sensors that can be used for example as dynamic strain gauges and contact microphones for vibration or impact detection. They can be readily adhered to a surface with double-sided tape or epoxy [12].

During measurements two states of the freight car were analysed. Dynamical responses of the model without and with load were measured. In Fig. 5 results of the measurements conducted using PVDF piezoelectric foil glued in the position of the P2 measuring point are presented. It can be observed that this time maximum values of the voltage signal generated by the PVDF foil are very similar for both measurements – with and without load but it can be easily noticed that the time to damp vibrations is shorter for the system with load.

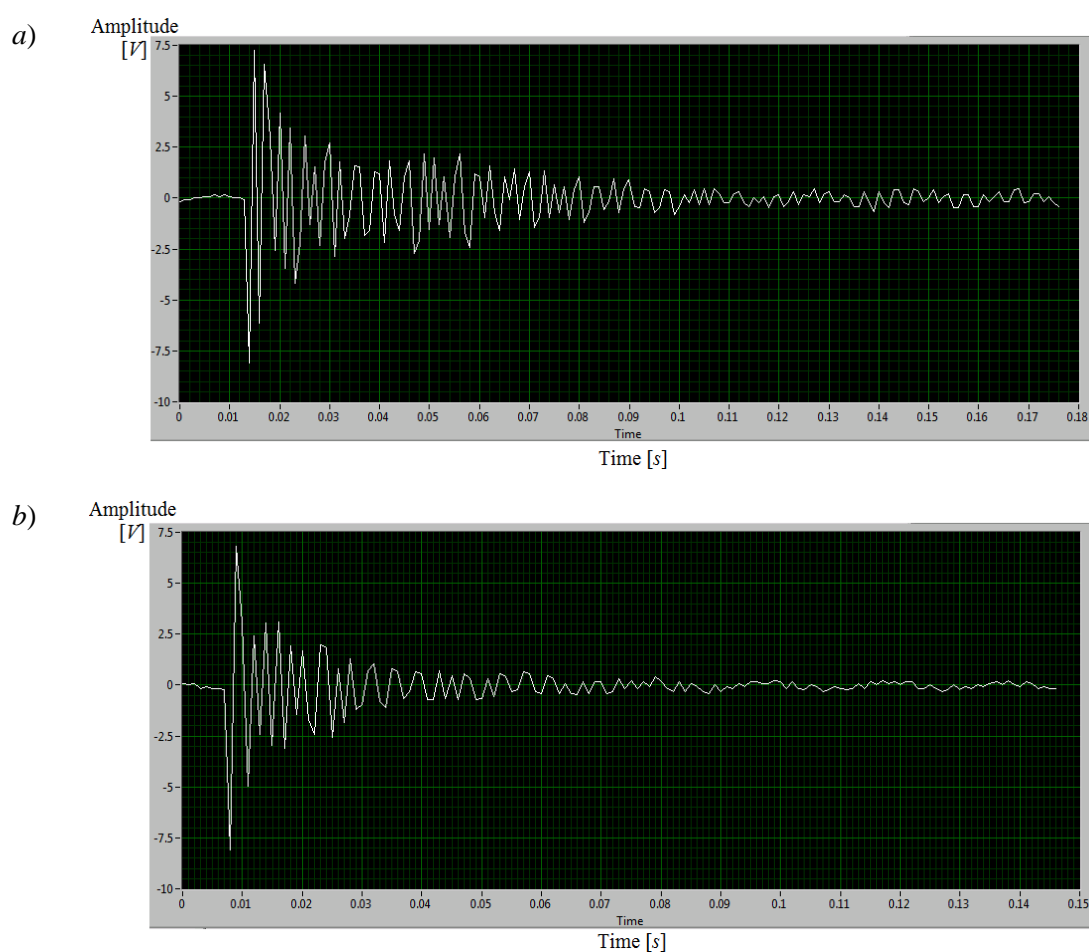


Fig.6. Results of measurements without (a) and with load (b)

Results of carried out tests were very repeatable so it can be assumed that proposed method of dynamical response measurements can be treated as very precise and successfully used in designed mechatronic system. During the future tests the analysis of the model dynamical response while driving will be carried out. Finally tests on the real object will be conducted in order to verify results obtained on the laboratory model.

4. Conclusion

The main aim of presented work was to verify if it is possible to measure dynamical response of the considered object using piezoelectric foils. The carried out tests proved that there is a possibility to create a mechatronic system that can be integrated with the freight car and used for its management during exploitation (collecting data about its location, condition, load etc.). Such system can be based on piezoelectric foils application. The system that is intended to be created will allow monitoring of the freight car dynamic parameters during its normal exploitation and inferred on its basis about the status of the wagon. It should be noticed that those results and proposed thesis must be verified by tests on the real objects during their normal exploitation.

References

1. Berghuvud A.: Freight car curving performance in braked conditions, Proceedings of the Institution of Mechanical Engineers, Part F: Journal of Rail and Rapid Transit, (2002), pp. 23-29.
2. Białas K.: Mechanical and electrical elements in reduction of vibrations, Journal of Vibroengineering, Vol. 14, Issue 1 (2012), pp. 123-128.
3. Baier A., Zolkiewski S.: Initial research of epoxy and polyester warp laminates testing on abrasive wear used in car sheathing, Eksploatacja i Niezawodność – Maintenance and reliability, Vol. 15, Issue 1 (2013), pp. 37–43.
4. Buchacz A., Gałęziowski D.: Synthesis as a designing of mechatronic vibrating mixed systems, Journal of Vibroengineering, Vol. 14, Issue 2 (2012), pp. 553 -559.
5. Buchacz A., Płaczek M., Wróbel A.: Control of characteristics of mechatronic systems using piezoelectric materials, Journal of Theoretical and Applied Mechanics, Vol. 51 (2013), pp. 225-234.
6. Buchacz A., Płaczek M., Wróbel A.: Modelling of passive vibration damping using piezoelectric transducers – the mathematical model, Eksploatacja i Niezawodność – Maintenance and reliability, Vol. 16, Issue 2 (2014), pp. 301–306.
7. Connolly D. P., Kouroussis G., Giannopoulos A., Verlinden O., Woodward P. K., Forde M. C.: Assessment of railway vibrations using an efficient scoping model, Soil Dynamics and Earthquake Engineering, Vol. 58 (2014), pp. 37-47.
8. Dymarek A., Dzitkowski T: Method of active synthesis of discrete fixed mechanical systems, Journal of Vibroengineering, Vol. 14, Issue 2 (2012), pp. 458-463.
9. Kovalev R., Lysikov N., Mikheev G., Pogorelov D., Simonov V., Yazykov V., Zakharov S., Zharov I., Goryacheva I., Soshenkov S., Torskaya E.: Freight car models and their computer-aided dynamic analysis, Multibody System Dynamics, Vol. 22, Issue 4 (2009), pp. 399-423.
10. Zhai W. M.: Modelling and experiment of railway ballast vibrations, Journal of Sound and Vibration, Vol. 270, Issues 4–5 (2004), pp. 673–683.
11. Zolkiewski S.: Testing composite materials connected in bolt joints. Journal of Vibroengineering, Vol. 13, Issue 4 (2011), pp.817-822.
12. <http://www.imagesco.com/catalog/sensors/film.html> (Access 15.10.2014).

SELECTED ENGINEERING PROBLEMS

NUMBER 5

INSTITUTE OF ENGINEERING PROCESSES AUTOMATION
AND INTEGRATED MANUFACTURING SYSTEMS

Piotr SAKIEWICZ^{1*}, Ryszard NOWOSIELSKI, Rafał BABILAS, Wirginia PILARCZYK,
Katarzyna CESARZ-ANDRACZKE,

¹ Institute of Engineering Materials and Biomaterials, Faculty of Mechanical Engineering,
Silesian University of Technology, Gliwice,
*piotr.sakiewicz@polsl.pl

WEEECONTAININGNANOWASTE -RISKFORENVIRONMENT AND HEALTH&SAFETY

Abstract: The quantities of waste electrical and electronic equipment (WEEE) will increase in the near future and the importance of its recycling has become more evident. This waste are mixture of materials and components that because of their hazardous content, can cause major environmental and health problems. In order to minimize risks two legislation acts have been put in place; the Directive on the restriction of the use of certain hazardous substances in electrical and electronic equipment (RoHS Directive) and Directive on waste electrical and electronic equipment (WEEE Directive). It has led to a reduction of hazardous substances which often are replaced by new ones for example nanomaterials. Actually, existing processes for the recycling of used electronic equipment focuses on separation of metals but there is not procedures taking into account the presence of nanowaste. It is significant subject not only from the point of waste treatment and the recovery of valuable materials but also from the risk for environment and health.

1. Introduction

Nanotechnology has developed in very short time in an uncontrolled manner in all areas of life including electronic and household goods industry. Waste electrical and electronic equipment (WEEE) is considered to be one of the fastest growing waste torrent in the EU, growing at 3-5 % per year. In 2005 it was generated 9 million Mg, and expected to grow to more than 12 million Mg by 2020 [1,2]. The advances is driven by revolution in material sciences. The electric and electronic equipment has been developed, applied, and consumed worldwide at a very high rate and its give an opportunity for the use of nanotechnologies in electronic components and products. Nanotechnology in electrical and electronic equipment is encountered as nano thin-films, nanofibers, nanowires, nanotubes, nanoparticles, nanopowders, nanocapsules, fullerenes, dendrimers, quantum dots, nanostructures, nanocoatings, nanoparticles, nanostructured films, nanofibers used in e.g.;

- displays,
- nanocomposites,
- organic electronics,
- optoelectronics and photonics,

- energy storage and generation devices e.g. batteries, solar cells, capacitors, fuel cells,
- heat management systems,
- nanosensors,
- memory and storage devices.

The WEEE and electronic industry waste include: products containing nanoparticles, pure nanomaterials, nano thin-films, nanofibers, nanowires, nanopowders, nanostructures, liquid suspensions containing nanoparticles, items contaminated with nanomaterials and solid matrixes with nanomaterials.

2. Risk for environment and health & safety

The importance of smart waste electrical and electronic equipment recycling has become more evident over the last years. WEEE are inhomogenous and complex in terms of materials and components. In order to develop a cost effective and environmental friendly recycling system, it is important to identify and quantify of materials and hazardous substances to understand the physical characteristic of this waste stream [2]. The restriction in use of hazardous substances in electrical and electronic equipment entered in 2003 cause necessity of replacing old materials by new. The maximum tolerated amount of the substance permitted in any homogenous material from which the application is comprised. At present the list of substances including e.g. : lead, mercury, cadmium, polybrominated diphenyl ethers (PBDE), hexavalent chromium, polybrominated biphenyls [3].

It has led to a reduction of hazardous substances, which often are replaced by new materials often containing nano solution. The industry produces ever smaller electronics devices improving costs, properties and performance often using nanotechnology. Development of nanotechnology causes miniaturization and the current electronic products tend to be smaller and more integrated. This impede reparability and shorten the product life cycle causing more amount of waste. The WEEE Directive has ten categories of electrical and electronic equipment and they are categorized as follows [4]:

- large household appliances ,
- small household appliances,
- it and telecommunications equipment,
- consumer equipment,
- lighting equipment,
- electrical and electronic tools with the exception of large scale stationary industrial tools,
- toys, leisure and sports equipment,
- medical devices with the exception of all implanted and infected products,
- monitoring and control instruments,
- automatic disperses.

The structure and chemical composition of the WEEE depends on the type and the age of the equipment. For example WEEE from IT contain a higher amount of precious metals and nanomaterials than scrap from household. In older devices the amount of nanowaste is low but content of valuable metals and hazardous substances is higher [1]. Due to their hazardous material contents, if WEEE are not correctly treated may cause environmental and health problems during the waste management, recycling or landfill phases. Commonly, the mechanical separation, electrochemical treatment, thermal treatment and hydrometallurgical

treatment methods are used for the treatment of electrical and electronic waste [5]. None of this method takes into account the prevalence of a variety of nanowaste.

The worst way of recycling WEEE with nanotechnology seems to be mechanical separation because of dust and nanoparticles formation. This nanowaste cause water, air and soil pollution leading to risk for environment and health & safety. After segregation the obtained fractions have to be treated further in other processes or have to be landfilled as it is done at present with plastic fractions (e.g. at the world's poorest countries). Very important aspect is that this nanowaste are inhomogeneous, it means that this material can't be mechanically disjointed or separated into different materials, by use of actions such as cutting, crushing, grinding and abrasive processes.

It is expected [2] that quantities of WEEE contain nanowaste will increase rapidly in the near future. Usually nanowaste are generated during the product end of life operations (e.g. recycling, landfill incineration etc.). The nanowaste are generated also during the usage of products containing nanomaterials or nanotechnology (e.g. abrasion, degradation, etc).

A useful tool may be establishing classification standards of nanowaste operation. Managing risk and uncertainty should be primarily on authority draws attention to the need to develop research in the area of dealing with nanowaste. In order to avoid the potential risks of uncontrolled and unexpected impact of nanowaste into the environment and health and safety EU supports many R&D programs (tab. 1).

Table 1. Selected nano - projects in the EU.

NANoREG	A common European approach to the regulatory testing of Nanomaterials
eNanoMapper	A Database and Ontology Framework for Nanomaterials Design and Safety Assessment
ENNSATOX	Engineered Nanoparticle Impact on Aquatic Environments: Structure, Activity and Toxicology
GUIDENANO	Assessment and mitigation of nano-enabled product risks on human and environmental health
LICARA	Life cycle approach and human risk impact assessment, product stewardship and stakeholder risk/benefit communication of nanomaterials
ModNanoTox	Modelling nanoparticle toxicity: principles, methods, novel approaches.
NANODEVICE	Novel Concepts, Methods, and Technologies for the Production of Portable, Easy-to-Use Devices for the Measurement and Analysis of Airborne Engineered Nanoparticles in Workplace Air
NANOMMUNE	Comprehensive Assessment of Hazardous Effects of Engineered Nanomaterials on the Immune System
NanoPolyTox	Toxicological impact of nanomaterials derived from processing, weathering and recycling of polymer nanocomposites used in various industrial applications
Scaffold	Innovative strategies, methods and tools for occupational risk management of manufactured nanomaterials (MNMs) in the construction industry
Nephh	Nanomaterials Related Environmental Pollution and Health Hazards Throughout their Life Cycle
NanoMILE	Engineered nanomaterial mechanisms of interactions with living systems and the environment: a universal framework for safe nanotechnology

A wide range of nanotechnology applications and lack of comprehensive knowledge on social and health consequences of its use made politicians in many countries to take steps to prepare the relevant regulations associated with the development of new technologies.

3. Conclusion

The RoHS and WEEE directive requirements force constructors and manufacturers a need to use new materials for example nanomaterials. These materials are being used as possible replacements for traditional materials. Each manufacturer have to take into account managing risks and uncertainties associated with the use of materials with not fully known properties. Especially risk for environment, health and safety associated with waste electrical and electronic equipment and the process of their recycling. The omnipresence of electronic devices in people's everyday lives requires the introduction of procedures taking into account these aspects already at the product design stage. This also applies to industrial design which use both applied science and applied art to improve the aesthetics of design products, new materials and technologies offer new opportunities. Nanotechnologies in future electronics development will play a key role. The commercialization of nanotechnology incomplete knowledge will be today profitable for industry, but in the future would be costly for all of us.

Legislation does not yet cover nanowaste. It is very important to remember that nanotechnology has many advantages, but there is also many unpredictable risks for environment, health and safety. Interdisciplinary character of nanotechnology forcing scientists from many disciplines to develop rational procedures. People should be informed about advantages and disadvantages of nanotechnology applications to reduce hazards and risk of new technology and nanowaste quantity. Nanowaste are a new kind of waste containing nanoscale materials and appointment of entirely new standards of the waste treatment is a new challenge for scientists and lawyers. The majority of nanomaterials do not exist in the natural environment and nobody is able to determine the long term effects of its creation. Intensive industrial development of nanotechnology and lack of environmental standards caused penetration of natural environment by waste also WEEE containing nanowaste.

References

1. Gramatyka P., Nowosielski R., Sakiewicz P., Recycling of waste electrical and electronic equipment., *J. Achiev. Mater. Manuf. Eng.* 2007 vol. 20 iss. 1/2, s. 535-538,
2. www.eea.europa.eu,
3. Directive 2002/95/EC of the European Parliament and of the Council of 27 January 2003 on the restriction of the use of certain hazardous substances in electrical and electronic equipment (RoHS).
4. Directive 2002/96/EC of the European Parliament and of the Council of 27 January 2003 on waste electrical and electronic equipment (WEEE),
5. J.A.S. Williams, A review of electronics demanufacturing processes, *Resources, Conservation and Recycling*, 47 (2006) 195-208.

SELECTED ENGINEERING PROBLEMS

NUMBER 5

INSTITUTE OF ENGINEERING PROCESSES AUTOMATION
AND INTEGRATED MANUFACTURING SYSTEMS

Rafał ZBICIAK

Institute of Engineering Processes Automation and Integrated Manufacturing Systems,
Faculty of Mechanical Engineering, Silesian University of Technology, Gliwice, Poland
rafal.zbiciak@polsl.pl

THE ORIGINAL SOFTWARE SUPPORTING DESIGN OF GEARS IN SIEMENS NX ENVIRONMENT

Abstract: The study presents a description of the original software supporting gears design. The discussed software is destined to make 3D models of spur and helical gears in Siemens NX environment. It is characterized by higher involute profile gear tooth accuracy. The main benefit of the original software is primarily reducing modelling time of gears up to a few seconds. It is also possible to create models using an individual parameters (including non-standard modules of the gear). The software was programmed using C# programming language and SNAP it is Simple NX Application Programming.

1. Introduction

One of the fundamental machine or device components is gearbox. Gearboxes are used in the small precision clockworks as well as industrial machinery or aircraft. Particularly important in industry are high power gearboxes. Warn-out gearbox replacement is linked not only to bear costs for buying a new one but also to lengthy production process interval. That is the reason why gearboxes have to qualify requirements of reliability.

Contemporary trend in mechanical engineering is tendency for reducing manufacturing costs. It means material saving, simplifying a technology, design form optimization. Taking the above facts into account it can be concluded that designer should find compromise between reliability requirements and economic and technical aspects. Design supporting software can be helpful in design process of gears. This software allows to create precise 3D models according to given parameters. This solution enables to omit frequently appearing errors and reduce time for element modeling. Using advanced CAD (Computer Aided Design) systems like Siemens NX one can perform gears analysis without wasting time for repeated modeling. For example Finite Element Method (FEM) – numerical technique for finding solutions for the differential equations that describe, or approximately describe a wide variety of physical (and non-physical) relations. FEM is the basic tool which occurs in many CAD environments like Siemens NX, CATIA, Solid Edge.

Gears generator is enable in Solid Edge and also Siemens NX system contains similar plugin. Moreover a tooth profile created due to above mentioned software is a curve (spline) probably based on the three points. It is the minimal sum of points needed to sketch a curve. Taking into account above the model accuracy might appear low.

To make sure that generated model has features relating to the high mapping of the tooth's cooperating part geometry the original software was created.

2. Gears generator

The software was programmed using C# programming language and SNAP it is .NET library. The first one was used for creating a graphic user interface (Fig.1).

The screenshot displays the 'Gears generator' software interface, which is divided into two main sections: 'Basic gear parameters' and 'Advanced gear parameters'.

Basic gear parameters:

- Gear type:** Radio buttons for 'spur' (selected) and 'helical'.
- 3D models:** Two 3D models of gears, labeled 'Form A' and 'Form B', are shown side-by-side.
- Module m (wg PN-78/M88502):** A dropdown menu set to '2'.
- Number of teeth Z:** A text input field containing '20'.
- Face width B [mm]:** A text input field containing '10'.
- Bore diameter Do [mm]:** A text input field containing '17'.
- Tooth depth coefficient y:** A text input field containing '1'.
- Pressure angle:** A text input field containing 'α = 20°'.
- Helix angle [°]:** A dropdown menu set to 'β = 15'.
- Hand of helix:** A dropdown menu set to 'right'.
- Buttons:** 'Calculate' and '3D model of gear Generate' buttons are located at the bottom of this section.

Advanced gear parameters:

- Edit:** A checkbox that is currently unchecked.
- Module M:** A text input field containing '2'.
- Pitch diameter D:** A text input field containing '40,00 mm'.
- Base diameter Db:** A text input field containing '37,59 mm'.
- Outside diameter Da:** A text input field containing '44,00 mm'.
- Root diameter Df:** A text input field containing '35,20 mm'.
- Tooth depth H:** A text input field containing '4,40 mm'.
- Addendum Ha:** A text input field containing '2,00 mm'.
- Dedendum Hf:** A text input field containing '2,40 mm'.
- Slot width b:** A text input field containing '5,00 mm'.
- Slot depth h:** A text input field containing '2,30 mm'.
- Slot radius r:** A text input field containing '0,25 mm'.
- Hub diameter Dp:** A text input field containing '27,20 mm'.
- Hub length B1:** A text input field containing '5,10 mm'.
- Helix angle β:** A text input field containing '15,00 °'.
- Buttons:** '3D model of gear Generate' button is located at the bottom of this section.

Fig.1. User interface

The second one (SNAP) was used in conjunction with C# to create 3D model. Combination of these two elements has been edited and compiled in an Integrated Development Environment (IDE) it is in Microsoft Visual Studio.

In order to generate 3D model of gears it is necessary to choose basic parameters of the gear. After completing all needed parameters it is possible to calculate advanced parameters of the gear or just to generate 3D model in Siemens NX (Fig. 2).



Fig.2. The example of the 3D model of gear: $m = 2$, $z = 15$, $y = 1$

Very important aspect is a possibility to edit the advanced parameters. It means that using GEARS GENERATOR, it is possible to generate special gears with the individual parameters.

Involute gear tooth profile generated in the original software has been based on the 11 points. The same gear tooth profile based on 3 points is not as precise as the first one (Fig. 3).

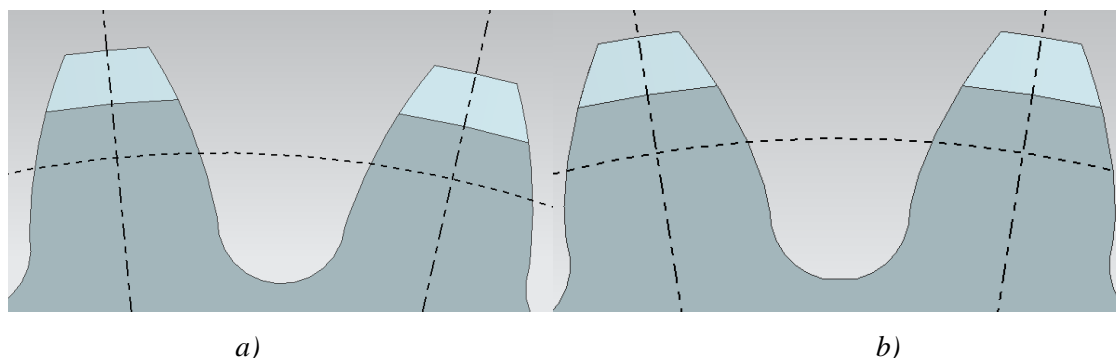


Fig.3. Automatically generated involute gear tooth profile: a) based on 3 pts, b) based on 11 pts

These differences are more evident with comparison of involute curves as the fig. 4 shows. The difference in the point of extreme reaches about 0.1 mm.

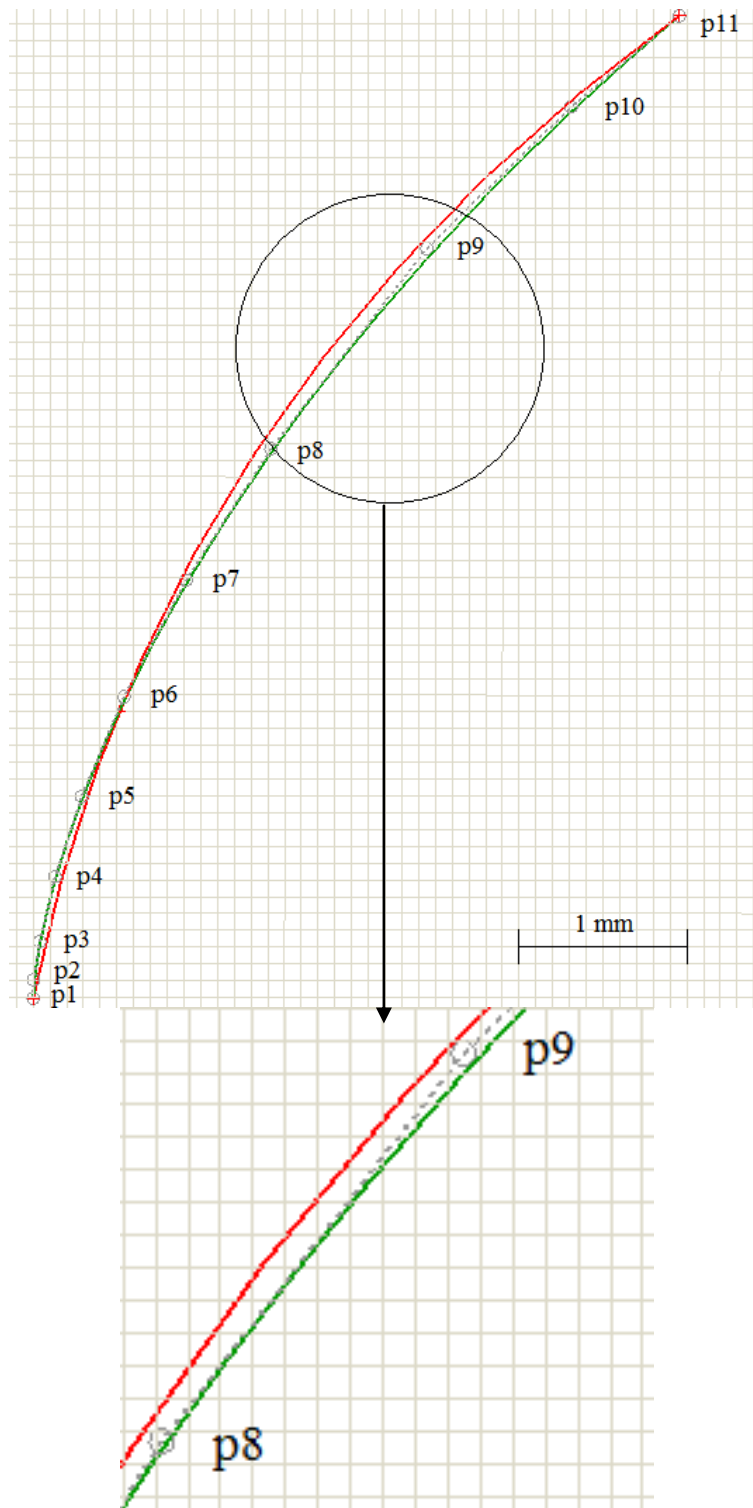


Fig.4. Involute curves: the red line – based on 3 pts, the green line – based on 11 pts

For a more detailed analysis of these teeth profiles the finite element method was used. For this purpose Design Simulation module of Siemens NX was used. During the numerical

simulation for the one particular tooth flank normal force of 500 N was applied (perpendicular to the surface at each point). The following results were presented in Fig. 5 and Fig 6.

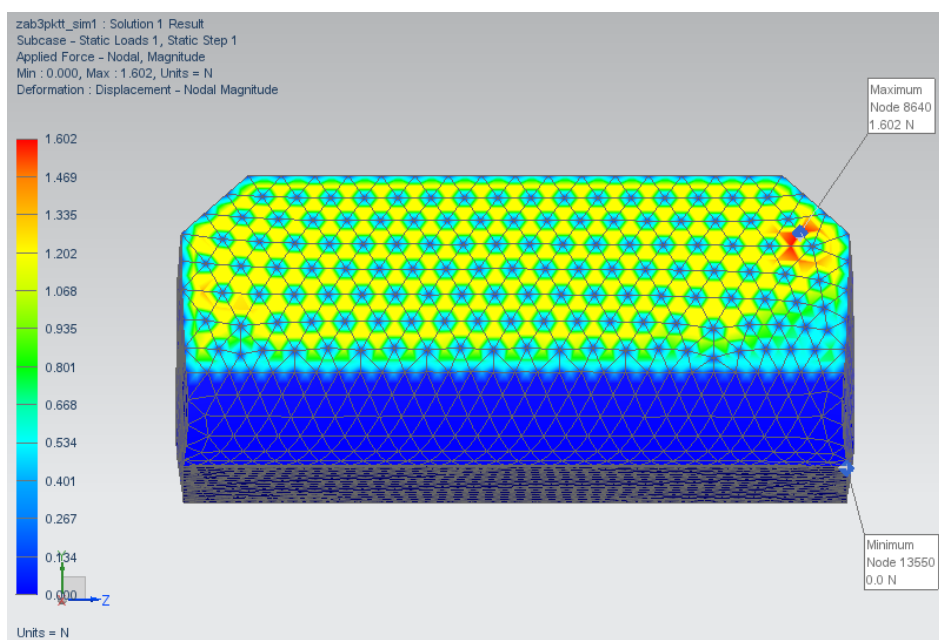


Fig.5. Analysis of force distribution for 3 pts

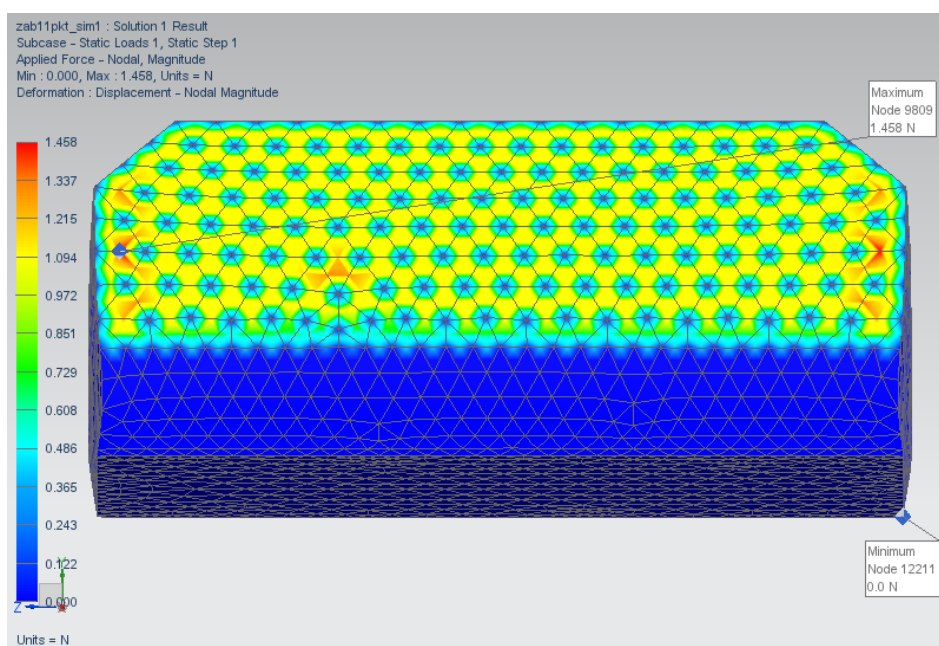


Fig.6. Analysis of force distribution for 11 pts

In case of the 3 pts tooth profile the maximum force acting on the node equals to 1.602 N.

In case of the second tooth is about 0.144 N smaller and amounts to 1.458 N. For less accurate tooth there is an asymmetric forces distribution (Fig. 5). The tooth profile based on

a larger number of points has a relatively symmetrical forces distribution on both sides of the engaging surface (Fig. 6). This phenomenon can also has positive influence on the fatigue strength of the gear.

3. Conclusion

Based on FEM analysis the inaccuracy models of gears with involute tooth profile based on three points was stated. These differences in results between the two outlines were small but in key situations the quality of the outline can make a big difference in case when high accuracy is required. 3D models generated in the NX environment using the original software can serve as a basis for analysis for gears certainly.

References

1. Al-Khafaji A. W., Tooley J.R.: Numerical methods in engineering practice. Canada: Holt, Rinehart & Winston, 1986.
2. Dietrych J.: Podstawy konstrukcji maszyn – tom 3. Warszawa: Wydawnictwa Naukowo-Techniczne, 1970.
3. Feld M.: Podstawy projektowania procesów technologicznych typowych części maszyn. Warszawa: Wydawnictwa Naukowo-Techniczne, 2003.
4. Müller L.: Przekładnie zębate. Warszawa: Wydawnictwa Naukowo-Techniczne, 1996.
5. Ochęduszek K.: Koła zębate. Warszawa: Wydawnictwa Naukowo-Techniczne, 1985.
6. Siemens Product Lifecycle Management Software Inc.: Getting Started With SNAP: NX 8.5 Documentation, 2012.

INDEX OF AUTHORS

B

BABILAS Rafał	33, 47, 103, 119
BAIER Maja	5
BĄCZKOWICZ Magdalena	11
BOGNÁR Eszter	15

C

CESARZ-ANDRACZKE Katarzyna	119
----------------------------	-----

Ć

ĆWIKŁA Grzegorz	21, 41, 53, 87
-----------------	----------------

D

DÉVÉNYI László	15
DUSIK Dawid	5

F

FOIT Krzysztof	27
----------------	----

G

GAWLAS-MUCHA Agnieszka	33, 47
GOŁDA Grzegorz	37, 57
GRABOWIK Cezary	21, 41, 53, 87
GUWER Aleksandra	33, 47, 103
GWIAZDA Aleksander	11, 99

H

HETMAŃCZYK Mariusz Piotr	63, 93
--------------------------	--------

J

JANIK Witold	21, 41, 53, 87
--------------	----------------

K

KALINOWSKI Krzysztof	21, 41, 53, 87
KAMPA Adrian	37, 57
KERTÉSZ Anna	15

KILJAN Anna	47, 103
-------------	---------

KLARECKI Klaudiusz	63
--------------------	----

KRENCZYK Damian	67
-----------------	----

KRZYSTAŁA Edyta	71
-----------------	----

M

MAJCHRZAK Magdalena	109
---------------------	-----

MANDLA Łukasz	71
---------------	----

MAZUR Jarosław	41
----------------	----

MICHALSKI Piotr	81
-----------------	----

MIKOŁAJCZAK Magdalena	87
-----------------------	----

MOCZAŁA Marcin	93
----------------	----

MONICA Zbigniew	99
-----------------	----

N

NOWOSIELSKI Ryszard	33, 47, 103, 119
---------------------	------------------

O

OZSVÁTH Péter	15
---------------	----

P

PELYHE Liza	15
-------------	----

PILARCZYK Wirginia	109, 119
--------------------	----------

PŁACZEK Marek	113
---------------	-----

R

RABSZTYN Dominik	63
------------------	----

S

SAKIEWICZ Piotr	119
-----------------	-----

T

TKOCZ Krzysztof	81
-----------------	----

Z

ZBICIAK Rafał	123
---------------	-----

Printed 200 copies

Paper 80g

Submitted for printing 16 December, 2014

Printed in Epigraf s.c. Jan Kalnik, Teresa Kalnik

ul. Bernardyńska 19, 44-100 Gliwice, Poland
